

# The Seventh Korea-Japan Workshop on Digital Holography and Information Photonics

**December 20-22, 2017**

**DGDC, Daegu, South Korea**

**Organizers:**

Optical Society of Korea (OSK)

**The Optical Society of Japan (OSJ)**

School of Electronics Engineering, Kyungpook National University (KNU)

**Sponsored by:**

Center for Research and Development of Police Science and Technology

ITRC on Hologram Convergence Technology

**Korea Photonics Technology Institute (KOPTI)**

**Korea Electronics Technology Institute (KETI)**

ICT Fundamental Laboratory



# Program

December 20(Wed)

## Session 1: 9:00 – 10:40

Chair: Jae-Hyeung Park, Inha University

<b>Key20a-1</b>	<b>Research and development of holographic optical element for three-dimensional display and microscopy</b>
9:00	Nam Kim, Munkh-Uchral Erdenebat, Ki-Chul Kwon, and Young-Tae Lim
	Chungbuk National University
9:50	.....01

<b>Inv20a-1</b>	<b>Three dimensional structure of subdiffraction limit optical patterns</b>
9:50	Yusuke Ogura and Jun Tanida
	Osaka University
10:15	.....02

<b>Inv20a-2</b>	<b>Research activities in KETI</b>
10:15	Hoonjong Kang
	Korea Electronics Technology Institute
10:40	.....03

## Session 2: 11:00 – 12:15

Chair: Naoya Tate, Kyushu University

<b>Inv20a-3</b>	<b>Ghost imaging for single photon counting</b>
11:00	Yasuhiro Mizutani <sup>1,2</sup> , Hiroki Taguchi <sup>1</sup> , Yasuhiro Takaya <sup>1</sup>
	<sup>1</sup> Osaka Univesity,
11:25	<sup>2</sup> JST/ERATO MINOSHIMA Intelligent Optical Synthesizer Project
	.....04

<b>Inv20a-4</b>	<b>Fast calculation of wide viewing angle depth-map computer-generated hologram</b>
11:25	Hwi Kim, Sungjae Park, and Jonghyun Lee
	Korea University
11:50	.....05

<b>Inv20a-5</b>	<b>Compound-eye imaging for forensics</b>
11:50	Yoshinori Akao
	National Research Institute of Police Science
12:15	.....06

Lunch Time

### Session 3: 13:30 – 14:45

Chair: Hwi Kim, Korea University

<b>Inv20p-1</b> 13:30   13:55	<b>3D display making light field inside volume</b>  Joonku Hahn Kyungpook National University	.....07
<b>Inv20p-2</b> 13:55   14:20	<b>Nanoscale character extraction for nano-optical metric system</b>  Naoya Tate Kyushu University	.....08
<b>Inv20p-3</b> 14:20   14:45	<b>Reflective-type reconfigurable digital hologram panel using Ge<sub>2</sub>Sb<sub>2</sub>Te<sub>5</sub> phase change material</b> Seung-Yeol Lee Kyungpook National University	.....09

### Session 4: 15:05 – 16:20

Chair: Yusuke Ogura, Osaka University

<b>Inv20p-4</b> 15:05   15:30	<b>Unstained tumor detection in digestive organs based on autofluorescence spectroscopy</b> Hidenobu Arimoto <sup>1</sup> , Keiichiro Kagawa <sup>2</sup> , Yoji Sanomura <sup>3</sup> , Shigeto Yoshida <sup>4</sup> , and Shinji Tanaka <sup>3</sup> <sup>1</sup> National Institute of Advanced Industrial Science and Technology, <sup>2</sup> Shizuoka University, <sup>3</sup> Hiroshima University Hospital, <sup>4</sup> JR Hiroshima Hospital	.....10
<b>Inv20p-5</b> 15:30   15:55	<b>Recent progress on 3D target tracking using optical scanning holography</b>  Taegeun Kim Sejong University	.....11
<b>Inv20p-6</b> 15:55   16:20	<b>Multi-frequency swept en-face optical coherence microscopy with supercontinuum comb for in-vivo measurement of inner ear</b> Samuel Choi <sup>1,4</sup> , Fumiaki Nin <sup>2,4</sup> , Takeru Ota <sup>2,4</sup> , Keita Sato <sup>3</sup> , Takamasa Suzuki <sup>3</sup> and Hiroshi Hibino <sup>2,4</sup> <sup>1,2,3,4</sup> Niigata University	.....13

## Poster Session: 16:40 – 18:00

<b>p20-1</b>	<b>Polarization Color Display Using Index Matching</b> Toshiki Matsuzaki, Huangyi Qin and Kenji Harada Kitami Institute of Technology	.....14
<b>p20-2</b>	<b>Polarization color optimization of birefringent material</b> Huangyi Qin, Toshiki Matsuzaki and Kenji Harada Kitami Institute of Technology	.....15
<b>p20-3</b>	<b>Object recognition through a multi-mode fiber based on machine learning</b> Ryosuke Takagi, Ryoichi Horisaki and Jun Tanida Osaka University	.....16
<b>p20-4</b>	<b>Spectral imaging based on single pixel camera</b> Ryo Sato, Kazuki Ota and Yoshio Hayasaki Utsunomiya University	.....17
<b>p20-5</b>	<b>Aerial Volumetric Display with Pyramid Structured LED Lattice and AIRR</b> Kazuki Shimose <sup>1</sup> and Hirotugu Yamamoto <sup>1,2</sup> <sup>1</sup> Utsunomiya University, <sup>2</sup> JST.ACCEL	.....18
<b>p20-6</b>	<b>Forming the aerial 3D image of your back in front of you with using AIRR</b> Ryosuke Kujime <sup>1,2</sup> and Hirotugu Yamamoto <sup>1,2</sup> <sup>1</sup> Utsunomiya University, <sup>2</sup> JST.ACCEL	.....19
<b>p20-7</b>	<b>Multi-layered head-mounted display for occlusion and accommodation effects</b> Mugoen Kim, Daerak Heo, and Joonku Hahn Kyungpook National University	.....20
<b>p20-8</b>	<b>Depth resolution enhancement of computational reconstruction of integral imaging with considering continuously non-uniform shifting pixel</b> Byungwoo Cho <sup>1</sup> , Hui Yun <sup>1</sup> , Kotaro Inoue <sup>1</sup> , Ki-Ok Cho <sup>1</sup> , Kyungtae Park <sup>1,2</sup> , Jungsik Koo <sup>2</sup> , Jiyong Park <sup>2</sup> , Cheol-su Kim <sup>3</sup> , Min-Chul Lee <sup>4</sup> and Myungjin Cho <sup>1</sup> <sup>1</sup> Hankyong National University, <sup>2</sup> Gumi Electronics & Information Technology Research Institute, <sup>3</sup> Gyeongju University, <sup>4</sup> Kyushu Institute of Technology	.....21



<b>p20-9</b>	<b>Pixel Blink Rate based Depth Estimation Technique in Integral Imaging with Markov Random Field Optimization</b> Kotaro Inoue <sup>1</sup> , Byeongwoo Cho <sup>1</sup> , Hui Yoon <sup>1</sup> , Ki-Ok Cho <sup>1</sup> , Kyungtae Park <sup>1,2</sup> , Jungsik Koo <sup>2</sup> , Jiyong Park <sup>2</sup> , Cheol-Su Kim <sup>3</sup> , Min-Chul Lee <sup>4</sup> , Myungjin Cho <sup>1</sup> <sup>1</sup> Hankyong National University, <sup>2</sup> Gumi Electronics & Information Technology Research Institute, <sup>3</sup> Gyeongju University, <sup>4</sup> Kyushu Institute of Technology .....22
<b>p20-10</b>	<b>Three-dimensional image sensing and visualization to enhance 3D resolution of integral imaging</b> Hui Yun <sup>1</sup> , Byeongwoo Cho <sup>1</sup> , Ki-Ok Cho <sup>1</sup> , Kyungtae Park <sup>1,2</sup> , Kotaro Inoue <sup>1</sup> , Jungsik Koo <sup>2</sup> , Jiyong Park <sup>2</sup> , Cheol-Su Kim <sup>3</sup> , MinChul Lee <sup>4</sup> , Myungjin Cho <sup>1</sup> <sup>1</sup> Hankyong National University, <sup>2</sup> Gumi Electronics & Information Technology Research Institute, <sup>3</sup> Gyeongju University, <sup>4</sup> Kyushu Institute of Technology .....23
<b>p20-11</b>	<b>Multiple projection 3D display on diffusive fog screen</b> Jiman Yu, Minwoo Jung, Daerak Heo, Geunseop Choi, and Joonku Hahn Kyungpook National University .....24
<b>p20-12</b>	<b>Complex object wave extraction using time-multiplexing in off-axis digital holography</b> Erkhembaatar Dashdavaa, Munkh-Uchral Erdenebat, Nyamsuren Darkhanbaatar, Anar Khuderchuluun, and Nam Kim Chungbuk National University .....25
<b>p20-13</b>	<b>Fast calculation method for full-color holographic system of real existing objects</b> Yu Zhao <sup>1</sup> , Ki-Chul Kwon <sup>1</sup> , Seok-Hee Jeon <sup>2</sup> , Sang-Keun Gil <sup>3</sup> , Nam Kim <sup>1</sup> <sup>1</sup> Chungbuk National University, <sup>2</sup> Incheon National University, <sup>3</sup> Suwon University .....26
<b>p20-14</b>	<b>A refractive index sensor based on an extraordinary optical transmission in a floated metal nano-slit array</b> Hee-Dong Jeong <sup>1</sup> , Yong-Sang Ryu <sup>2</sup> and Seung-Yeol Lee <sup>1</sup> <sup>1</sup> Kyungpook National University, <sup>2</sup> Korea Institute of Science and Technology .....27
<b>p20-15</b>	<b>Analysis on random plasmonic nanopillar structure using Bruggeman effective medium theory</b> Youngkyu Bae <sup>1</sup> , Yong-Sang Ryu <sup>2</sup> , and Seung-Yeol Lee <sup>1</sup> <sup>1</sup> Kyungpook National University, <sup>2</sup> Korea Institute of Science and Technology .....28
<b>p20-16</b>	<b>Fabrication of camera lens using photopolymer</b> Seo-Yeon Park, Jae-Min Lee, Chang-Won Shin, Hui-Ying Wu, and Nam Kim Chungbuk National University .....29
<b>p20-17</b>	<b>Universal light engine with three digital micromirror devices</b> Kwangsoo Kim, Geunseop Choi, Daerak Heo, and Joonku Hahn Kyungpook National University .....30

<b>p20-18</b>	<b>Spherical light field display</b>	
	Daerak Heo, Mugeon Kim and Joonku Hahn Kyungpook National University	.....31
<b>p20-19</b>	<b>Time-sequential super multi-view display</b>	
	Sungjin Lim, Geunseop Choi, Mugeon Kim, Kwangsoo Kim and Joonku Hahn Kyungpook National University	.....32
<b>p20-20</b>	<b>Cylindrical light field display</b>	
	Geunseop Choi <sup>1</sup> , Hosung Jeon <sup>1</sup> , Kwangsoo Kim <sup>1</sup> , Hwi Kim <sup>2</sup> and Joonku Hahn <sup>1</sup> <sup>1</sup> Kyungpook National University, <sup>2</sup> Korea University	.....33
<b>p20-21</b>	<b>Orthographic projection based holography with low density modeling point cloud</b>	
	Yan-Ling Piao <sup>1</sup> , Alam MD Shahinur <sup>1</sup> , Jong-Rae Jeong <sup>2</sup> and Nam Kim <sup>1</sup> <sup>1</sup> Chungbuk National University, <sup>2</sup> Suwon Science College	.....34
<b>p20-22</b>	<b>Analysis of 360-degree Non-Mechanical Table Top Electronic Holographic Display system</b>	
	Soobin Kim and Hwi Kim Korea University	.....35
<b>p20-23</b>	<b>Geometrical optical modeling and diffraction efficiency analysis of diffractive augmented reality system</b>	
	JungBeom Choi, JongHa Park, SooBin Kim, and Hwi Kim Korea University	.....36
<b>p20-24</b>	<b>Fast Calculation Method of High-Definition Computer-Generated Hologram</b>	
	Sungjae Park, Jonghyun Lee and Hwi Kim Korea University	.....37
<b>p20-25</b>	<b>Analysis of Moiré Deflectometry in Display System using Talbot Effect</b>	
	Junghwan Park and Hwi Kim Korea University	.....38
<b>p20-26</b>	<b>Localization Method of Depth-map Computer Generated Hologram for Fast Calculation</b>	
	JongHa Park, JiSung Yoon, SungJae Park, JongHyun Lee and Hwi Kim Korea University	.....39
<b>p20-27</b>	<b>Comparison of LED and LD as a light source for near-eye holographic display</b>	
	Dukho Lee, Gang Li, Byounghyo Lee and Byoungho Lee Seoul National University	.....40

<b>p20-28</b>	<b>Augmented-Reality Display for Supporting Ametropia using Maxwellian view and Edge Enhancement</b> Byounghyo Lee <sup>1</sup> , Seungjae Lee <sup>1</sup> , Dukho Lee <sup>1</sup> , Hee-Jin Choi <sup>2</sup> and Byoungho Lee <sup>1</sup> <sup>1</sup> Seoul National University, <sup>2</sup> Sejong University	.....42
<b>p20-29</b>	<b>Apparatus for measuring large field of view embossed hologram</b> Sunggyun Ahn, Geunseop Choi, Mugeon Kim and Joonku Hahn Kyungpook National University	.....44
<b>p20-30</b>	<b>Time division multiplexed holographic display using electronic beam steering method</b> Hyun-Eui Kim, Minsik Park and Jinwoong Kim Electronics and Telecommunications Research Institute (ETRI)	.....45
<b>p20-31</b>	<b>Improving the image quality of a digital holographic display system by estimating a virtual spatial light modulator plane</b> Yongjun Lim, Keehoon Hong, Minsik Park, Jinwoong Kim Electronics and Telecommunications Research Institute (ETRI)	.....46
<b>p20-32</b>	<b>3D smart table display</b> Sang-Hyeok Mun, Muhan Choi Kyungpook National University	.....47
<b>p20-33</b>	<b>Tunable Graphene Metasurface Application</b> Yong-Hoon Lee, Sang-Hyeok Mun, Inbo Kim and Muhan Choi Kyungpook National University	.....48
<b>p20-34</b>	<b>Compressive holographic optical sectioning</b> Junkyu Yim, Seungwhi Yoo, and Sung-Wook Min Kyung Hee University	.....49
<b>p20-35</b>	<b>Digital Holographic Tabletop display with vertical parallax by pupil tracking</b> Jaehan Kim, Hyongon Choo, Minsik Park and Jinwoong Kim Electronics and Telecommunications Research Institute (ETRI)	.....50
<b>p20-36</b>	<b>Optical design of table-top light field display</b> Kwangsoo Kim, Daerak Heo, and Joonku Hahn Kyungpook National University	.....51

<b>p20-37</b>	<b>Augmented Reality Near-eye Light-field 3D Display Using Retroreflector</b> Hyeongkyu Do, Young Min Kim, Hyunsik Sung, Ki-Hong Choi, Sungwon Choi and Sung-Wook Min Kyung Hee University .....	52
<b>p20-38</b>	<b>Improvement in Phase Pattern Design for Holographic Shack-Hartmann Wavefront Sensor with High Sensitivity</b> Yusuke Saita and Takanori Nomura Wakayama University .....	53
<b>p20-39</b>	<b>GPU acceleration of hologram calculation using an orthographic ray-sampling plane</b> Shunsuke Igarashi <sup>1</sup> , Tomoya Nakamura <sup>1,2</sup> , Kyoji Matsushima <sup>3</sup> , and Masahiro Yamaguchi <sup>1</sup> <sup>1</sup> Tokyo Institute of Technology, <sup>2</sup> Japan Science and Technology Agency, <sup>3</sup> Kansai University .....	54
<b>p20-40</b>	<b>Angular spectrum convolution based occlusion processing in computer generated hologram</b> Mehdi Askari and Jae-Hyeong Park Inha University .....	56
<b>p20-41</b>	<b>Speckle reduction using angular spectrum interleaving for triangular mesh based computer generated hologram</b> Seok-Beom Ko and Jae-Hyeong Park Inha University .....	57
<b>p20-42</b>	<b>See-through Maxwellian display using waveguide and multiplexing holographic optical element</b> Seong-Bok Kim, Jae-Hyeong Park Inha University .....	58
<b>p20-43</b>	<b>Acceleration of fully analytic mesh based computer generated hologram using foveated rendering technique</b> Yeon-Gyeong Ju and Jae-Hyeong Park Inha University .....	59
<b>p20-44</b>	<b>An analysis of light field type head-up displays for vehicles</b> KwangSoo Shin, Jae-Hyeong Park Inha University .....	60

## Session 5: 9:00 – 10:40

Chair: Yoshio Hayasaki, Utsunomiya University

<b>Key21a-1</b> 9:00   9:50	<b>Full-parallax light-field and holographic displays</b>  Masahiro Yamaguchi Tokyo Institute of Technology	.....61
<b>Inv21a-1</b> 9:50   10:15	<b>Table-top Holographic Display with Full Parallax</b>  Minsik Park, Yongjun Lim, Keehoon Hong, Eun-Young Chang, Hayan Kim, Jaehan Kim and Jinwoong Kim Electronics and Telecommunications Research Institute (ETRI)	.....62
<b>Inv21a-2</b> 10:15   10:40	<b>Enlargement of viewing zone of holographic 3D display using a parabolic mirror</b>  Yusuke Sando <sup>3</sup> , Kazuo Satoh <sup>3</sup> , Takahiro Kitagawa <sup>3</sup> , Makoto Kawamura <sup>3</sup> , Daisuke Barada <sup>1,2</sup> and Toyohiko Yatagai <sup>1</sup> <sup>3</sup> Osaka Research Institute of Industrial Science and Technology, <sup>1,2</sup> Utsunomiya University	.....63

## Session 6: 11:00 – 12:15

Chair: Kwang-Hoon Lee, Korea Photonics Technology Institute (KOPTI)

<b>Inv21a-3</b> 11:00   11:25	<b>Formation of dynamic viewing zone in autostereoscopic 3D display</b>  Sung-Kyu Kim, Ky-Hyuk Yoon, and Min-Koo Kang Korea Institute of Science and Technology	.....64
<b>Inv21a-4</b> 11:25   11:50	<b>Aerial Multi-Modal Information Display</b>  Hirotsugu Yamamoto <sup>1,2</sup> , Tomoyuki Okamoto <sup>1</sup> , Shusei Ito <sup>1</sup> and Ryosuke Kujime <sup>1,2</sup> <sup>1</sup> Utsunomiya University, <sup>2</sup> JST. ACCEL	.....66
<b>Inv21a-5</b> 11:50   12:15	<b>Metasurfaces for holograms</b>  Byoungho Lee and Gun-Yeal Lee Seoul National University	.....67

**Lunch Time**



## Session 7: 13:30 – 14:45

Chair: Hee-Jin Choi, Sejong University

<b>Inv21p-1</b> 13:30   13:55	<b>Common-path incoherent digital holography</b>  Osamu Matoba <sup>1</sup> , Xiangyu Quan <sup>1</sup> and Yasuhiro Awatsuji <sup>2</sup> <sup>1</sup> Kobe University, <sup>2</sup> Kyoto Institute of Technology .....68
<b>Inv21p-2</b> 13:55   14:20	<b>Photonic meta-devices based on optical path control</b>  Muhan Choi, Inbo Kim, Jinhang Cho, and Sang-Hyeok Mun Kyungpook National University .....69
<b>Inv21p-3</b> 14:20   14:45	<b>Multidimensional imaging with phase-shifting interferometry</b>  Tatsuki Tahara <sup>1,2</sup> , Reo Otani <sup>3</sup> , Yasuhiko Arai <sup>1</sup> and Yasuhiro Takaki <sup>4</sup> <sup>1</sup> Kansai University, <sup>2</sup> Japan Science and Technology Agency, <sup>3</sup> SIGMAKOKI CO. LTD, <sup>4</sup> Tokyo University of Agriculture and Technology .....70

## Session 8: 15:05 – 16:20

Chair: Minsik Park, Electronics and Telecommunications Research Institute (ETRI)

<b>Inv21p-4</b> 15:05   15:30	<b>Quantitative verification for whether LF display system can serve accommodative function to the observer</b>  Kwang-Hoon Lee and Seon Kyu Yoon Korea Photonics Technology Institute .....71
<b>Inv21p-5</b> 15:30   15:55	<b>How to control polarization color</b>  Kenji Harada, Toshiki Matsuzaki and Huangyi Qin Kitami Institute of Technology .....72
<b>Inv21p-6</b> 15:55   16:20	<b>Research on effects of physiological depth cues on the visual discomfort of augmented reality displays</b>  Hee-Jin Choi, Hanul Lee, Minyoung Park, and Jaehee Seo Sejong University .....73

**Session 9: 9:00 – 10:40**

Chair: Hirotugu Yamamoto, Utsunomiya University

<b>Inv22a-1</b> 9:00   9:25	<b>Volumetric Bubble Display</b>  Yoshio Hayasaki and Kota Kumagai Utsunomiya University	.....74
<b>Inv22a-2</b> 9:25   9:50	<b>Accommodative optical-see-through near-to-eye displays using waveguide and holographic optical elements</b> Jae-Hyeung Park, Seong-Bok Kim, Seok-Beom Ko, Kwang-Soo Shin, Yeon-Gyeong Ju, Dae-Yeol Park, and Askari Mehdi Inha Univesity	.....75
<b>Inv22a-3</b> 9:50   10:15	<b>Incoherent holography without depth of field</b>  Takanori Nomura <sup>1</sup> , Takuya Matsuda <sup>2</sup> <sup>1,2</sup> Wakayama University	.....76
<b>Inv22a-4</b> 10:15   10:40	<b>Recent researches for two type 3D screens: Reflection-type and Transmission-type</b> Sung-Wook Min and Hyunsik Sung Kyung Hee University	.....77

## Research and development of holographic optical element for three-dimensional display and microscopy

Nam Kim\*, Munkh-Uchral Erdenebat, Ki-Chul Kwon, and Young-Tae Lim  
 School of Information and Communication Engineering, Chungbuk National University,  
 Cheongju, Chungbuk 28644, South Korea  
 Tel.:82-43-261-2482, \*E-mail: [namkim@chungbuk.ac.kr](mailto:namkim@chungbuk.ac.kr)

**OCIS codes:** (090.2890) Holographic optical elements; (110.3010) Image reconstruction techniques; (180.6900) Three-dimensional microscopy

The holographic optical element (HOE) can be applied in various fields of three-dimensional (3D) applications such that the light field camera, head-mounted display (HMD), holographic printer, hologram memory and so on. Due to the advantageous function of HOE that it can be applied as a lens/lens array and mirror etc., according to high diffraction efficiency and narrow-band frequency characteristics, the design of optical systems can be lighter, thinner and smaller. For example, the HOE film can be applied as the in and out-coupling elements in the waveguide-type 3D HMD, the HMD is getting lighter, so it can be wearable for a long time, and applied to a glass-type display with an AR function. When the optical properties of microlens array are recorded onto the HOE film, it can be used in the light field camera and microscopy based on integral imaging technique. By using the spatial or rotational multiplexing methods, multiple microlens array's properties can be recorded, and single HOE film images the different 3D perspectives. Also, the HOE film is applied in the typical camera as a main lens instead of a huge and heavy glass lens.

In this report, we discussed the recent research and development of the HOE for the applications of 3D imaging field such as 3D display and microscopy. Figure 1 shows the example of full-color HOE for HMD and rotationally multiplexed HOE-MLA for integral imaging microscopy. Experimental results presented that the use of HOE has several advantages such as miniaturization of optical devices.

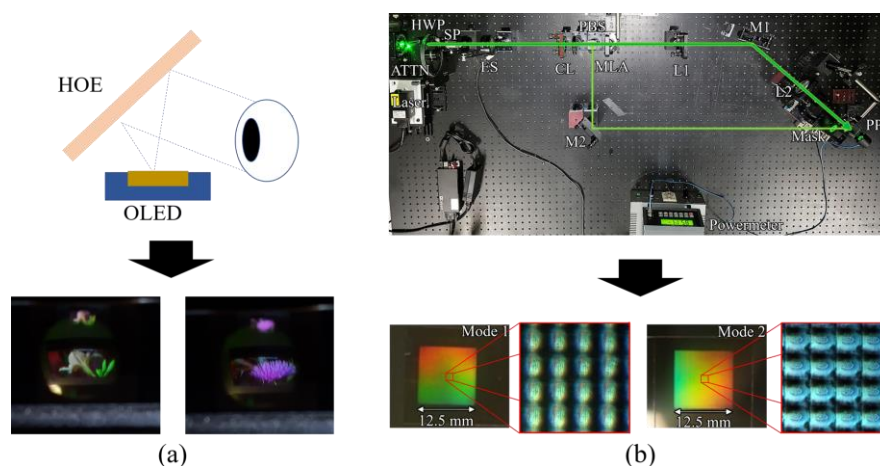


**Fig. 1. The examples for applications of HOE in the optical imaging systems: (a) full-color HOE for HMD, and (b) a visualization of rotationally multiplexed HOE micro lens array for integral imaging microscopy.**

### Acknowledgment

This research was supported by the Government of Korea, under the ITRC (Information Technology Research Center) support program (IITP-2017-2015-0-00448) supervised by the IITP (Institute for Information & communications Technology Promotion), and supported by the National Research Foundation of Korea (NRF) grant funded by the Government of Korea (No. NRF-2017R1A2B4012096).

### References

1. M.-L. Piao and N. Kim, *Appl. Opt.*, 53(10), 2180 (2014).
2. M.-L. Piao, H.-Y. Wu, and N. Kim, *Digital Holography and 3-D Imaging* 2016, JW4A.50 (2016).

## Three dimensional structure of subdiffraction limit optical patterns

*Yusuke Ogura and Jun Tanida*

Graduate School of Information Science and Technology, Osaka University, Suita, Osaka 565-0871, Japan

Tel.:81-6-6879-7849, E-mail: ogura@ist.osaka-u.ac.jp

**OCIS codes:** (090.1760) Computer holography; (050.1940) Diffraction; (070.6120) Spatial light modulators

Diffractive optical elements (DOEs) have high design flexibility, and they can provide a variety of functions as a single device. However, these functions are based on diffraction, and therefore, the behavior of the DOEs is governed by the diffraction limit. To enhance the functionality under the diffraction limit, we have demonstrated DOEs that generate an array of spots smaller than a single diffraction-limited spot [1,2]. We refer such fine patterns as subdiffraction limit optical patterns. This strategy is effective to realize fine patterns using propagating light; thus distinctive properties such as spatial parallelism, remote accessibility, and multiplexing capability are utilizable straightforwardly in optical application systems.

In this paper, we focus on generation of subdiffraction limit light sheets. A light sheet is, for example, used in light sheet fluorescence microscopy (LSFM), which enables three-dimensional imaging of a sample with low damage and high contrast. The resolution along the optical axis of this type of microscopy depends on the thickness of a light sheet used as illumination, so that generation of a thin light sheet is an important factor for the axial resolution. Furthermore, patterned light sheets are realized by a DOE, which is useful to provide a new function in LSFM.

To use a subdiffraction limit light sheet in LSFM, it is important to know the three-dimensional structure. For the purpose, we analyzed intensity distributions of subdiffraction limit light sheets at many planes, and experimentally observed them. As an example of the analyses, Fig. 1 shows the intensity distribution on a plane parallel to the optical axis ( $z$  axis) and the direction of the sheet's width ( $x$  axis) for DOEs generating a single and three subdiffraction limit light sheets. The result shows that the  $z$ -direction length of the central light sheet of the three light sheets is longer than that of a single light sheet. In summary, this kind of investigation is effective to understand the diffraction characteristics of subdiffraction limit optical patterns. It is demonstrated that subdiffraction limit optical patterns offer distinctive features and they are valuable in microscopy applications.

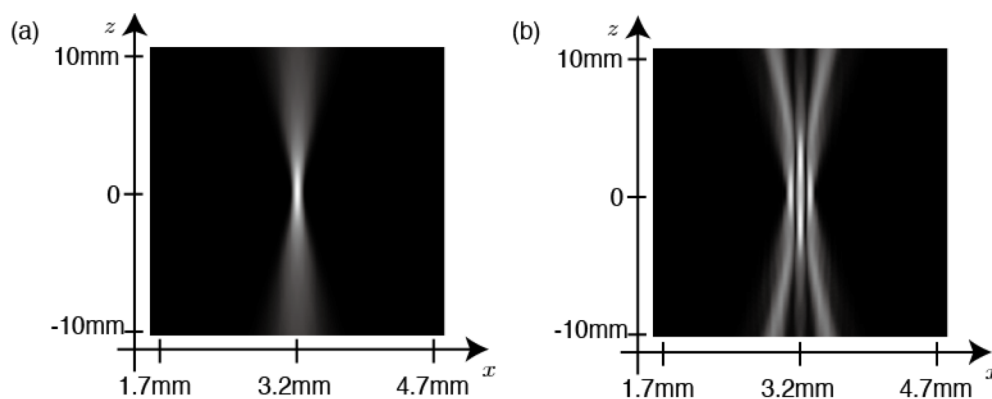


**Fig. 1.** The intensity distribution on the  $xz$ -plane when generating (a) a single subdiffraction limit light sheet and (b) three subdiffraction limit light sheets.

### Acknowledgment

This work was supported by Research Foundation for Opto-Science and Technology and JSPS KAKENHI Grant Number 17H02084.

### References

1. Y. Ogura, M. Aino, and J. Tanida, *Opt. Express*, 22(21), 25196 (2014).
2. Y. Ogura, M. Aino, and J. Tanida, *Appl. Opt.*, 55(23), 6371 (2016).

## **Research activities in KETI**

*Hoonjong Kang*

**Korea Electronics Technology Institute, 11, World Cup buk-ro 54-gil, Mapo-gu, Seoul, South Korea**



# Ghost imaging for single photon counting

Yasuhiro Mizutani<sup>1,2</sup>, Hiroki Taguchi<sup>1</sup>, Yasuhiro Takaya<sup>1</sup>

<sup>1</sup>Dept. of Mechanical Engineering, Osaka University, 2-1 Yamadaoka, Suita, Osaka 5605-0871, Japan

Tel.: 82-6-6879-7319, E-mail: mizutani@mech.eng.osaka-u.ac.jp

<sup>2</sup>JST/ERATO MINOSHIMA Intelligent Optical Synthesizer Project, Japan

**OCIS codes:** (110.1758) Computational imaging; (110.2970) Image detection systems; (030.5260) Photon counting

We propose a novel single pixel imaging based on the Ghost Imaging (GI) in a photon limited imaging. In this paper, in order to obtain image using few photons, the First Photon-detection Time (FPT) is applied to the GI. The proposed signal detection method is able to obtain a signal with only 1 photon. The FPT has variations that are due to a shot noise. Using a correlation, effect of the noise on images is removed. As a result, the GI with FPT (FPGI) was able to obtain high quality image than a conventional imaging method using same photon numbers.

A basic configuration of the FPGI is shown in fig. 1 (a). Random-patterned excitation lights ( $\lambda=560\text{nm}$ ) from a DMD projector (Texas Instruments, DLP Lightcrafter) are projected on a fluorescent sample thorough an objective lens (OLYMPUS, x50, N.A. 0.8). Then fluorescence signals thorough a band pass filter for cutting the excitation light are detected by a photo-multiplier tube (PMT, Hamamatsu: H10682-110). Finally, by analyzing a correlation between the illuminated patterns and the detected signals, a fluorescence image can be detected as a 2D distribution of a correlation efficient. For realizing the ghost image with more high sensitivity, we have used arrival times after excitation as fluorescent signals by using photon counting technique as shown in fig. 1 (b). The time depending on the light power, the ghost image using correlation between the patterns and the time is possible to detect a fluorescent image with weak light intensity.

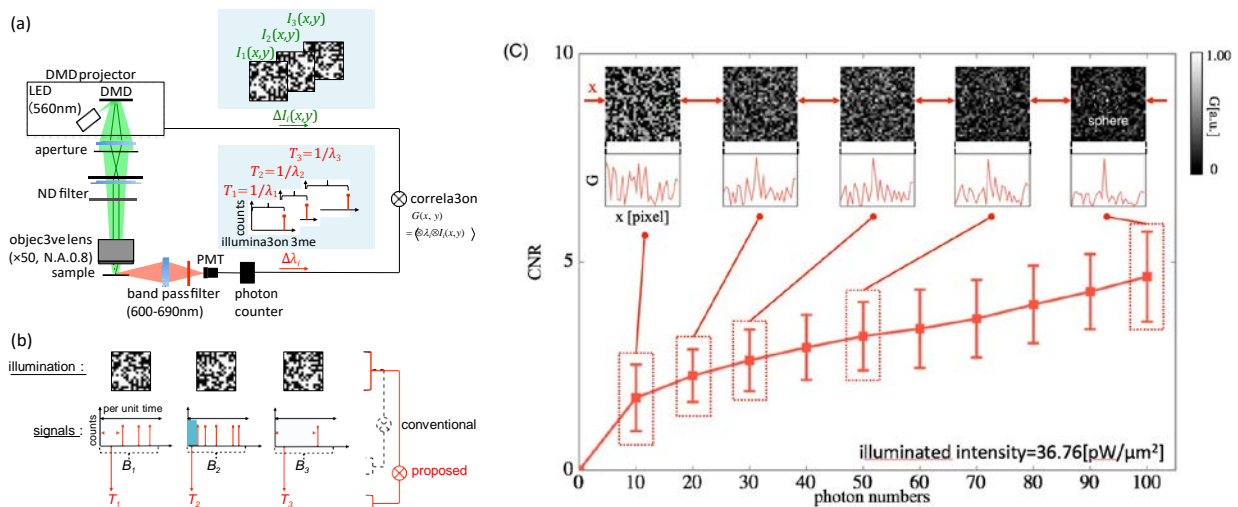


**Fig. 1.** Experimental setup of first photon detection ghost imaging (FPGI) and results. (a) optical configuration, (b) data detection analogy and (c) qualities of fluorescent images using sub 100 photons.

Figure 1(c) shows experimental results of fluorescent microsphere ( $\phi=8\mu\text{m}$ ) images by using the FPGI. To evaluate the images quantitatively, we used the contrast-to-noise ratio (CNR) like visibility<sup>(2)</sup>. As the photon numbers beyond 50 numbers, the image can be detected by using FPGI. Therefore, it has been found that the proposed method is well suited for imaging when photon number is limited.

## References

1. T. B. Pittman, Y. H. Shih, D. V. Strekalov, and A. V. Sergienko, Phys. Rev. A 52, R3429 (1995).
2. K. W. C. Chan, M. N. O'Sullivan and R. W. Boyd, Opt. Express **18**, 5562 (2010).

# Fast calculation of wide viewing angle depth-map computer-generated hologram

Hwi Kim,\*, Sungjae Park, and Jonghyun Lee

Department of Electronics and Information Engineering, College of Science and Technology, Korea University,  
Sejong-Campus, 2511 Sejong-ro, Sejong 30019, Korea

[hwikim@korea.ac.kr](mailto:hwikim@korea.ac.kr)

**OCIS codes:** (090.2870) Holographic display; (090.1760) Computer holography

In this presentation, we introduce our recent research on on-going classical theme of computer-generated holograms (CGHs). The wide-viewing angle depth-map CGH is designed and related idea to enhance computational speed is tested. The wide viewing angle computer-generated hologram (CGH) shows realistic and high-quality holographic three-dimensional (3D) images, and so much attention and research effort have been devoted to develop complex-modulation and full-color CGHs [1-2]. However, the design and fabrication of full-color complex modulation CGH remains challenge and also the computational efficiency of the design of wide viewing angle CGH is still limited. It requires a lot of computational time and great memory. Therefore, fast calculation method is an important key element of CGH research [3].

In this paper, we introduce the localized wide viewing angle depth-map CGH calculation method and check the calculation efficiency enhancement. The localization method is the spatial and frequency domain division of the depth-map image at regular intervals. The sub-division area with non-zero image signal is calculated, if not, the calculation is skipped. The sub CGHs representing the sub-division images are coherently stamped in the CGH plane. The schematic diagram of the process is represented in Fig. 1(a). In Fig. 1(b), it is seen that the computation time decreases as the number of sub-region increases for several cases of CGHs with various resolution. Also, the graph shows that the enhancement of the computational efficiency becomes more vivid with an increase of CGH resolution. It can be said that the ultimate goal of our research is the development of the optimized parallel fast algorithm of the high-definition wide viewing angle depth-map CGH with high quality.

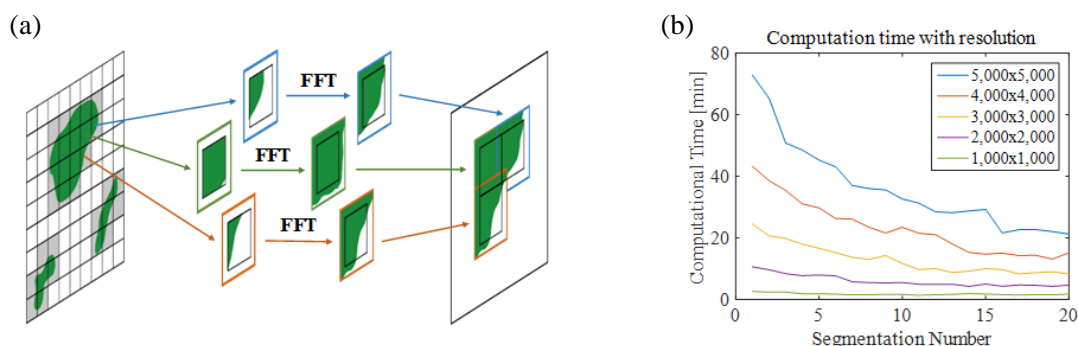


Fig. 1. (a) The schematic diagram of the localized localization method, (b) computation time with resolution

## Acknowledgment

This work was supported by the Industrial Strategic technology development program (10052641, Development of the commercialization platform technology for diffractive optical element based on 3D surface nanostructure for full-color implementation) funded by the Ministry of Trade, industry & Energy (MI, Korea).

## References

1. Y. Tsuchiyama, K. Matsushima, S. Nakahara, and Y. Sakamoto, "Full-Color High-Definition CGH Using Color Filter and Filter Design Based on Simulation," in *Imaging and Applied Optics 2016*, OSA Technical Digest (online) (Optical Society of America, 2016), paper DW5I.4.
2. K. Matsushima and S. Nakahara, "Extremely high-definition fullparallax computer-generated hologram created by the poly-gon-based method," *Applied optics* 48, H54-H63 (2009).
3. J. Cho, J. Hahn, and H. Kim, "Fast reconfiguration algorithm of computer generated holograms for adaptive view direction change in holographic three-dimensional display," *Optics Express*, Vol. 20, No. 27, pp. 28282-28291, (2012).

# Compound-eye imaging for forensics

Yoshinori Akao

Information Sci. Sec., National Research Institute of Police Science, Kashiwa, Chiba 277-0882, Japan

Tel.: 81-4-7135-8001, E-mail: akao@nrrips.go.jp

**OCIS codes:** (110.2970) Image detection systems; (110.4190) Multiple imaging; (120.4630) Optical inspection

Compound-eye imaging system [1] is fascinating since multiple images are captured within single shot whereas each image has different properties. It is so versatile that the field of forensics are also included within its application range. In this presentation, we show examples of efficient gonio-imaging [2] by compound-eye imaging system for forensic document examination.

Fig. 1(a) describes compound-eye imaging system for the examination of holograms [3]. It has four (2 by 2) compound eyes which captures sample images at different observation angles. With the combination of illuminating light sources at 12 directions achieved gonio-imaging at 48 kinds of geometries. Objective lens placed at its focal length from sample surface made the diffraction light from hologram sample quasi-parallel. Compound-eye lens on image sensor resulted in four images with different diffraction angles. The result showed different color of diffracted light was imaged at each individual eye. The system is small-sized and handheld. All optical end electronic devices are in the housing, therefore hologram inspection outside of dark room was enabled.

Fig. 1(b) shows compound-eye imaging system for the examination of handwritings [4]. Compound-eye camera (Pi Photonics, TOMBO USB3.0), which has nine (3 by 3) individual eyes with 1.2 mm interval between adjacent compound-eye, was used for the acquisition of compound-eye image. In front of the camera, coaxial illumination module (Optomecha Engineering, DRS-5) was installed. The gloss specular reflection was observed at the bottom or side wall of handwritten strokes in nine individual images of a compound-eye image.

Multi-angle imaging that captures reflected light at different angle were achieved based on compound-eye optical systems. It is one of the promising application to examine holograms or handwritings in the field of forensic document examination. High resolution imaging and zooming remain as future works.

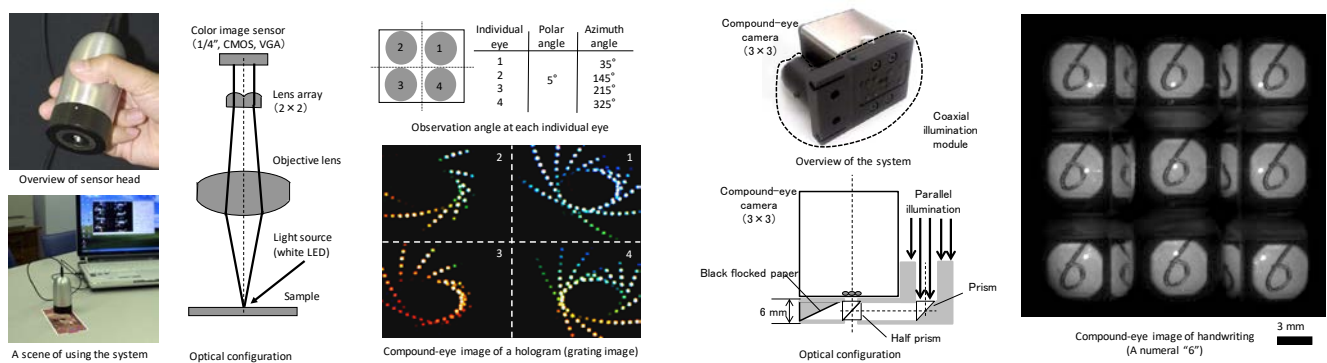


**Fig. 1. Compound-eye imaging for forensic examination: (a) hologram, (b) handwriting.**

## Acknowledgment

Author express gratitude to Prof. Tanida of Osaka University for his supervising in the development of systems. A part of this work was supported by JSPS KAKENHI Grant Number 15K00260.

## References

1. J. Tanida *et al.*, Appl. Opt., 40, 1806 (2001).
2. Y. Akao *et al.*, Opt. Exp., 19, 3353 (2011).
3. Y. Akao *et al.*, Proc. JSAP-OSA Joint Symposia 2015, 15p-2F-14 (2015).
4. Y. Akao, Proc. DHIP2016, 186 (2016).

### 3D display making light field inside volume

*Joonku Hahn*

School of Electronics Engineering, Kyungpook National University, 80 Daehak-ro, Buk-gu, Daegu 41566, South Korea

Tel.:82-53-950-5514, E-mail: [jhahn@knu.ac.kr](mailto:jhahn@knu.ac.kr)

OCIS codes: (100.6890) Three-dimensional image processing; (220.0220) Optical design and fabrication.

In general, light field is formed by integral imaging [1] and it resembles Talbot image as shown in Fig. 1(a). Directional displays covering closed surface makes light field inside volume [2] and they can be categorized according to the location and convergence of projection optics. When the projection optics are aligned along a circle [3,4] the light field is formed as shown in Fig. 1(b). The light fields with converging optics [5,6] and diverging optics [7] are the same inside volume as shown in Figs. 1(c) and (d).

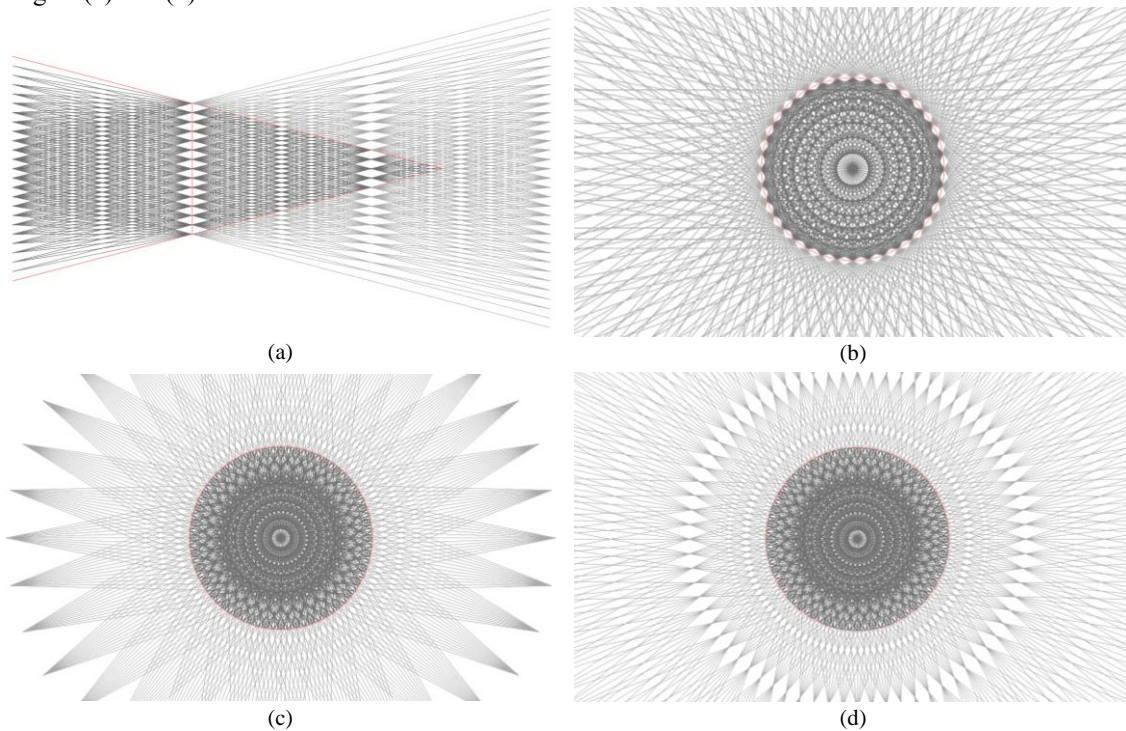


**Fig. 1. Light fields from (a) planar and (b) cylindrical alignment of projection optics. Light fields from rotation of (c) converging and (d) diverging projection optics.**

#### Acknowledgment

This work was supported by Samsung Research Funding Center of Samsung Electronics under Project Number SRFC-IT1301-07.

#### References

1. J. Hahn, Y. Kim, and B. Lee, "Uniform angular resolution integral imaging display with boundary folding mirrors," *Appl. Opt.* **48**, 504-511 (2009).
2. H. Kim, J. Hahn, and B. Lee, "Image volume analysis of omnidirectional parallax regular-polyhedron three-dimensional displays," *Optics Express* **17**, 6389-6396 (2009).
3. G. Choi, H. Jeon, H. Kim and J. Hahn, "Cylindrical directional display with multiple spinning slits," The 16th International Meeting on Information Display, Jeju, Korea, P2-65, Aug. 2016.
4. M. Jung, C. Lee, S. Lim and J. Hahn, "Computation of elemental images in convexly curved lenticular display," The 16th International Meeting on Information Display, Jeju, Korea, P2-67, Aug. 2016.
5. Y. Lim, K. Hong, H. Kim, H.-E. Kim, E.-Y. Chang, S. Lee, T. Kim, J. Nam, H.-G. Choo, J. Kim, and J. Hahn, "360-degree tabletop electronic holographic display," *Optics Express* **24**, 24999-25009 (2016).
6. D. Heo, M. Kim, G. Choi, and J. Hahn, "Full parallax crystal ball three-dimensional display," The 17th International Meeting on Information Display, Busan, Korea, F46-4, Aug. 2017.
7. K. Kim, S. Lim, H. Kim and J. Hahn, "Full-color tabletop light-field display," Digital Holography and Three-Dimensional Imaging, Heidelberg, Germany, paper DT4D.5, July 2016.



# Nanoscale character extraction for nano-optical metric system

Naoya Tate

Dept. of Electrical Engineering and Computer Science, Kyushu University,  
Fukuoka, Nishi-ku, 744 Motooka, Japan

Tel.: 81-92-802-3694, E-mail: tate@ed.kyushu-u.ac.jp

**OCIS codes:** (060.4785) Optical security and encryption; (200.3050) Information processing; (350.4238) Nanophotonics and Photonic crystals

Recently, we investigated the realization of advanced physical security that we defined as *nano-optical metrics* [1]. In the case of the simplest setup consisting of a sample and a reader, their performance is affected by technological difficulty in duplicating nanoscale structures and fundamental impossibility of estimating the characteristic behavior of optical near-field interactions [2] between the sample and the reader. In order to experimentally demonstrate our concept, it is necessary to realize the stable detection of nanoscale fluctuations due to optical near-field interactions and to appropriately define their characteristics for the development of our original authentication algorithm. In this paper, we mainly focus on the latter topic. Firstly, for mathematical demonstration, the signal detection via the optical near-field interactions is modeled and the corresponding nanoscale fluctuations are calculated. Then, the characteristics are quantitatively defined for further studies.

The prototype setup of nano-optical metrics is based on non-scanning near-field optical microscopy (NOM). In the field of nano-photonics, the probe is continuously fluctuated to maintain the distance between the sample. During the fluctuations, based on the size resonance effect of optical near-field interaction [3], various scales of interactions between the probe and the target are sequentially induced. This means that only by fluctuations on a single detection point, the probe induces interactions between not only the structure just beneath it but also the surrounding structures on the sample. Therefore, readout signals during the fluctuations are expected to include some information about spatial structures of the sample. This is one of the most important matters of nano-optical metrics, because the precise scanning process is not suitable for actual use as a common security system.

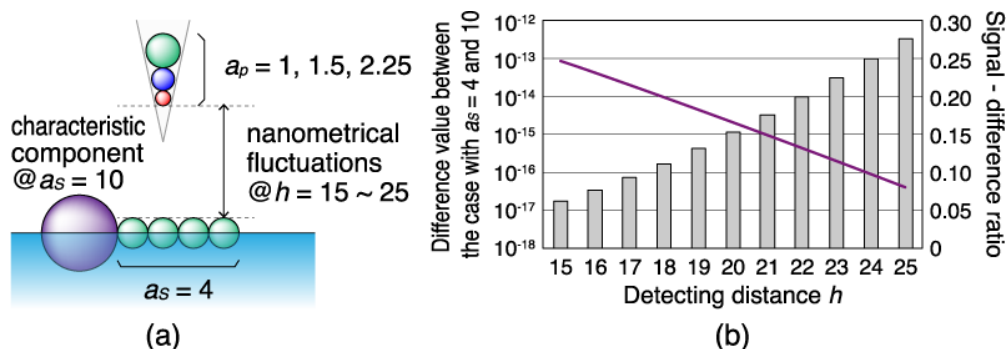


**Fig. 1. (a) A model of nano-scale fluctuations between the sample and the probe, which is modeled using a combination of spheres. (b) Detecting distance dependency of the calculated interactions.**

Figures 1(a) and (b) show one of the simplest model of optical near-field interactions and the calculated results with some variations in the detecting distance between the sample and the probe. Results in Fig. 1(b) indicates that while one of the five similar spheres were displaced by another sphere with a different size, as shown in Fig. 1(a), some clear differences are surely obtained during the fluctuations. As further studies, we are now discussing the definition of their characteristics and development of our original authentication algorithm based on the definition. *This work was supported by JST KAKENHI Grant Number JP17K14125.*

## References

1. N. Tate, et al., *Appl. Phys. A*, Vol. 121, Issue 4, pp. 1383-1387 (2015).
2. M. Ohtsu, *Dressed Photons—Concepts of Light-Matter Fusion Technology* (Springer, Berlin, 2013).
3. S. Sangu, et al., *J. Microscopy*, Vol. 202, pp. 279-285 (2001).



# Reflective-type reconfigurable digital hologram panel using $\text{Ge}_2\text{Sb}_2\text{Te}_5$ phase change material

Seung-Yeol Lee<sup>1</sup>

<sup>1</sup>School of Electronics Engineering, Kyungpook National University, Bukgu, Daegu 702-701, Republic of Korea  
Tel.:82-53-950-6608, E-mail: seungyeol@knu.ac.kr

**OCIS codes:** (240.6680) Surface plasmons; (280.4788) Optical sensing and sensors; (310.6628) Subwavelength structures, nanostructures

Recently, digital hologram using various spatial light modulators (SLMs) has been reported for developing a dynamic hologram movie system. For a high-resolution hologram image with wide viewing angle, an optical modulating device below 1~2  $\mu\text{m}$  scale pixel pitch are needed which has reconfigurable or tunable characteristic. According to our previous works, both reconfigurable characteristic and high compactness of 1  $\mu\text{m}$  scale pixel pitch have been simultaneously achieved by using a thermally-driven phase change material,  $\text{Ge}_2\text{Sb}_2\text{Te}_5$  (GST) [1]. It has been known that the reflection spectrum of thick GST is usually gray due to its broadband highly loss characteristics. However, the ITO-GST-ITO composite layer can provide its own structural color depends on the thickness of surrounding ITO, when a multiple reflection inside the ITO cavity is enhanced due to the Fabry-Perot (FP) resonance. When such kind of composite layer is applied, diffraction efficiency caused by phase change of thin GST region was dramatically enhanced and absorption characteristic caused by GST layer is also increased [2].

Based on an absorption resonance of ITO-GST-ITO composite layer, a reconfigurable digital hologram with 1  $\mu\text{m}$  scale can be written by excimer laser lithography on thin ITO-GST-ITO composite film. We also find that FP resonances of dielectric layer have significant role for determining the optimized GST film location, and by using such characteristics, it is also possible to make the light illuminating to digital holography pattern can be diffracted wavelength-selectively. Numerical simulations based on rigorous coupled wave analysis (RCWA) has been shown to find the appropriate location of thin GST film within the dielectric layer.

Moreover, nano-slit structure that can sustain surface plasmon polaritons (SPPs) has been numerously researched for shaping the subwavelength-scale optical signals. For example, increasing the intensity of light passing through the nano-slit is quite important to improve the performance of light detection using the nano-slit. Therefore, methods for optical reflection phase control within subwavelength size unit pixel using phase change materials (PCMs) and plasmonic metasurfaces are quite important for developing novel type of 3D optical imaging system. Diffractive optical systems such as PCM-based hologram panel, plasmonic metalens, and polarization multiplexing techniques of surface plasmon polaritons will be presented.

## Acknowledgment

This work is supported by the National Research Foundation of Korea and the Ministry of Science and ICT (NRF-2017R1C1B2003585).

## References

1. S.-Y. Lee, Y.-H. Kim, S.-M. Cho, G. H. Kim, T.-Y. Kim, H. Ryu, H. N. Kim, H. B. Kang, C.-Y. Hwang, and C.-S. Hwang, *Sci. Rep.* 7, 41152 (2017).
2. P. Hosseini, C. D. Wright and H. Bhaskaran *Nature* 511, 206–211 (2014).
3. S.-Y. Lee, H. N. Kim, Y.-H. Kim, T.-Y. Kim, S.-M. Cho, H. B. Kang, and C.-S. Hwang, *ETRI J.* 39, 3, 390-397, (2017).

## Unstained tumor detection in digestive organs based on autofluorescence spectroscopy

*Hidenobu Arimoto<sup>1</sup>, Keiichiro Kagawa<sup>2</sup>, Yoji Sanomura<sup>3</sup>, Shigeto Yoshida<sup>4</sup>, and Shinji Tanaka<sup>3</sup>*

<sup>1</sup>Electronics and Photonics Research Institute, National Institute of Advanced Industrial Science and Technology, Tsukuba, Ibaraki 305-8565, Japan

<sup>2</sup>Research Institute of Electronics, Shizuoka University, Hamamatsu, Shizuoka 432-8011, Japan

<sup>3</sup>Department of Endoscopy, Hiroshima University Hospital, Hiroshima, Hiroshima 734-8551, Japan

<sup>4</sup>Department of Gastroenterology, JR Hiroshima Hospital, Hiroshima, Hiroshima 732-0057, Japan  
Tel.:81-29-861-7880, E-mail: arimoto-h@aist.go.jp

**OCIS codes:** (170.0170) Medical optics and biotechnology; (170.6280) Spectroscopy, fluorescence and luminescence; (170.2150) Endoscopic imaging

Early detection of the tumors in digestive organs is quite important for the better prognosis. In the endoscopic diagnosis, narrow band imaging (NBI) is widely used. NBI investigates angiogenesis patterns using particular spectral band for the illumination light so that the angiogenesis is clearly seen. However, earlier detection of the tumor is possible if we can measure the metabolic change which is caused by the tumor cell divisions. For this purpose, we focus our attention on the coenzymes NADH and FAD those density ratio change according to the oxygen partial pressure in an organ. The ratio of NADH and FAD is estimated from their autofluorescence spectra, and the tumor region is determined by the REDOX index which is defined as the intensity ratio of the autofluorescence intensities.

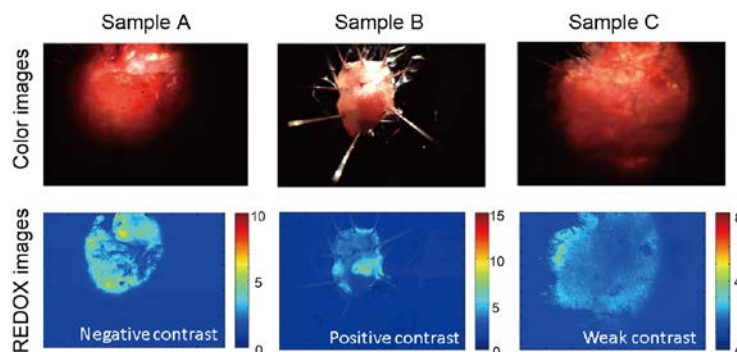


**Fig. 1. Example of the REDOX images for the digestive tumor detection.**

In a tumor cell, NADH increases while FAD decreases compared to the normal cell. Then we use two excitation wavelengths 365 and 405 nm; 365 nm excites almost only NADH while 405 nm excites both NADH and FAD. Hence the intensity ratio [365 nm ex.]/[405 nm ex.] (ratio REDOX index) is expected to increase in the tumor region. Lower images in Figure 1 are the 2D map of the REDOX index (REDOX image), expecting the tumor region appears bright. Sample A, B, and C are the resected digestive tissues including tumor in their middle areas. The REDOX image of sample B indicates the tumor region with the bright area as we expected. We took 32 REDOX images in total, and 78% of the REDOX images show the positive contrast. However the REDOX images of sample A and C have the negative contrast and weak contrast, respectively, probably because of the appearance of the collagen in the lower layer of the tissue. More precise determination may be possible by introducing additional parameters.

### References

1. H. Arimoto, A. Iwata, K. Kagawa, Y. Sanomura, S. Yoshida, S. Kawahito, and S. Tanaka, Proc. SPIE 10068, Imaging, Manipulation, and Analysis of Biomolecules, Cells, and Tissues XV, 100681L (2017).
2. M. Ozaki, K. Kagawa, H. Arimoto, Y. Kominami, Y. Sanomura, S. Yoshida, M-W. Seo, S. Kawahito, and S. Tanaka, 2015 37th Annual International Conference of the IEEE Engineering in Medicine and Biology Society (EMBC), 5879 (2015).

## Recent progress on 3D target tracking using optical scanning holography

**Taegeun Kim**

*E-mail: takim@sejong.ac.kr*

**Dep. of Electrical Eng., Sejong Univ. Korea**

**OCIS codes:** (090.1995) Holography; (070.0070) Fourier optics and signal processing

Three-dimensional (3D) target tracking using optical scanning holography (OSH) has a long standing history [1-5]. In first generation, we propose an algorithm based on Wigner distribution analysis, which extracts depth location of a matched object without searching process.[1,2] However, this technique is limited to the 3D location extraction of the 3D matched object and the 3D matching process is not robust to rotation and distortion of the target object. In second generation, an algorithm which extracts depth location of an object without prior knowledge of target object [3,4]. In the proposed algorithm, we first record the complex hologram of a target object using OSH. After that, we synthesize a real-only spectrum hologram and extract the depth location of the object using Wigner distribution or axis transformation after power-fringe adjusted filtering. [3,4] Figure 1,2. show OSH that records the complex hologram of an object and the flow chart that extracts the depth location of the object. This makes it possible to extract the depth location of an object without prior knowledge. Using the depth location, we get the focused image of the object by digital refocusing. Here we note that hologram contains information of depth as well as lateral distributions of an object as a form of fringe pattern and the phase of a complex hologram recorded by OSH in incoherent mode is not contaminated by speckle noise. This make the fringe analysis of the hologram recorded by OSH give the depth location of a target object and focused image without prior knowledge. Meanwhile, in computer vision area, rotation and distortion invariant image recognition algorithms have been proposed. However, these rotation and distortion invariant features extraction techniques are limited to 2D because the object's image is the projection of a 3D object onto 2D plane and does not contain depth information. Recently, we propose a 3D target recognition and tracking technique[5]. This composes two stages. One is feature extraction stage and the other is recognition and location extraction stage. In the feature extraction stage, we first record the complex hologram of a reference object using OSH. Second, we extract the depth location of the object by searching the focused depth using sharpness function metric. Third, we recover the 2D image of the object by reconstructing the hologram using the depth location. Fourth, we extract the features of the object using SURF(speeded up robust feature) algorithm.

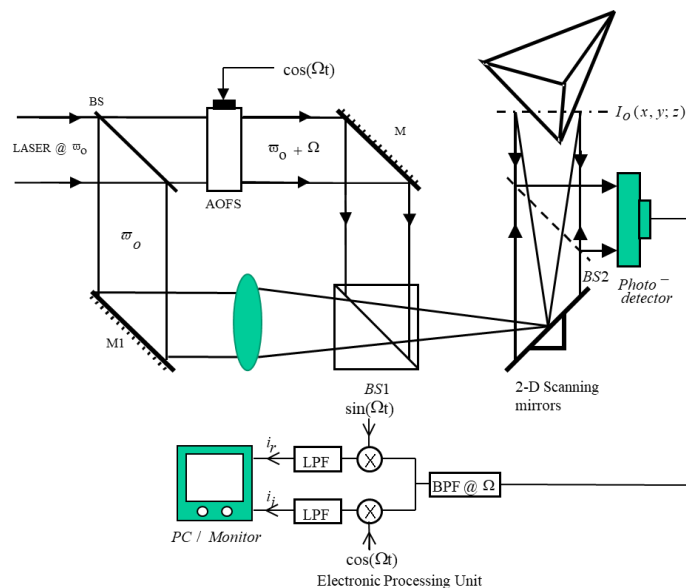


Fig. 1. Optical Scanning Holography (BS: beam splitter, M: mirror)

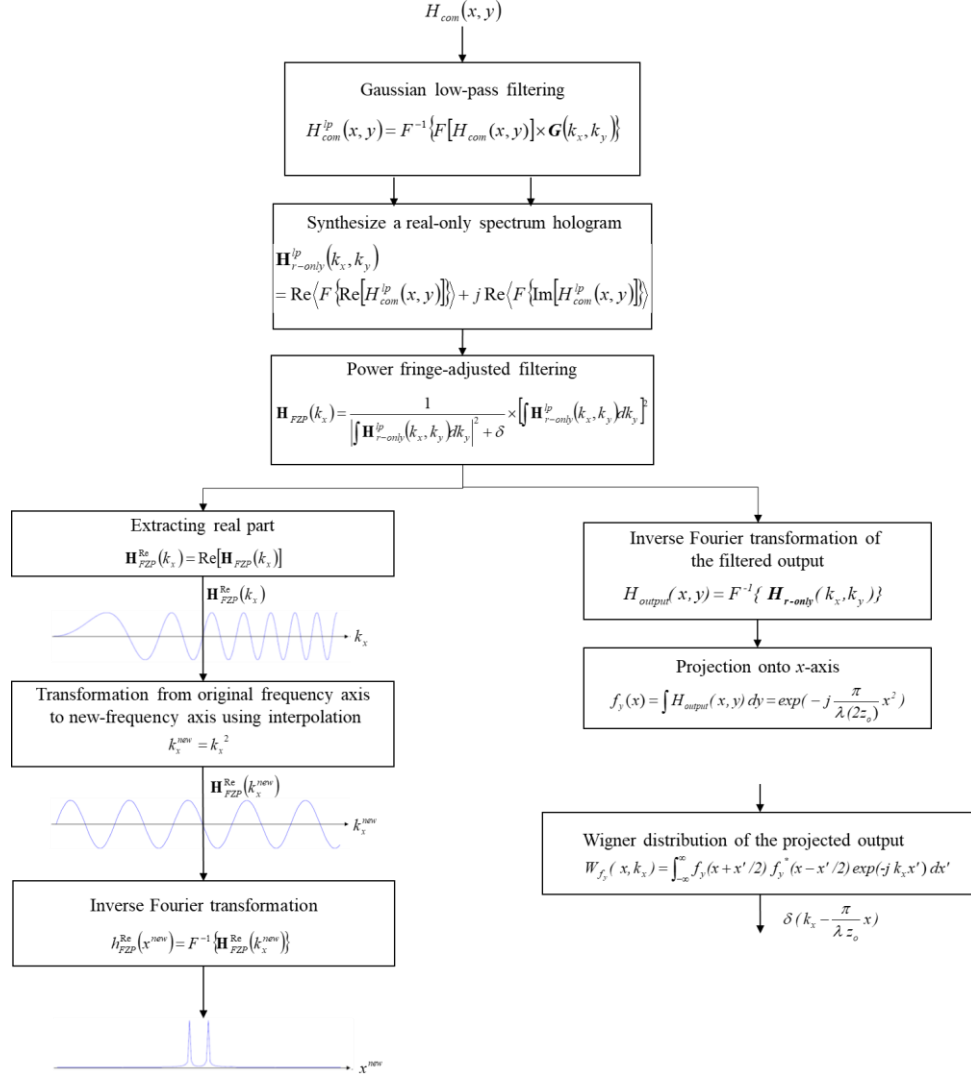


Fig. 2. Depth detection algorithm [3,4]

In the recognition and location extraction stage, first we record the complex hologram of a target object using OSH. After that, we extract the depth location by searching algorithm and matches features of the target object using SURF algorithm. Matching the features of the reference and target objects gives the lateral location of the matched object. This gives the lateral location of the rotation and distortion invariantly recognized target object. Including the depth location of the target object extracted in the depth searching process, finally, we extract 3D location of recognized target object.

### Acknowledgment

This research was supported by the MSIT(Ministry of Science and ICT), Korea, under the ITRC(Information Technology Research Center) support program(IITP-2017-2015-0-00448) supervised by the IITP(Institute for Information & communications Technology Promotion)

### References

1. T. Kim and T.-C. Poon, *Opt. Eng.*, 38(12), 2176 (1999).
2. T. Kim and T.-C. Poon, *J. Opt. Soc. Am.*, 17(12), 2025 (2000).
3. T. Kim and T.-C. Poon, *Opt. Eng.*, 41(6), 1331 (2002).
4. T. Kim and Y.-S. Kim, *JOSK*, 14(2), 104 (2010).
5. U.-J. Lee, Y.-S. Kim and T. Kim, *Proc. of Photonics Conference 2016*, 287, (2016).

# Multi-frequency swept *en-face* optical coherence microscopy with supercontinuum comb for in-vivo measurement of inner ear

Samuel Choi<sup>1,4</sup>, Fumiaki Nin<sup>2,4</sup>, Takeru Ota<sup>2,4</sup>, Keita Sato<sup>3</sup>, Takamasa Suzuki<sup>3</sup> and Hiroshi Hibino<sup>2,4</sup>

1 Niigata University, Department of Electrical and Electronics Engineering, Niigata, Japan

Tel.: 81-25-262-6761, E-mail: schoi@eng.niigata-u.ac.jp

2 Niigata University, School of Medicine, Department of Molecular Physiology, Niigata, Japan

3 Niigata University, Graduate School of Science and Technology, Niigata, Japan

**OCIS codes:** (180.3170) Interference microscopy; (110.4500) Optical coherence tomography; (170.3880) Medical and biological imaging; (120.7280) Vibration analysis

A variety of optical coherence tomography (OCT) techniques are being widely adopted for imaging cross-section and vibrational distributions in subsurface tissue [1]. As concrete examples, the phase-sensitive spectral domain (SD)-OCT [2], and swept-source (SS)-OCT [3] have been developed for measuring high-speed vibrations from various surfaces within the organ of Corti and the tympanic membrane. However, these techniques involve scanning single measurement points along the two lateral dimensions based on fiber-optic OCT. Therefore, conventional SS-OCT and SD-OCT cannot simultaneously measure the wide-range dynamics of bio-tissues, which is thought to be crucial for elucidating the biomechanics. To address this issue, tomographic wide-field vibrometry, which we term “multifrequency swept optical coherence microscopic vibrometry[4]” (MS-OCMV) has been developed. The irradiation power in MS-OCMV was insufficient to detect the reflection from the organ of Corti (sensory epithelium) due to lack of output power of the super luminescent diode (SLD) employed as a light source. In this paper, we report the improvement of MS-OCMV system employing a supercontinuum (SC) light source instead of SLD. In-vivo *en-face* OCT and vibrational measurements of guinea pig sensory epithelium in organ of Corti were successfully conducted as shown in Fig. 1(b). The effective depth scan range and the imaging resolution in the OCT mode were approximately 980  $\mu\text{m}$  and 1.8  $\mu\text{m}$ , respectively. 3-D volume data acquisition speed was 2Gvoxel/sec. In the vibrometry mode, the vibration distributions with the sinusoidal sound inducing of 15-25 kHz, 90 dBspl were imaged on the microscopic *en-face* images. The effective detectable vibrational amplitude was approximately 10 nm in the *in-vivo* measurement.

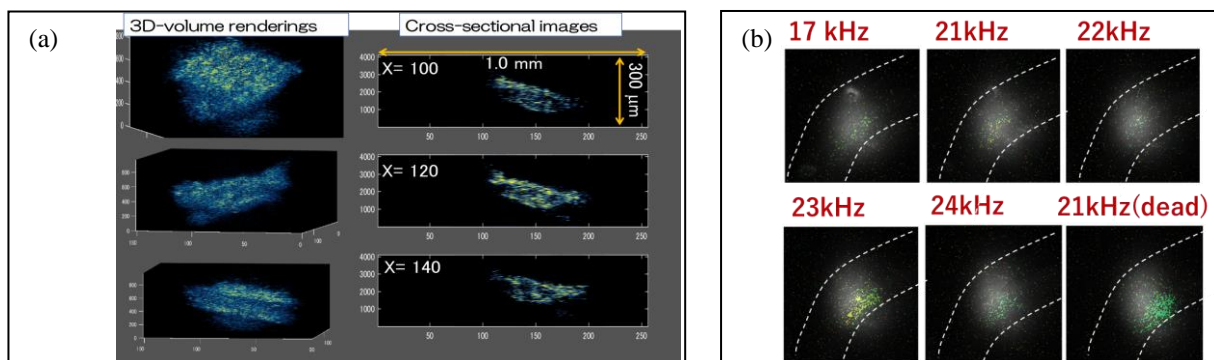


**Fig. 1** *In-vivo* measurement results, (a) 3D volume and (b) vibration distributions of sensory epithelium.

## Acknowledgment

This work was supported by AMED-CREST, AMED, Grant-in-Aid for Scientific Research (B) (16H03164) and Grant in-Aid for Young Scientists (A) (15H05683).

## References

1. N. Choudhury, et al., *Hear. Res.* 220(1-2), 1–9 (2006).
2. S. S. Gao, et al., *J. Neurophysiol.* 112(5), 1192–1204 (2014).
3. D. MacDougall, et al., *Opt. Express* 7(11), 4621–4635 (2016).
4. S. Choi, et al., *Biomed Opt. Express* 8(2), 608–621 (2017).



## Polarization Color Display Using Index Matching

*Toshiki Matsuzaki, Huangyi Qin and Kenji Harada*

Dept. of Computer Science, Kitami Institute of Technology, 165 Koen-cho, Kitami, Hokkaido 090-8507, Japan

Tel.: 81-157-26-9357, E-mail: m1652400113@std.kitami-it.ac.jp

**OCIS codes:** (260.1440) Birefringence; (260.5430) Polarization; (330.1690) Color;

The polarization color is displayed by sandwiching the retarder film between two polarizer and by incidence of white light. The color tone varies depending on the arrangement angle of the retarder film and the stacking number of the retarder films. In the conventional polarization color display, the difference in the number of retarder films is observed as a difference in transmittance without using a polarizer, and there is a possibility that a display image is guessed. This causes loss of pleasure and wonder when you see the images, which is an advantage of polarization color display. Also, when applying polarization color to the art field, it will cause harm to the color of the work.

Therefore, in this research, we propose a method of index matching using optical adhesive and make the transmittance uniform. Optical adhesives have high transmittance and refractive index matching and are known to be suitable for bonding optically precise instruments such as optical fibers. It also cures rapidly by ultraviolet irradiation (sunlight, UV light, etc.). The transmittance when using the optical adhesive was measured using a spectrophotometer and compared with the conventional polarization color display. Also, it was applied to a polarization color display in which no difference in the number of retarder films was observed.

The refractive index of the optical adhesive used in this research is 1.56. The refractive index of the retarder film used is 1.58. The transmittance  $T[\%]$  when light incidents a substance with a refractive index  $n_a$  from a substance with a refractive index  $n_b$  is calculated by

$$T = \left(1.0 - \left|\frac{n_a - n_b}{n_a + n_b}\right|^2\right) \times 100. \quad (1)$$

Therefore, the transmittance when light incidents the air from the retarder film is about 94%. On the other hand, the transmittance when light incidents the optical adhesive from the retarder film is about 99%. Therefore, by adhering the retarder films with the optical adhesive, the transmittance is improved. Figure 1 show a state of 1 to 10 quarter wave retarder films stacked and observed. The numbers in the figure 1 indicate the number of films. Compared to Fig. 1(a), Figure 1(b) shows that the transmittance of the portion with a large number of retarder films is improved and it is difficult to observe the difference of the stacking number of retarder films. Also, Figure 1(c) and 1(d) shows that the optical adhesive does not affect the polarization color. Figure 2 shows a graph obtained by measuring the transmittance when white light is incident. Without the optical adhesive, the transmittance decrease from 90.2% to 30.0% by stacking 10 retarder films. On the other hand, when the optical adhesive is used, a high transmittance of 81.6% is maintained with 10 retarder films. The transmittance when stacking the retarder films were improved using index matching by the optical adhesive. In this presentation, we will also exhibit polarization color art using this transmittance improvement method.

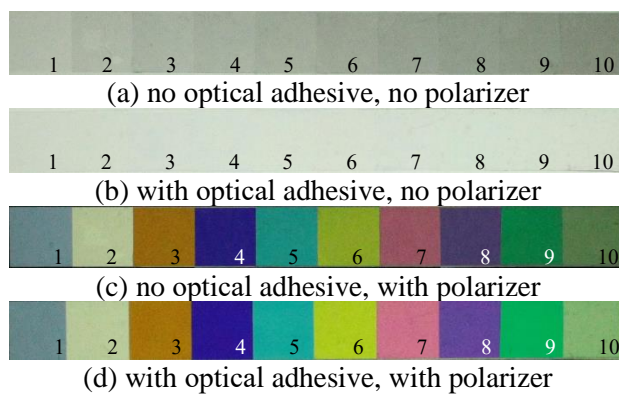


**Fig. 1. Transmission state of retarder films**

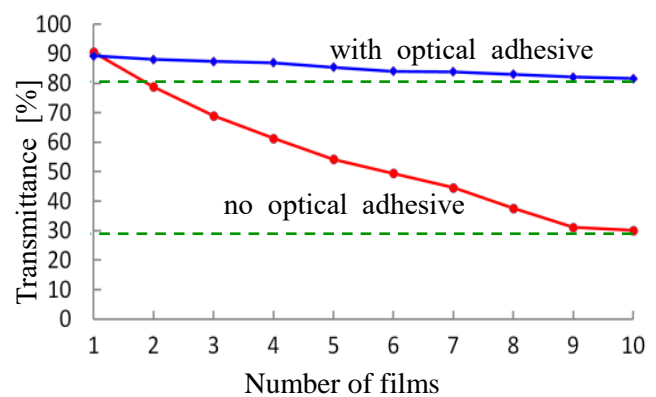


**Fig. 2. Transmittance of each number of films**

## Polarization color optimization of birefringent material

*Huangyi Qin, Toshiki Matsuzaki and Kenji Harada*

Dept. of Computer Science, Kitami Institute of Technology, 165 Koen-cho, Kitami, Hokkaido 090-8507, Japan

Tel.:81-0157-26-9357, E-mail: m1752400132@std.kitami-it.ac.jp

**OCIS codes:** (260.1440) Birefringence; (260.5430) Polarization; (330.1690) Color;

Retarder film exhibits polarization color by polarizer. We propose a method that uses waveplate and polarizers to display polarization color. The output color can be designed hardly by mathematic way analytically. Because the calculation contains invertible functions which make the computation of output color unsolvable. To make this color design possible, we introduce differential evolution algorithm.

Jones Matrix is a proper tool for discrimination of interference color phenomena. A retarder can be described as below by Jones Matrix.

$$M(\theta, \lambda) = \begin{pmatrix} \cos \theta & -\sin \theta \\ \sin \theta & \cos \theta \end{pmatrix} \begin{pmatrix} e^{-i\frac{\pi R}{\lambda}} & 0 \\ 0 & e^{i\frac{\pi R}{\lambda}} \end{pmatrix} \begin{pmatrix} \cos \theta & -\sin \theta \\ \sin \theta & \cos \theta \end{pmatrix}$$

$R$  is retardation of the retarder and  $\lambda$  is incident light's wavelength.

$$M_{out} = M_n \cdot \dots \cdot M_2 \cdot M_1$$

$$T(\theta_{M_n}, \dots, \theta_{M_2}, \theta_{M_1}, \lambda) = \begin{pmatrix} 1 & 0 \\ 0 & 0 \end{pmatrix} \cdot M_{out} \cdot \begin{pmatrix} 0 & 0 \\ 0 & 1 \end{pmatrix} = (M_{out})_{1,2}$$

$$X = \frac{\int_{380}^{780} S(\lambda) \cdot T(\dots, \lambda) \cdot x(\lambda) d\lambda}{\int_{380}^{780} S(\lambda) \cdot y(\lambda) d\lambda}, Y = \frac{\int_{380}^{780} S(\lambda) \cdot T(\dots, \lambda) \cdot y(\lambda) d\lambda}{\int_{380}^{780} S(\lambda) \cdot y(\lambda) d\lambda}, Z = \frac{\int_{380}^{780} S(\lambda) \cdot T(\dots, \lambda) \cdot z(\lambda) d\lambda}{\int_{380}^{780} S(\lambda) \cdot y(\lambda) d\lambda}$$

To optimize  $\theta_{M_n}, \dots, \theta_{M_2}, \theta_{M_1}$  by given XYZ we introduce differential evolution algorithm (DE). DE is similar to genetic algorithm (GA) which has steps of mutation, recombination and selection. Comparing to GA, DE's mutation has a very simple form as equation (3). Recombination described as equation (4). Selection is showed as equation (5).

$$v = g_1 + F(g_2 - g_3) \dots \dots \dots (3)$$

At equation (3),  $g_1, g_2$  and  $g_3$  are individuals chosen from the population group.  $F$  is constant called mutation factor.  $v$  is the mutated target.

$$u_j = \begin{cases} v_j & \text{if rand}[0,1] \leq CR \text{ or } j = \text{randint}[0, \text{dim}] \\ g_{1,j} & \end{cases} \dots \dots \dots (4)$$

At equation (4),  $j$  is the index of data dimension. In our previous research, we thought to use 5 retarder films is proper choice. Thus, the data here have 5 dimensions of each film's rotation angle. CR is called crossover ratio.

$$\text{new } g_1 = \begin{cases} u & \text{if } f(g_1) < f(u) \\ g_1 & \end{cases} \dots \dots \dots (5)$$

At equation (5),  $f$  is the fitness function which here is squared error of given XYZ.

### References

1. K. Harada, D. Sakai, Y. Sone, Y. Harada and S. Kamemaru, Jpn. J. of Appl. Phys. Education, 34 (2010) 35-40 [in Japanese].
2. Storn, R.; Price, K. Journal of Global Optimization. 11: 341-359 (1997)

# Object recognition through a multi-mode fiber based on machine learning

Ryosuke Takagi, Ryoichi Horisaki and Jun Tanida

Graduate School of Information Science and Technology, Osaka University,  
1-5 Yamadaoka, Suita, Osaka 565-0871, Japan

Tel.: +81-6-6879-4398, E-mail: r-takagi@ist.osaka-u.ac.jp

**OCIS codes:** (060.2350) Fiber optics imaging; (070.5010) Pattern recognition; (110.0113) Imaging through turbid media; (110.1758) Computational imaging;

Sensing and control of light in optically scattering media like in vivo biological tissues have been important problems. Against these problems, researchers have proposed many approaches based on structured illumination [1], integral photography [2], estimating the scattering process [3] and so on. These methods are effective, but they require complex setups like requirements of a reference light, multiple measurements or heavy computational costs for the reconstruction.

In this study, we propose a machine-learning-based approach for object recognition through a multi-mode fiber (MMF), which is known as a strongly scattering medium. In this case, optical setup is simpler because of a single-shot measurement and the computational costs are mitigated by omitting the reconstruction process. The method consists of training and test processes. In the training process, speckle patterns from face and non-face objects in the training database are provided for the classifier based on machine learning. In the test process, unknown speckle patterns are categorized into the two classes of the face and non-face. The support vector machine (SVM), adaptive boosting (AB), neural network (NN) were used to compare their efficiencies [4].

The optical setup in our experimental demonstration is shown in Fig. 1. Object images are displayed on a spatial light modulator (SLM). The SLM is illuminated with a collimated beam from a laser diode. The intensity patterns after propagating through the MMF are captured with an image sensor without reference light. In the training process, the radial basis function was applied to the SVM. The number of weak learners in the AB was 500. The NN had one hidden layer with ten nodes and it was constructed based on the back-propagation method.

The graph in Fig. 2 shows the relationship between the number of sampling pixels in a speckle pattern and the accuracy rate of the binary classification with the three algorithms. In this case, the number of training pairs of the objects and speckles was 2000 (face class: 1000, non-face class: 1000). The number of the test pairs was 400 (face class: 200, non-face class: 200). The accuracy rates at the 800 sampling pixels of the SVM, the AB, the NN were 92.2%, 87.7% and 89.1%, respectively. The accuracy rates of the SVM were the best in any case.

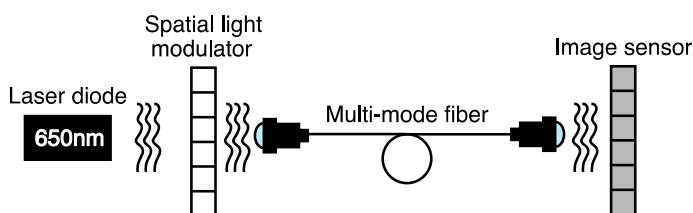


Fig. 1. Optical setup.

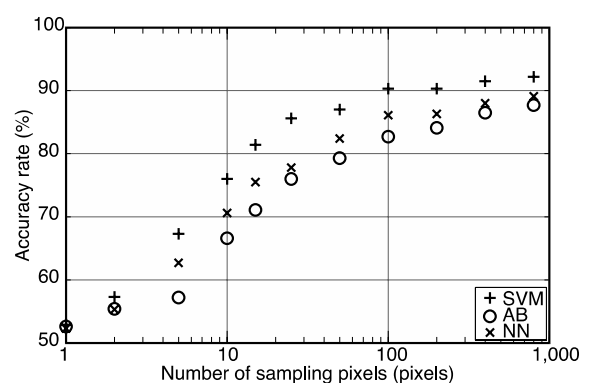


Fig. 2. Accuracy rate with each number of sampling pixels.

## References

1. V. Durán. *et al.*, *Opt. Express* 23, 14424-14433 (2015).
2. M. Cho and B. Javidi, *Disp. Technol. J.* 6, 544-547 (2010).
3. M. Kim. *et al.*, *Opt. Express* 23, 12648-12668 (2015).
4. R. Takagi. *et al.*, *Opt. Rev* 24, 117-120 (2017).

## Spectral imaging based on single pixel camera

*Ryo Sato, Kazuki Ota and Yoshio Hayasaki*

Center for Optical Research and Education (CORE), Utsunomiya University

7-1-2 Yoto, Utsunomiya 321-8585, Japan

Tel.: +81-28-689-7128, E-mail: sato\_ry@opt.utsunomiya-u.ac.jp

**OCIS codes:** (110.0110) Imaging systems; (300.0300) Spectroscopy; (110.1758) Computational imaging

Spectral imaging is very effective in various fields of biology, food science, health science, medicine, remote sensing, and astronomy. It acquires the wavelength information in addition to the two-dimensional light intensity distribution. There are two different approaches. In one approach, an object is illuminated with a light source with narrow wavelength width and the change of the wavelength. The transmission, reflection, and scattered light from the object are detected by an ordinary image sensor. In the other approach, an object is illuminated by a light with a wide wavelength, and the light from the object is detected by a specially-customized camera with a spectral separation ability.

In this paper, we propose a spectral imaging based on a single pixel camera. The single-pixel camera [1] is composed of optical coding masks and a photo detector. An object image is spatially encoded by the masks and the light intensity summation of the encoded image is detected by the photo detector. And the light detection was iterated the same number of the pixels while changing the masks. The object image is reconstructed by the inverse matrix calculation from the encoded images and the light detections. The number of the light detection is reduced by the compressive sensing technique [1]. The biggest feature of the single-pixel camera can perform an imaging with a photodetector, that is, without an image sensor. Therefore, it has simple optics and simple electronics, and consequently it can perform the imaging in a wide variety of wavelengths with very low cost.

A spectral imaging based on a single pixel camera (single pixel spectral camera) is easily constructed by replacing the photodetector to a conventional spectroscope, in this research, with an optical fiber input. The coding mask consists of holes on a substrate for ultrawideband spectroscopy in future. The masks are placed on a rotatory disk. It has no wavelength dependence except for an optical absorption of air.

The light source was a halogen light source. The  $4 \times 4$  coding mask is made of holes arranged on the circumference of the disk and switched by rotation of the disk. The encoded image was detected by a fiber-based spectroscope (C7473, Hamamatsu) through a lens. The light intensity values were continuously detected while the disk was rotating, and the peak values corresponding to each mask were extracted at the indication position.

Spectral images had a spectrum from 300 nm to 700 nm with same spectral resolution of the spectroscope. Figure 1 shows an object composed of red and blue films, and the spectroscopic images with  $4 \times 4$  pixels. The spectrum of the obtained image corresponded to the spectral properties of films.

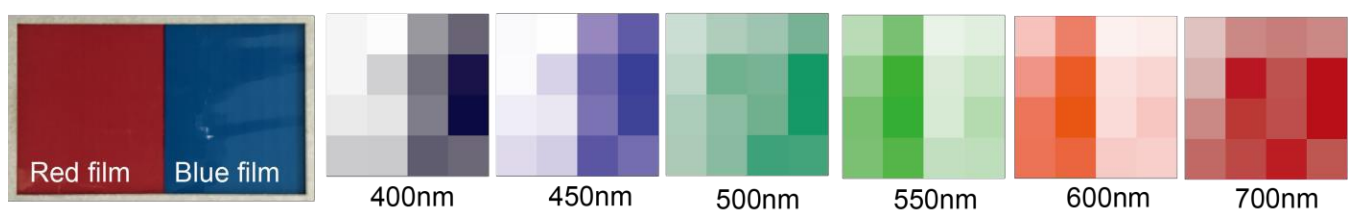


**Figure 1** Object composed of red and blue films and the obtained spectroscopic images with  $4 \times 4$  pixels. The color is pseudo.

### Reference

- [1] M. F. Duarte, M. A. Davenport, D. Takhar, J. N. Laska, T. Sun, K. F. Kelly, and R. G. Baraniuk, "Single-Pixel Imaging via Compressive Sampling", IEEE Signal Process. Mag. 25, 83-91 (2008).

# Aerial Volumetric Display with Pyramid Structured LED Lattice and AIRR

Kazuki Shimose<sup>1</sup> and Hirotugu Yamamoto<sup>1,2</sup>

<sup>1</sup> Dept. of Optical Engineering, Utsunomiya University, Utsunomiya City, Tochigi, 3210904, Japan  
Tel.:81-28-689-7120, E-mail: hirotugu@yamamotolab.science

<sup>2</sup> JST.ACCEL, Japan

OCIS codes: (110.0110) Imaging systems; (300.0300) Spectroscopy; (110.1758) Computational imaging

The aerial volumetric display is a three-dimensional (3D) aerial imaging technique that can show 3D information intact in the air. A user can touch all light spots displayed in the depth direction. The purpose of this research is to realize an aerial volumetric display with a wide viewing angle, which is free from the occlusion problem occurring in 3D space. The occlusion problem is the inconsistency between the depth of the aerial image and the occlusion, which occurs in the conventional aerial 3D display by use of an LED cube. Our solution employs a pyramid structured LED lattice. Our proposed aerial volumetric display is useful for displaying realistic objects in the air. Furthermore, it is effective for applications that intuitively show the orientation three-dimensionally in the air. As a volume display for drawing stereoscopic images directly in three-dimensional space, the three-dimensional structure that displays different directional images according to the viewing direction has been proposed<sup>1</sup>. For a volumetric display that three-dimensionally distributes bright spots in the air to form a three-dimensional image, it has been proposed that three-dimensional display by scanning two-dimensional plane<sup>2</sup>. However, large-scale equipment such as scanning is required. In order to make full use of motion parallax for volumetric display, we utilize aerial imaging by retro-reflector (AIRR)<sup>3</sup>, which features a wide viewing angle, for aerial volumetric 3D display. When an 3D LED lattice is imaged in the air with AIRR, it is possible to form a volumetric image without a scanning mechanism.

A volumetric display by use of an LED cube and our proposed aerial volumetric display with a pyramid structured LED lattice are shown Fig. 1. The lights from the LEDs are partially reflected by the half mirror. Then, the reflected lights are retro-reflected on the retro-reflectors. Finally, the retro-reflected lights transmit the half mirror and form aerial images of the LEDs. As shown in Fig. 1(a), since the LED of Layer 3 in the LED cube is occluded by the LED of Layer 1 and Layer 2, not only the light utilization efficiency decreases, when forming an image in the air, an occlusion problem occurs in which the aerial image of Layer 3 to be observed in front is hidden in aerial image of Layer 1 and Layer 2 formed at the back. We avoid this occlusion problem by using pyramid structured LED lattice. As shown in Fig. 1(b), by designing that the LED of Layer 3 does not overlap the LED of Layer 1 and Layer 2, it is possible to observe the aerial image of all the LEDs from the range of the fixed viewing angle.

Experimental results are shown in Fig. 1(c), (d) and (e). Even with the naked eyes, it was confirmed that a three-dimensional arrow was formed in the air. Furthermore, observations of the aerial image using the screen are shown in Fig. 1(f), (g) and (h), which show the aerial images of Layer 1, Layer 2, and Layer 3, respectively. We have confirmed that each aerial image is formed at the different depths.

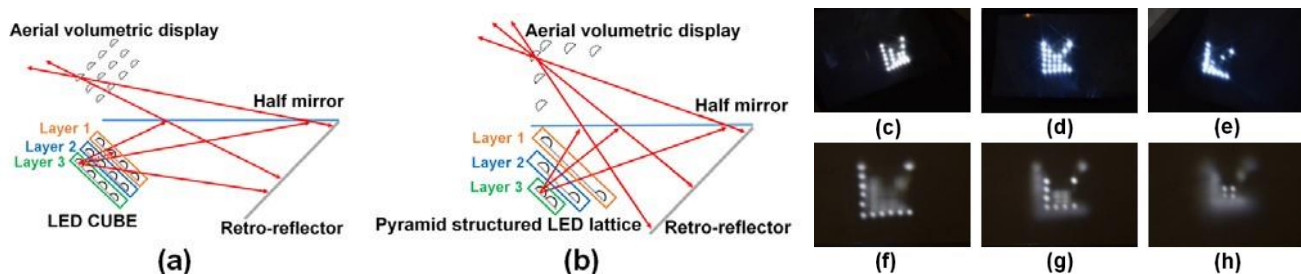


**Fig. 1. Aerial volumetric display by use of (a) an LED CUBE and (b) a pyramid-shape LED array. Observations (c) from a left, (d) in front, (e) from a right of the aerial image, screen observations of (f) Layer 1 LEDs, (g) Layer 2 LEDs, and (h) Layer 3 LEDs.**

## References

1. R. Hirayama, *et al.*, Opt. Exp. **24**, 7319 (2016).
2. D. Miyazaki, *et al.*, Opt. Exp. **14**, 12760 (2014).
3. H. Yamamoto, Y. Tomiyama, and S. Suyama, Opt. Exp. **22**, 26919 (2014).



# Forming the aerial 3D image of your back in front of you with using AIRR

Ryosuke Kujime<sup>1,2</sup> and Hirotsugu Yamamoto<sup>1,2</sup>

<sup>1</sup> Utsunomiya University, 7-1-2, Yoto, Utsunomiya City, Tochigi, 321-0904, Japan

Tel.: 81-28-689-6137, E-mail: r\_kujime@yamamotolab.science

<sup>2</sup>JST, ACCEL, 7-1-2, Yoto, Utsunomiya City, Tochigi, 321-0904, Japan

OCIS codes: (110.6880) Three-dimensional image acquisition

In this paper, we propose a system to form the aerial 3D image of the back of a viewer in front of the viewer without delay. The proposed system is expected to be utilized for sport training: when an athlete check their moving form, delay influences their training. We have proposed aerial imaging by retro-reflection (AIRR) to realize a large aerial display [1, 2]. Since AIRR forms a real image in all optical process, we can form the aerial image of a viewer without photoelectric conversion delay.

Fundamental composition of AIRR is shown in Fig. 1. Aerial display with AIRR is composed of a light source, a beam splitter, and a retro-reflector. Incident rays are reflected on the beam splitter and impinge the retro-reflector. The retro-reflected rays transmit through the beam splitter and form the aerial image of the light source. Aerial image is formed at the position of the plane symmetry of the light source regarding the beam splitter.

Our proposed system in this paper is shown in Fig. 2. Our system consists of two AIRR modules and two mirrors. The first AIRR module forms the aerial 3D image of a mirrored image of the back of an object. The rays converging the aerial image are reflected by a mirror before the second AIRR module. The second AIRR module forms the aerial image of the reflected aerial image. As shown in Fig. 2, the second AIRR module forms the aerial 3D image of the back of the object in front of the object. This system uses only reflection for forming aerial image. Thus, this system can form aerial image without delay. The distance between the aerial image and the object is determined by the distance between the second mirror and the beam splitter in the second AIRR module, and the angle of the second mirror and the beam splitter in the second AIRR module. The Distance of the aerial image and the object  $D$  is expressed by  $D = d[\tan(2\theta-90^\circ)-1/\cos(2\theta-90^\circ)+1]$ , where  $d$  and  $\theta$  are the distance between the first mirror and the beam splitter in the first AIRR module, and the incident angle of the second mirror, which is equal to the angle of the beam splitter in the second AIRR module.

Fig. 3 shows the theoretical curve of the distance  $D$  when  $d = 2000$  mm. The distance increases with the angle of the second mirror. When  $\theta$  is 45 degrees, the aerial image position is the same as the object position. Thus, the distance can be controlled by angle of mirror.

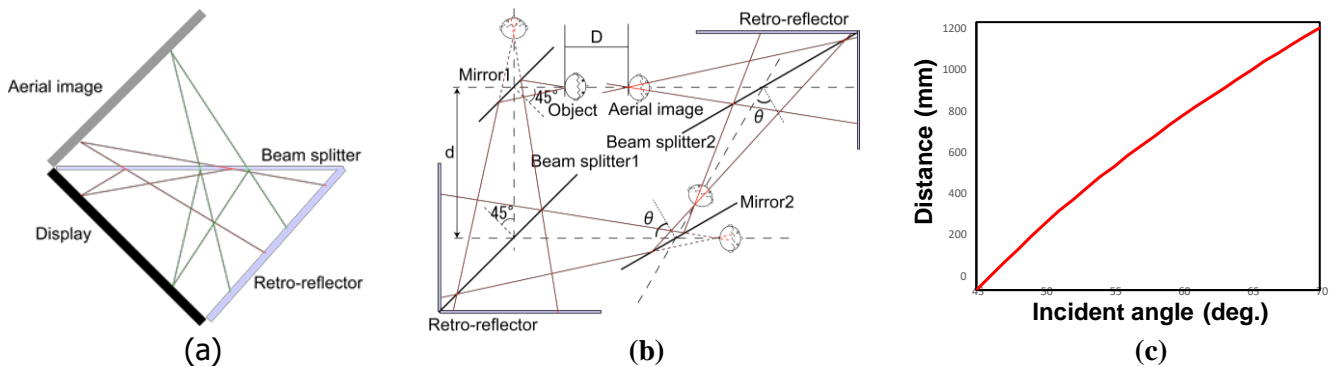


**Fig. 1 (a) Configuration of AIRR. AIRR is consisted of a display, a beam splitter, and a retro-reflector. (b) Configuration of proposed system. This system can form aerial image of its own back face at your front without delay. (c) Dependences of the distance from an object to its aerial image upon the mirror angle.**

## Acknowledgment

This work was partially supported by JST ACCEL Grant Number JPMJAC1601.

## References

1. H. Yamamoto, Y. Tomiyama, and S. Suyama, *Opt. Exp.* **22**, pp. 26919-26924 (2014).
2. R. Kujime, and H. Yamamoto, *Proc. IDW'16*, pp. 468-471 (2016).

# Multi-layered head-mounted display for occlusion and accommodation effects

*Mugoen Kim, Daerak Heo, and Joonku Hahn*

School of Electronics Engineering, Kyungpook National University, 80 Daehak-ro, Buk-gu, Daegu, 41566, South Korea

Tel.:82-53950-5514, E-mail:jhahn@knu.ac.kr

**OCIS codes:** (100.6890) Three-dimensional image processing; (220.4830) Systems design;

Various studies of near-eye display systems have been reported [1]. Among them, the double layer display has great advantages to integrate lots of pixels within a given area by stacking the pixels vertically [2,3]. However, the background image is overlapped with object images. Also, the object image is illuminated by the background image light, and the object image is blended with the background image. The study by M. Holroyed shows the possibility of natural three dimensional view with multi-layer structure [4]. In this paper, we propose the multi-layer head-mounted display for occlusion effect and accommodation effect.

The system consists of four parts which are three liquid crystal panels of mobile phone, an optical film for combining the panels, an external light source, and a pair of eyepieces. Three panels are used to represent the background image, the mask blocking the part of background image and the object image, respectively. The first panel is located on the focal plane of the eyepiece and expresses the background image from optically infinite. The second panel is a masking panel that provides occlusion effects for prevent the overlap of the background image on the first panel over the object image on the third panel. The last panel expresses an object image which is displayed at a certain distance in front of the background. It is illuminated by an additional light source from the edge of it. Figure 1 shows the structure of multi-layer head-mounted display system. This system is operated by using a properties of polarization state. The masking panel determines whether the background image is seen through the object panel or not.

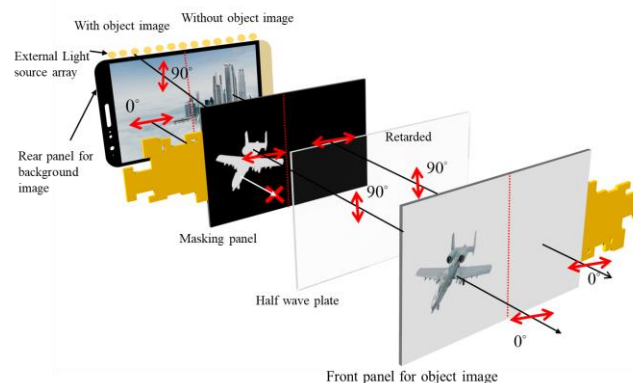


**Fig. 1. Structure of multi-layer head-mounted display**

## Acknowledgment

This work was supported by Samsung Research Funding Center of Samsung Electronics under Project Number SRFC-IT1301-07.

## References

1. D. Lamman and D. Luebke, "Near-eye light field displays," *ACM Transactions on Graphics (TOG)* **32**, 6(2013).
2. F.-C. Huang, G. Wetzstein, B.A. Barsky, and R. Raskar, "Eyeglasses-free display: Towards correcting visual aberrations with computational light field displays," *ACM Transactions on Graphics (TOG)* **33**, 4 (2014)
3. C. Lee, J. Seok, M. Kim, and J. Hahn, "High-resolution light field stereoscope," *The 16th International Meeting on Information Display (IMID)* (2016).
4. M. Holroyed, I. Baran, J. Lawrence, and W. Matusik, "Computing and fabricating multilayer models," *ACM Transactions on Graphics (TOG)* **30**, 6 (2011).

## Depth resolution enhancement of computational reconstruction of integral imaging with considering continuously non-uniform shifting pixel

Byungwoo Cho<sup>1</sup>, Hui Yun<sup>1</sup>, Kotaro Inoue<sup>1</sup>, Ki-Ok Cho<sup>1</sup>, Kyungtea Park<sup>1,2</sup>, Jungsik Koo<sup>2</sup>, Jiyong Park<sup>2</sup>, Cheol-su Kim<sup>3</sup>, Min-Chul Lee<sup>4</sup> and Myungjin Cho<sup>1\*</sup>

<sup>1</sup>Dept. of Electrical, Electronic and Control Engineering, Hankyong National University, 327 Chungang-ro, Anseong-si, Gyeonggi-do 456-749, Korea

E-mail: mjcho@hkun.ac.kr

<sup>2</sup> 3D Display Components Support Center, Gumi Electronics & Information Technology Research Institute, Korea

<sup>3</sup> Dept. of Electric Energy and Computer Engineering, Gyeongju University, Korea

<sup>4</sup> Dept. of Computer Science and Electronics, Kyushu Institute of Technology, Fukuoka 820-8502, Japan

OCIS codes: (110.6880) Three-dimensional image acquisition; (100.6890) Three-dimensional image processing

Three-dimensional (3D) image sensing and visualization of integral imaging technique has been studied for several applications including unmanned automatic vehicle system, object recognition, and so on. A general integral imaging system is composed of two primary process : pickup and reconstruction process. Recently many computational reconstruction techniques are reported ; computational volumetric reconstruction [1], PERT [2], and so on. One of these computational reconstruction techniques is computational volumetric reconstruction. Since conventional computational volumetric reconstruction uses the pixelated process and the number of shifting pixels for reconstruction is the fixed integer value in general, the depth resolution of the reconstructed 3D image is not continuous. Further, the reconstructed 3D images have insufficient quality when elemental images with row resolution are used. In this paper, we present the new computational volumetric reconstruction technique to improve depth resolution of the reconstructed 3D images by using continuously non-uniform shifting pixels instead of integer uniform shifting pixels in conventional computational volumetric reconstruction. Figure 1 is shown the reconstructed planes of the conventional computational volumetric reconstruction and our method.

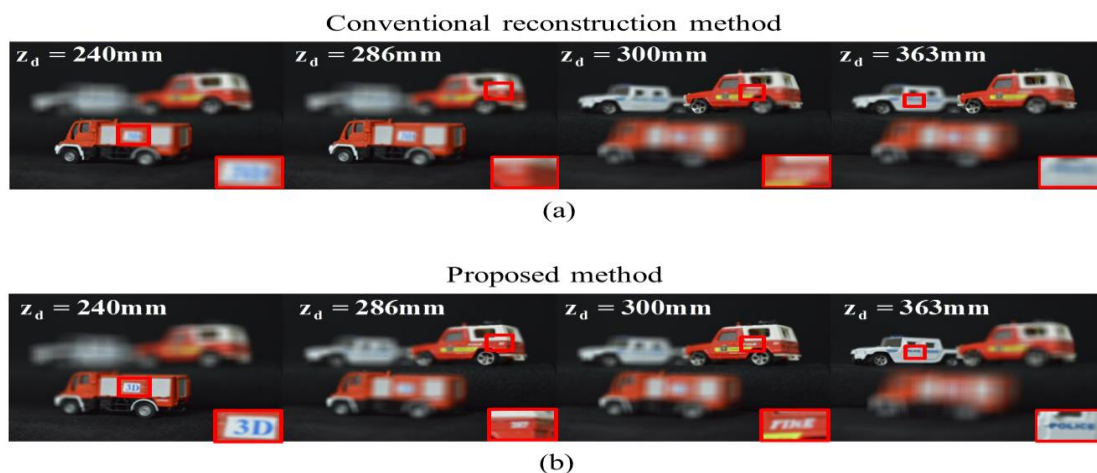


**Fig. 1. Result of comparison of (a) the conventional computational volumetric reconstruction method and (b) our method**

### Acknowledgment

This research was supported by Basic Science Research Program through the National Research Foundation of Korea(NRF) funded by the Ministry of Education(NRF-2016R1E1A2A01952377).

### References

1. M. Cho and B. Javidi, J. of Display Technol., 5, 61-65, (2009).
2. S.-H. Hong, J.-S. Jang and B. Javidi, Opt. Express, 12, 483, (2004).



# Pixel Blink Rate based Depth Estimation Technique in Integral Imaging with Markov Random Field Optimization

Kotaro Inoue<sup>1</sup>, Byeongwoo Cho<sup>1</sup>, Hui Yoon<sup>1</sup>, Ki-Ok Cho<sup>1</sup>, Kyungtae Park<sup>1,2</sup>, Jungsik Koo<sup>2</sup>, Jiyong Park<sup>2</sup>, Cheol-Su Kim<sup>3</sup>, Min-Chul Lee<sup>4</sup>, Myungjin Cho<sup>1,\*</sup>

<sup>1</sup>Department of Electrical, Electronic, and Control Engineering, IITC, Hankyong National University, Korea

\*E-mail: mjcho@hknu.ac.kr

<sup>2</sup>3D Display Components Support Center, Gumi Electronics and Information Technology Research Institute, Korea

<sup>3</sup>Department of Electric Energy and Computer Engineering, Gyeongju University, Korea

<sup>4</sup>Department of Computer Science and Electronics, Kyushu Institute of Technology, Fukuoka 820-8502, Japan

**OCIS codes:** (110.0110) Imaging systems; (110.6880) Three-dimensional image acquisition

Integral imaging is expected as a convenient three-dimensional (3D) imaging and display technique since it can obtain multi-view images with single shoot using a lenslet array. However, it has a critical problem that the resolution of multi-view images will be low. Therefore, reconstructed 3D images may be also low-resolution images. Pixel of elemental images rearrangement technique (PERT) is one of solution for this problem [1]. The reconstructed 3D images by PERT can be obtained by pixel rearranging of the multi-view images. Although it saves high-frequency components of multi-view images compared with conventional reconstruction algorithms[2], the defocus area of reconstructed images looks like particle noise, unlike blur images. Thus, it is difficult to apply current depth estimation algorithms. In this study, we solve this problem using pixel blink rate in depth domain. Figure 1 shows the optical experimental results. We compared with stereo matching based algorithm [3]. Our results show high resolution depth maps and the optimized map by markov random field (MRF) optimization shows better result. The number of pixels of our results are 100 times higher than conventional one.

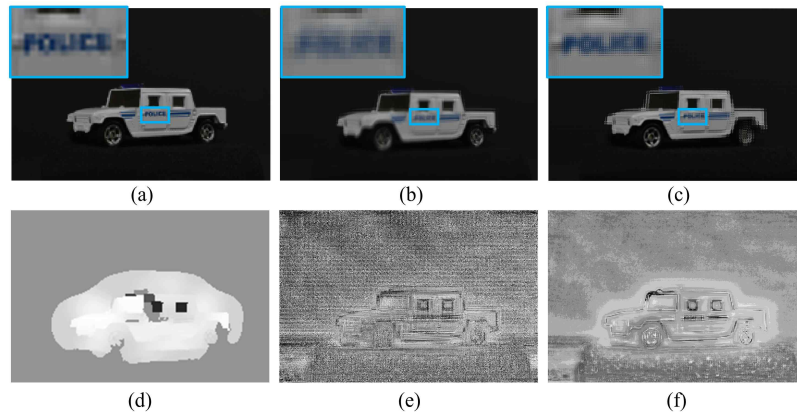


**Fig 1. Optical experimental results, (a) Original scene, (b) Reconstructed image by VCR [2], (c) Reconstructed image by PERT [1], (d) Depth maps by Jeon. et al. [3], (e) Our depth map, (f) Our depth map with MRF optimization.**

## Acknowledgment

This research was supported by Basic Science Research Program through the National Research Foundation of Korea(NRF) funded by the Ministry of Education(NRF-2016R1E1A2A01952377).

## References

1. M. Cho, and B. Javidi, J. of Disp. Technol. 5(2), 61, (2009).
2. S.-H. Hong, J.-S. Jang, and B. Javidi, Opt. Express, 12, 483, (2004).
3. H.-G. Jeon, J. Park, G. Choe, J. Park, Y. Bok, Y.-W. Tai, and I. S. Kweon, CVPR2015, 1555, (2015).

# Three-dimensional image sensing and visualization to enhance 3D resolution of integral imaging

Hui Yun<sup>1</sup>, Byeongwoo Cho<sup>1</sup>, Ki-Ok Cho<sup>1</sup>, Kyungtae Park<sup>1,2</sup>, Kotaro Inoue<sup>1</sup>, Jungsik Koo<sup>2</sup>, Jiyong Park<sup>2</sup>, Cheol-Su Kim<sup>3</sup>, MinChul Lee<sup>4</sup>, Myungjin Cho<sup>1,\*</sup>

<sup>1</sup>Dept. of Electrical, Electronic, and Control Engineering, Hankyong National University, Anseong, Korea

\*E-mail: mjcho@hknu.ac.kr

<sup>2</sup>3D display Components Support Center, Gumi Electronics & Information Technology Research Institute, Korea

<sup>3</sup>Dept. of Electric Energy and Computer Engineering, Gyeongju University, Korea

<sup>4</sup>Dept. of Computer Science and Electronics, Kyushu Institute of Technology, Fukuoka 820-8502, Japan

**OCIS codes:** (110.6880) Three-dimensional image acquisition; (100.6890) Three-dimensional image processing; (090.1760) Computer holography

There is the integral imaging technique [1] that can obtain 3D information by using multiple perspective 2D images. However, low viewing resolution, narrow viewing angle and shallow depth of focus in the integral imaging system are still unsolved problems. Therefore, We propose a new 3D image sensing and visualization technique to improve the lateral and depth resolutions.

In the proposed method, we assume that the 2D elemental images are important information for the 3D performance of integral Imaging since they include lateral and depth resolutions of 3D objects. We use the concept of the resolution priority integral imaging (RPII) and the depth priority integral imaging (DPII) [2] in pickup of proposed method. And then we analyze resolution of 2D elemental images by using characteristic of camera (or lens) parameter. The our proposed method is simple. In the reconstruction of the proposed method, the element image RPII focused on the distance of object result overlaps the reconstruction image of the conventional method using the element images of DPII.

To show the feasibility of our proposed method, we implemented experiments by using proposed method. We represent the result images by using the proposed method in Fig. 1-(a). And also Fig. 1-(b) shows PSNR [3] for both conventional and our methods via different reconstruction depths to evaluate the proposed method.



**Fig. 1. The result of the optical experiment (a) result images (b) PSNR**

## Acknowledgment

This research was supported by Basic Science Research Program through the National Research Foundation of Korea(NRF) funded by the Ministry of Education(NRF-2016R1E1A2A01952377).

## References

1. G. Lippmann, C. R. Acad. Sci., 146, 451, (1908).
2. J-S. Jang and F. Jin, Opt. Lett, 28, 1421-1423, (2003).
3. Q. Huynh-Thu, M. Ghanbari, Electronics Letters, 44, 800-801, (2008)

## Multiple projection 3D display on diffusive fog screen

*Jiman Yu, Minwoo Jung, Daerak Heo, Geunseop Choi, and Joonku Hahn*

<sup>1</sup>School of Electronics Engineering, Kyungpook National University, Buk-Gu Sankyuk-Dong, Daegu 702-701, South Korea

Tel.:82-2-950-5514, E-mail: jhahn@knu.ac.kr

**OCIS codes:** (100.6890) Three-dimensional image processing; (220.2740) Geometric optical design; (110.2990) Image formation theory;

The multi-view displays have been studied in many ways due to their various configuration choices and high-quality three-dimensional(3D) contents. Fog display has two advantages to be applied to multi-view display[1]. First, the fog screen is easy to change its form and it is possible for real objects to pass through the screen. Second, the fog screen functions as the diffusive screen and it fills in the vacant dark region between the two adjacent views. Therefore, dreamy 3D contents can be demonstrated on the fog screen, but there is a disadvantage that observers watch unclear images. In this paper, we improved our previous work by introducing viewing window technology and making density of fog uniform[2]. So, observers can watch high-definition 3D contents with large field of view on table-top.

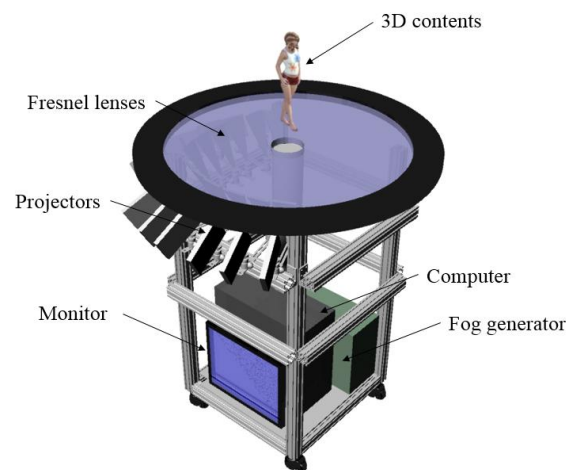


**Fig. 1. Schematic of multiple projection 3D display on diffusive fog screen**

Figure 1 shows the schematic of our system. It is divided into two main parts, the fog screen and elemental projection units(EPU). In the fog screen part, a cylindrical pipe is positioned at the center of the table and it delivers fog from a fog generator. Air curtain surrounding the fog screen helps the fog maintain straight upward uniformly. Twelve projectors are positioned under the top of the table with the same interval in azimuth angle. A fresnel lense aligned in front of the each projector reduces the distortion of the image plane and cross-talk. Moreover, it helps projector's numerical apertures much larger than those of the conventional projectors.

### Acknowledgment

This work was supported by Giga KOREA project, [GK13D0100, Development of Telecommunications terminal with Digital Holographic Table-top Display]

### References

1. A. Yahi, M. Imura, Y. Kuroda, and O. Oshiro, "360-degree fog projection interactive display," ACM SIGGAPH Asia 2011 Emerging Technologies, No. 19 (2011).
2. J. Yu, J. Seok, J. Yun, C. Park, H. Jeon and J. Hahn, "Table-top multi-view fog display based on viewing window technology" IMID2016, Jeju, Korea, Aug. 2016.

# Complex object wave extraction using time-multiplexing in off-axis digital holography

Erkhembaatar Dashdavaa, Munkh-Uchral Erdenebat, Nyamsuren Darkhanbaatar, Anar Khuderchuluun, and Nam Kim\*

<sup>1</sup>School of Information and Communication Engineering, Chungbuk National University, Cheongju, Chungbuk 28644, Korea

Tel.: 82-43-267-9957, E-mail: [namkim@chungbuk.ac.kr](mailto:namkim@chungbuk.ac.kr)

**OCIS codes:** (090.1995) Digital Holography; (100.6890) Three-dimensional image processing; (090.1760) Computer holography

In off-axis digital holography as with conventional digital holography, the reconstructed image contains a zero-order of diffraction which is transmitted background intensity and two twin or conjugate images called the virtual and real images. The zero-order term and twin images can be separated from the reconstructed image using off-axis recording geometry proposed by Leith and Upatnieks [1-2]. Even if the three parts appear at the different locations in the reconstructed images, the elimination of these undesired terms is necessary to increase the recordable bandwidth of the object, thereby improving the image quality of the reconstructed image.

In this paper, we propose a digital method to suppress the zero-order image in off-axis digital holography. Firstly, the proposed approach utilizes digital time-multiplexing technique, in which 90-degree rotated two off-axis holograms are recorded in sequence and corresponding spectrums are subtracted in the computed Fourier domain to eliminate the DC term. Then two subtracted holograms are digitally multiplexed into one complex hologram in the same plane and by shifting the spatial frequency spectrums of the subtracted hologram in the spatial frequency domain, one of the two cross-correlations can be obtained in the center as shown in Fig. 1.

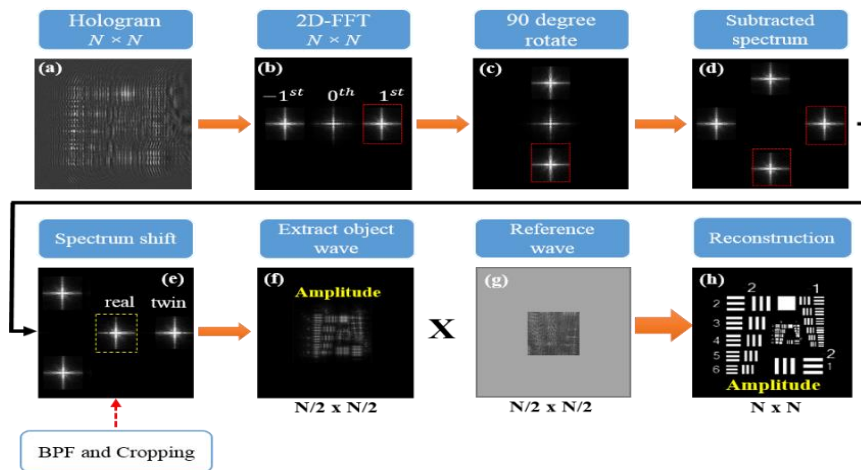


**Fig. 1. Reconstruction steps of the proposed approach**

## Acknowledgment

This work was supported by Institute for Information & communications Technology Promotion (IITP) grant funded by the Korea government (No.2017-0-00417, Openholo library technology development for digital holographic contents and simulation). This research was supported by the Korea government, under the ITRC (Information Technology Research Center) support program (IITP-2017-2015-0-00448) supervised by the IITP (Institute for Information & communications Technology Promotion).

## References

1. E. N. Leith, and J. Upatnieks, *J. Opt. Soc. Am.* 52, 1123 (1962).
2. I. Yamaguchi, and T. Zhong, *Opt. Lett.* 22, 1268 (1997).

# Fast calculation method for full-color holographic system of real existing objects

Yu Zhao<sup>1</sup>, Ki-Chul Kwon<sup>1</sup>, Seok-Hee Jeon<sup>2</sup>, Sang-Keun Gil<sup>3</sup>, Nam Kim<sup>1\*</sup>

<sup>1</sup>School of Information and Commu. Eng., Chungbuk Univ., Cheongju, Chungbuk 361-763, Korea

<sup>2</sup>Department of Electronics Eng., Incheon National University, 119 Academic-ro, Yeonsu-gu, Incheon 22012, Korea

<sup>3</sup>Department of Electronics Eng., Suwon University, San 2-2 Wau-ri, Bongdam-eup, Hwaseong-si, Gyeonggi-do, Korea

Tel.: 82-43-261-2482, E-mail: namkim@chungbuk.ac.kr

**OCIS codes:** (100.6890) Three-dimensional image processing; (090.1760) Computer holography

With the development of computing technologies over the past decades, optical holography can be totally through a digital processing method. CGH has significant benefits [1] including that a hologram of a physical object can be created quickly. Over the past decade, a lot of research based on the CGH technique has been proposed, among them, real object-based methods are very popular [2].

In this paper, we propose a full-color polygon-based holographic system for real 3D objects captured by a depth camera. Our proposed method consists of three steps. In the first step, the point cloud produce by a depth camera usually has a lot of depth information, The depth and color data of the real scene are acquired simultaneously through a depth camera connected with a personal computer (PC), where the depth camera consists of a red-green-blue (RGB) sensor that detects the color, and an infra-red (IR) sensor to detect depth data. The second step is to classify each point into sub-layers according to depth information. In the third step, each point of the point cloud can be distributed accurately according to the exact coordinates of each layer in a generated grid, and we obtain a CGH by executing the diffraction calculation on the sub grids using FFT techniques.

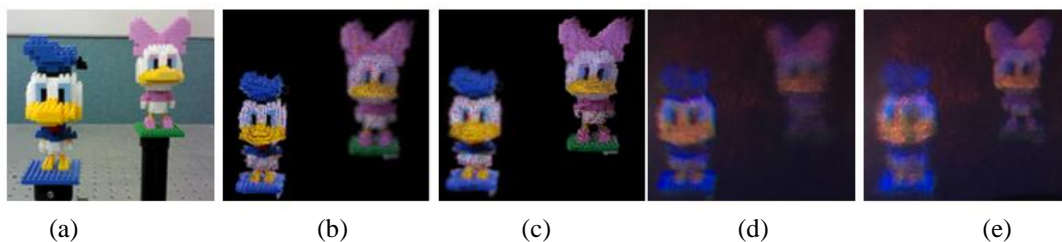


**Fig. 1. (a) Real 3D object, (b) point cloud model, numerical reconstructed images focus on the (b) first toy and (c) second toy, optical reconstructed images focus on the (d) first toy and (e) second toy**

**Table 1. Generation time for  $1,024 \times 1,024$  holograms (seconds)**

	Conventional algorithm (CPU)	Conventional algorithm (GPU)	Proposed method (CPU)	Proposed method (GPU)
toys	827.06	60.17	24.55	0.68

In this research, we propose a gridding method to generate holograms for real objects captured with a depth camera. We show that this method can accelerate the generation of the hologram. The numerical and experimental results both indicate that real 3D objects can be reconstructed clearly. The authors believe that this method will be useful for creating CGHs for a real-time full-color holographic display.

## Acknowledgment

This work was supported by Institute for Information & communications Technology Promotion(IITP) grant funded by the Korea government (No.2017-0-00417, Openholo library technology development for digital holographic contents and simulation). This research was supported by the Korea government, under the ITRC (Information Technology Research Center) support program (IITP-2017-2015-0-00448) supervised by the IITP (Institute for Information & communications Technology Promotion).

## References

1. A. W. Lohman and D. P. Paris, "Binary Fraunhofer holograms generated by computer," Appl. Opt. 6, 1739 (1967).
2. Y. Zhao, K. C. Kwon, Y. L. Piao, S. H. Jeon, and N. Kim, "Depth-layer weighted prediction method for a full-color polygon-based holographic system with real objects." Optics Letters (42.13), 2599-2602. (2017)



# A refractive index sensor based on an extraordinary optical transmission in a floated metal nano-slit array

Hee-Dong Jeong<sup>1</sup>, Yong-Sang Ryu<sup>2</sup> and Seung-Yeol Lee<sup>1\*</sup>

<sup>1</sup>School of Electronics Engineering, Kyungpook National University, Bukgu, Daegu 702-701, Republic of Korea

<sup>2</sup>Sensor System Research Center, Korea Institute of Science and Technology, Seoul 02792, Republic of Korea

Tel.:82-53-950-6608, E-mail: seungyeol@knu.ac.kr

**OCIS codes:** (240.6680) Surface plasmons; (280.4788) Optical sensing and sensors; (310.6628) Subwavelength structures, nanostructures

The surface plasmon polaritons (SPPs) are surface electromagnetic waves propagating along the plane interface between metal and dielectric [1]. SPPs has been applied to various optical devices such as waveguides, near-field optics, optical data storage, solar cells, and surface-enhanced Raman scattering (SERS) based optical sensors because it can confine light into sub-wavelength scale and overcome diffraction limit.

SPPs attracted the attention of scientists since the work of the Ebbesen's research group has been reported in 1998. They found that the transmission of light through Ag or Au films with nanohole arrays can be dramatically increased compared to the amount they predicted [2]. This phenomenon, called extraordinary optical transmission (EOT), can improve the sensing performance of the sensor system. Especially, as the sensing area of the nanohole and nano-slit structure becomes smaller, it can be used in biosensors, chemical sensors, etc. Also, refractive index sensing is possible by using the characteristic of EOT that the resonant wavelength of EOT depends on the refractive index of the surrounding environment [3]. In this study, we propose a floated nanoslit array structure for high-performance refractive index (RI) sensors based on an EOT.

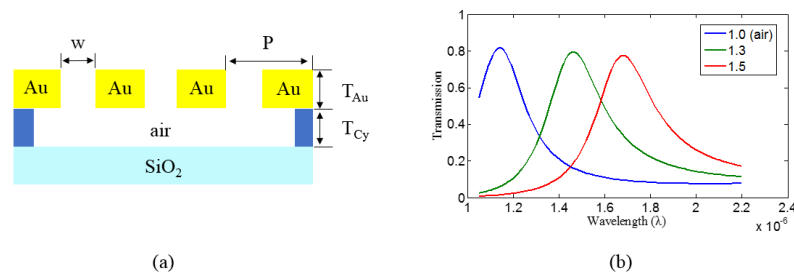


**Fig. 1. (a) A floated RI sensor structure. (b) Simulated transmission spectra of floated RI sensor with sensing material of  $n = 1.0, 1.3$ , and  $1.5$ .**

Figure 1(a) shows a cross-sectional view of the proposed structure. First, we simulated the optimal conditions of the EOT generated in our structure using a rigorous coupled-wave analysis (RCWA) method. Based on the numerical results, CYTOP was spin-coated on a  $\text{SiO}_2$  substrate with a thickness of 500 nm ( $T_{\text{Cy}}$ ), and Au was deposited on the CYTOP with a thickness of 350 nm ( $T_{\text{Au}}$ ). After that, a metal was patterned with period ( $P$ ) of 650 nm and width ( $W$ ) of 350 nm using focused ion beam (FIB) process. Then, etching of the CYTOP under the nanoslit pattern is done for design a tunable RI sensor structure. We can freely tune the resonant condition of EOT by filling a space under the pattern with a various refractive indexes. Figure 1(b) shows the result of index tuning simulation of the proposed structure. Each of the graphs was obtained by simulating a material with refractive index of 1.0 (air), 1.3, and 1.5 under the pattern, and a transmittance close to 0.8 was obtained.

## Acknowledgment

This work is supported by the National Research Foundation of Korea and the Ministry of Science and ICT (NRF-2017R1C1B2003585).

## References

1. S. A. Maier, *Plasmonics : Fundamentals and Applications* (springer-Verlag, New York, 2007).
2. T. W. Ebbesen, H. J. Lezec, H. F. Ghaemi, T. Thio, and P. A. Wolff, *Nature*, 391, 667 (1998).
3. R. Gordon, D. Sinton, K. L. Kavanagh, and A. G. Brolo, *Accounts of chemical research*, 41, 1049 (2008).

## Analysis on random plasmonic nanopillar structure using Bruggeman effective medium theory

Youngkyu Bae<sup>1</sup>, Yong-Sang Ryu<sup>2</sup>, and Seung-Yeol Lee<sup>1\*</sup>

<sup>1</sup>School of Electronics Engineering, Kyungpook National University, Bukgu, Daegu 702-701, Republic of Korea

<sup>2</sup>Sensor System Research Center, Korea Institute of Science and Technology, Seoul 02792, Republic of Korea

Tel.: 82-53-950-6608, E-mail: [seungyeol@knu.ac.kr](mailto:seungyeol@knu.ac.kr)

**OCIS codes:** (240.6680) Surface plasmons; (280.4788) Optical sensing and sensors; (310.6628) Subwavelength structures, nanostructures

Due to the improvement of recent nano-fabrication technology, various sensing devices using surface plasmon polaritons (SPPs) have been developed recently [1]. Mostly, these subwavelength-scale devices have been utilized with a periodic structure. However, fabrication of periodic structure often needs high costs when they are executed in a large-scale. In order to cope with this problem, it has been attempted to adopting an irregular structure, deviating from the regularity of devices. Unfortunately, to fully compute the electromagnetic characteristics of these irregular structures with a well-known EM-wave analysis methods such as finite-difference time-domain (FDTD) method, it involves significant error unless perfectly expressing all of random nature of the irregular structure, which significantly wastes computation time and memory. Therefore, it is necessary to have a different interpretation modeling for these kinds of structures. In this presentation, we apply an Bruggeman effective medium theory (BEMT) as one of the solutions to analyze random plasmonic nanopillar geometry [2].

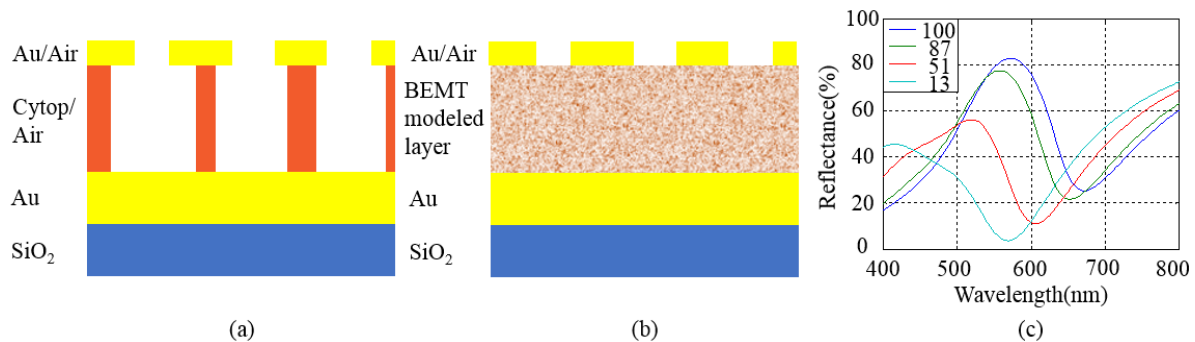


**Fig. 1. (a) A schematic of plasmonic nanopillar structure that used in experiment. (b) A simplified structure using BEMT on Cytop layer. (c) Reflection spectra of proposed structure using BEMT.**

BEMT provides a mixed permittivity taking into account the mutual electromagnetic effects of a mixture of dielectric and metal in the microscopic nature of the subwavelength scale. We used this mixed permittivity to predict the reflection spectra of EM waves in a plasmonic nanopillar geometry that is randomly mixed with metal and dielectric medium as shown in Fig. 1, which was also experimentally compared.

The calculated nanopillar structure has 4 layers, which are randomly distributed Au nano-island (30nm), Cytop nanopillar (164nm), flat Au (100nm) and SiO<sub>2</sub> substrate from top to bottom. The top and second layer are randomly distributed by thermal evaporating and etching, respectively. Changing the filling factor of the Cytop layer to 100%, 87%, 51% and 13%, we simulated the reflectance of device at visible spectrum and compared with experimental results which showed satisfactory similarity by using the permittivity obtained from BEMT. We expected that BEMT modeling will be used in various ways in a irregular large-scale plasmonic sensor devices.

### Acknowledgment

This work is supported by the National Research Foundation of Korea and the Ministry of Science and ICT (NRF-2017R1C1B2003585).

### References

1. S. A. Maier, *Plasmonics : Fundamentals and Applications* (springer-Verlag, New York, 2007).
2. W. Cai and V. Shalaev, *Optical Metamaterials : Fundamentals and Applications* (Springer, New York, 2009)

## Fabrication of camera lens using photopolymer

Seo-Yeon Park, Jae-Min Lee, Chang-Won Shin, Hui-Ying Wu, and Nam Kim\*

School of Information and Communication Engineering, Chungbuk National University, Cheongju,  
Chungbuk 28644, South Korea

Tel.: 82-043-276-9957, E-mail: \*namkim@chungbuk.ac.kr

**OCIS codes:** (090.2890) Holographic optical element; (040.1490) Cameras; (220.0220) Optical design and fabrication

Recently, the Holographic optical element (HOE) has become a promising field in the holography. Two coherent beams are encountered as the principle of HOE and the interference is generated by the phase difference. The HOE is a diffractive optical element which is widely used because of its advantages such as thin, easy mass production, and complex functions. Photopolymer, dichromated gelatin, silver-halide emulsion, photoresist are commonly used recording material for HOE. Amongst them, the photopolymer is a nonlinear holographic recording material which is suitable for volume phase hologram.

The camera lens is an optical lens which transmits light to a film or image sensor. It is usually used in the form of a multi-lens, in which multiple lenses are superimposed rather than a single lens. Therefore, a multi-lens has the disadvantage that the camera device becomes bulky. To overcome these disadvantages, we propose a method to replace multiple lenses with photopolymer.

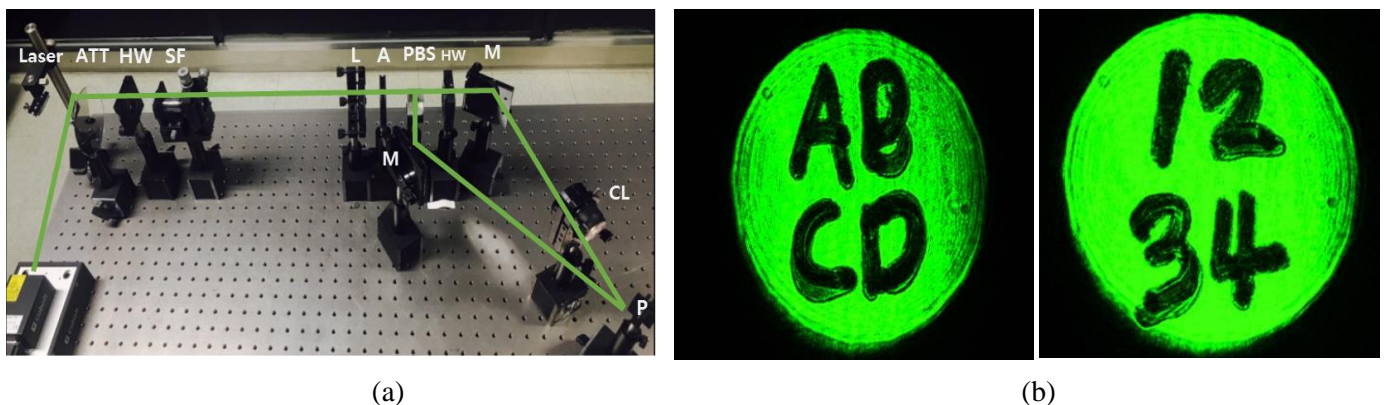


**Fig 1. (a) Experimental setup for recording Camera lens HOE (b) result**

The recording setup of the multi-lens HOE is shown in Fig 1(a). The wavelength of the laser was 532 nm. The camera lens with a focal length of 55 mm has been recorded at 30 degrees with a symmetrical transmission type structure in the photopolymer.

The experimental results are shown in Fig. 1(b). It is expected that this method will contribute to solving the bulky camera lens issues and also it will be adapted with smartphones or cameras.

### Acknowledgment

This work was supported by Institute for Information & communications Technology Promotion(IITP) grant funded by the Korea government(No.2017-0-00417, Openholo library technology development for digital holographic contents and simulation). This research was supported by the Korea government, under the ITRC (Information Technology Research Center) support program (IITP-2017-2015-0-00448) supervised by the IITP (Institute for Information & communications Technology Promotion)

### References

1. Y. M. Kim, B. Song, S.-W. Min, *Opt Lett*, 39(1), 105(2014).
2. J.-A. Piao, G. Li, M.-L. Piao, N. Kim, *J. Opt. Soc. Korea*, 242-248(2013).



## Universal light engine with three digital micromirror devices

*Kwangsoo Kim, Geunseop Choi, Daerak Heo, and Joonku Hahn*

School of Electronics Engineering, Kyungpook National University, 80 Daehak-ro, Buk-gu, Daegu 41566, South Korea

Tel.: 82-53-950-5514, E-mail: jhahn@knu.ac.kr

**OCIS codes:** (110.0110) Imaging system; (220.0220) Optical design and fabrication; (230.0230) Optical devices.

Digital micromirror device (DMD) has a great potential as a high-speed driving device for time-multiplexing 3D display. In recent years, 3D displays using the DMD have been actively studied by many researchers. We also have developed several 3D systems such as super multi-view display, cylindrical display, table top display, and crystal-ball display [1-4]. There is a growing demand for a universal light engines in 3D displays, but the universal light engine using the DMDs have not yet been developed. We suggest a universal light engine that can be used for various full-color 3D display systems. Figure 1 shows a system diagram with a universal light engine. The light engine designed to be available for various systems so it is possible to be used with one light engine design. In the light engine, we designed our own opto-mechanical adjusts for optics and it is easy to physically align the three DMDs. This system uses an LED light source, and each system can be attached to and detached from various systems with a single light engine using an adapter lens.

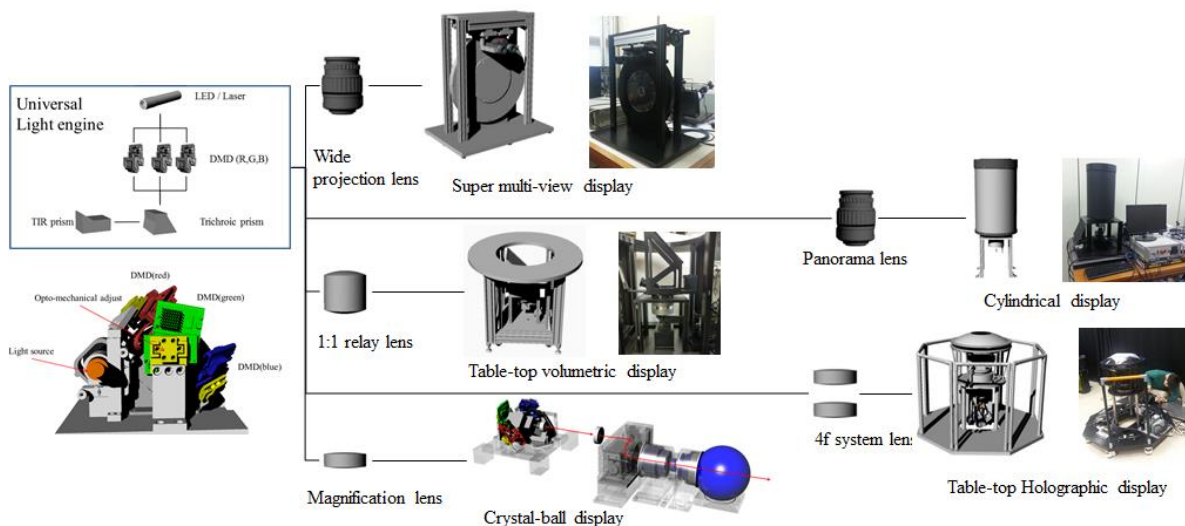


**Fig. 1. System diagram with a universal light engine.**

### Acknowledgment

This work was supported by GigaKOREA project, [GK GK13D0100, Development of Telecommunications Terminal with Digital Holographic Table-top Display] and by Samsung Research Funding Center of Samsung Electronics under Project Number SRFC-IT1301-07.

### References

1. C. Lee, S. Lim, H. Jeon, and J. Hahn, "Super multi-view display for analyzing human cognition," *Proc. SPIE* **9770**, paper 9970-06 (2016).
2. K. Kim, S. Lim, H. Kim, and J. Hahn, "Full-color Tabletop Light-field Display," in *Imaging and Applied Optics 2016*, OSA Technical Digest, DT4D.5 (2016).
3. G. Choi, H. Jeon, H. Kim, and J. Hahn, "Cylindrical directional display with multiple spinning slits," *The 16th International Meeting on Information Display*, Jeju, P2-65 (2016).
4. Y. Lim, K. Hong, H. Kim, H.-E. Kim, E.-Y. Chang, S. Lee, T. Kim, J. Nam, H.-G. Choo, J. Kim, and J. Hahn, "360-degree tabletop electronic holographic display," *Opt. Express* **24**, 24999-25009 (2016).

## Spherical light field display

*Daerak Heo, Mugeon Kim and Joonku Hahn\**

School of Electronics Engineering, Kyungpook National University, 80 Daehak-ro, Buk-gu, Daegu, South Korea  
Tel.:82-53-951-5514, E-mail: jhahn@knu.ac.kr

**OCIS codes:** (100.6890) Three-dimensional image processing; (120.5800) Scanners.

There have been many researches on three-dimensional(3D) display[1]. Various geometrical shapes of 3D displays have been suggested. Among them, 3D display with spherical symmetry is very interesting since it has a potential to provide 360-degree field of view. Only few studies on spherical 3D display have been reported and a crystal ball is applied to allow multiviews through its center[2]. But some practical problems such as alignment and maintenance may results from a large number of depth fused display units. One simple strategy to solve these problems is to replace space-division multiplexing with time-division multiplexing. For time-division multiplexing, a digital micromirror device(DMD) is usually used due to its driving speed[3].

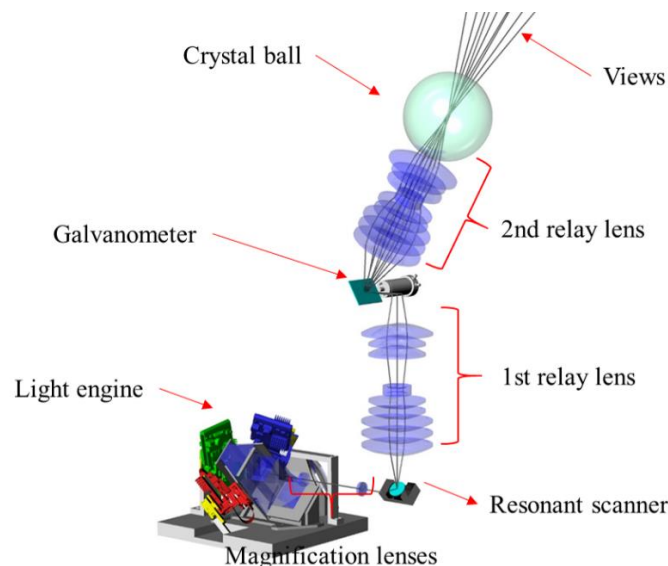


**Fig. 1. Spherical light field display.**

Figure 1 shows a schematic of our system and 3D contents appear in a crystal ball. Our system is composed of a light engine, magnification lenses, two scanners, two relay lenses and a crystal ball. The image is generated by the light engine in high speed and  $4f$  magnification lens delivers the image to the resonant scanner. After that, the first relay lens forms a conjugate plane of the resonant scanner at the galvanometer. Finally, the second relay lens forms an image plane inside of the crystal ball. The direction of views are controlled by two scanners and every view passes through the center of the crystal ball. Therefore, we observe 3D contents at the inside of the crystal ball with large field of view.

### Acknowledgment

This work was supported by Samsung Research Funding Center of Samsung Electronics under Project Number SRFC-IT1301-07

### References

1. J. Hong, Y. Kim, H.-J. Choi, J. Hahn, J.-H. Park, H. Kim, S.-W. Min, N. Chen, and B. Lee, "Three-dimensional display technologies of recent interest: principles, status, and issues," *Appl. Opt.* **50**, H87-H115 (2011).
2. M. Date, T. Kawakami, M. Sasai, and H. Takada, "Screen-free floating 3D image in a crystal ball using spatially imaged iris and multiview DFD(depth fused 3D) technologies," *SID'16 Digest* **47**, 146 (1984).
3. Y. Lim, K. Hong, H. Kim, H. Kim, E. Chang, S. Lee, T. Kim, J. Nam, H. Choo, J. Kim, and J. Hahn, "360-degree tabletop electronic holographic display," *Opt. Express* **24**, 24999-25009 (2016).

## Time-sequential super multi-view display

*Sungjin Lim, Geunseop Choi, Mugeon Kim, Kwangsoo Kim and Joonku Hahn\**

School of Electronics Engineering, Kyungpook National University, 80 Daehak-ro, Buk-gu, Daegu 41566, South Korea

Tel.:82-53-950-5514, E-mail: jhahn@knu.ac.kr

**OCIS codes:** (100.6890) Three-dimensional image processing; (090.1760) Display; (220.2740) Geometric optical design;

Three-dimensional (3D) display technologies have been regarded as one of the most popular issues and many researchers have tried various approaches to improve the quality of 3D display [1-3]. One of the approaches is a super multi-view (SMV) display and the SMV display has an advantage of reducing 3D sickness caused by the vergence-accommodation conflict since more than two views enter the pupil of the eye. We invented a SMV display which is able to change the number of views entering the pupil and our system is expected to clarify the principle of human cognition on 3D object [4].

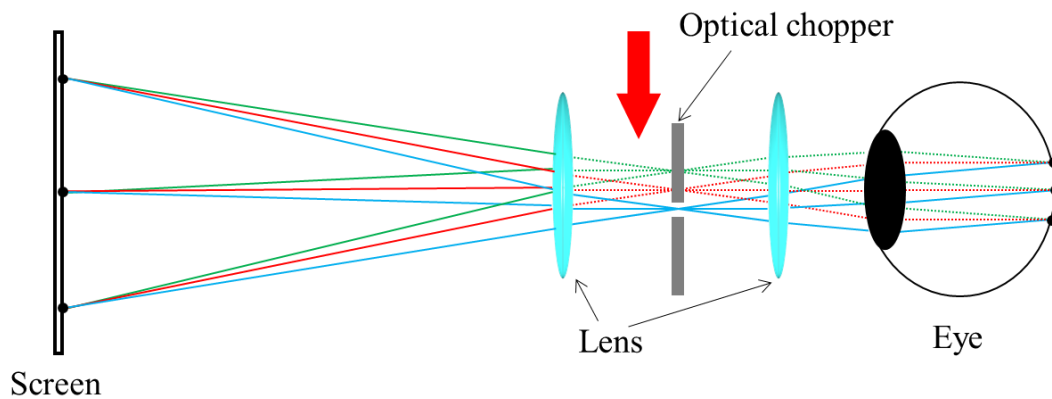


**Fig. 1. Time-sequential super multi-view display.**

In this paper, we improve our previous work on SMV display. Figure 1 shows a schematic of time-sequential SMV display. The system consists of the projection part and the observation part. The projection part is configured by the light engine which realize full-color images by using three digital micro-mirror devices. The projected image at the screen is observed through the observation part which has the optical system. The optical system consists of two lenses and an optical chopper between the lenses for defining the direction of the image entered into eyes.

### Acknowledgment

This work was supported by Samsung Research Funding Center of Samsung Electronics under Project Number SRFC-IT1301-07.

### References

1. J. Hong, Y. Kim, H.-J. Choi, J. Hahn, J.-H. Park, H. Kim, S.-W. Min, N. Chen, and B. Lee, "Three-dimensional display technologies of recent interest: principles, status, and issues," *Appl. Opt.* **50**, H87-H115 (2011).
2. N.S. Holliman, N.A. Dodgson, G.E. Favalora, and L. Pockett, "Three-Dimensional Displays: A Review and Applications Analysis," *IEEE Trans. Broadcast.* **57**, 362-371 (2011).
3. Y. Takaki, "Super Multi-View Display and Holographic Display," The 22nd Annual Meeting of the IEEE Photonics Society (LEOS), Belek-Antalya, Turkey (2009).
4. C. Lee, S. Lim, H. Jeon, and J. Hahn, "Super multi-view system for analyzing human cognition," *Pro. SPIE* **9770**, 9970-06 (2016).

## Cylindrical light field display

*Geunseop Choi<sup>1</sup>, Hosung Jeon<sup>1</sup>, Kwangsoo Kim<sup>1</sup>, Hwi Kim<sup>2</sup> and Joonku Hahn<sup>1</sup>*

<sup>1</sup>School of Electronics Engineering, Kyungpook National University, 80, Daehak-ro, Buk-gu, Daegu, 41566, South Korea

*Tel.: 82-53-950-5514, E-mail: jhahn@knu.ac.kr*

<sup>2</sup>Department of Electronics and Information Engineering, Korea University, Sejong Campus, Sejong-ro, 2511, Sejong 30019, South Korea

**OCIS codes:** (100.6890) Three-dimensional image processing; (230.6120) Spatial light modulators; (220.4830) Systems design

The light field display is the most natural three-dimensional(3D) display considering the visual perception factor. For this reason, various light field displays have been suggested in both industry and academy. We proposed a cylindrical light field display with rotating slits in last year[1]. Cylindrical shape has interesting advantages in providing 360-degree field of view and rotating the structure[2]. Until now, many systems providing 360-degree field of view have been realized by using multiplexing techniques. Some of them are implemented with plural projectors surrounding the screen. Others are implemented with a high-speed projector and the optics including a screen is usually rotating. In this paper, we propose a cylindrical light field display and it has two significant advantages. First, three digital micromirror device(DMD)s are used as a high-speed projector and it lessens the efforts for alignment of plural projectors. Second, the optics are also designed to have cylindrical symmetry and it is possible to let the optics stationary.

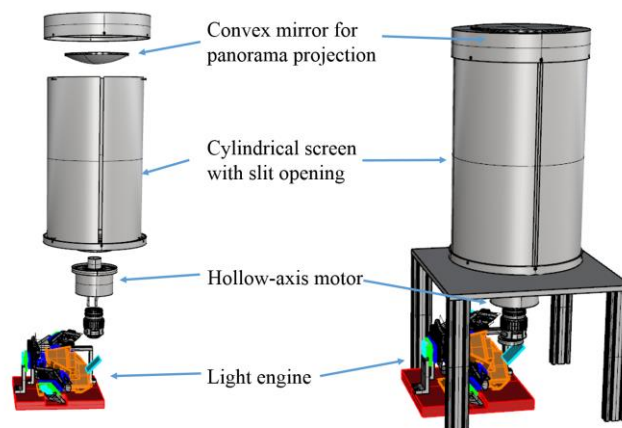


**Fig. 1. Cylindrical light field display.**

Figure 1 shows a schematic of cylindrical light field display. The image on the DMDs is projected upward along the axis of rotation and the light is reflected by the convex mirror at the top of the cylinder. Then, the image is projected on the rotating cylindrical screen. The observer watch 3D contents inside of the cylinder through the slits on the surface.

### Acknowledgment

This work was supported by Samsung Future Technology Fund of Samsung Electronics Inc. under Grant Number SRFC-IT1301-07.

### References

1. G. Choi, H. Jeon, H. Kim and J.Hahn, "Cylindrical directional display with multiple spinning slits," The 16th International Meeting on Information Display, Jaeju, Korea, P2-64, Aug. 2016
2. T. Yendo, N. Kawakami, and S. Tachi, "Seelinder: The Cylindrical Lightfield Display," in *Proceedings of ACM SIGGRAPH emerging technologies* (ACM, 2005) Article 16.

# Orthographic projection based holography with low density modeling point cloud

*Yan-Ling Piao<sup>1</sup>, Alam MD Shahinur<sup>1</sup> Jong-Rae Jeong<sup>2</sup> and Nam Kim<sup>1\*</sup>*

<sup>1</sup> Dept. of Electrical & Computer Engineering, Chungbuk National University, Korea

*Tel.:82-43-9957, E-mail: namkim@chungbuk.ac.kr*

<sup>2</sup>Dept. of Information and Communication, Suwon Science College, Korea

**OCIS codes:** (110.6880) Three-dimensional image acquisition; (100.6890) Three-dimensional image processing; (090.1760) Computer holography

Hologram generation methods can be classified depending on the type of input data: synthetic 3D scenes or multi-view data. Hologram computation from multi-view data have two approaches: the multi-viewpoint projection based methods and the holographic stereogram approach. With development of the science and technology, the device which extracted 3d information of real-existing scenes is improved such as depth camera, light field camera, etc. However, the extracted 3d information is not enough to describing the realistic scenes for generating synthetic hologram by usual synthetic model (point cloud, polygon, etc). It is possible to use multi-view data. But it is also challenging to provide all the human depth cues and accurate shading of the scene with only a few projection images. In order to improve the quality of CGH, we generate the multi-view image and depth information for synthetic CGH using low density point cloud which is modelling by 3D scan with depth camera.

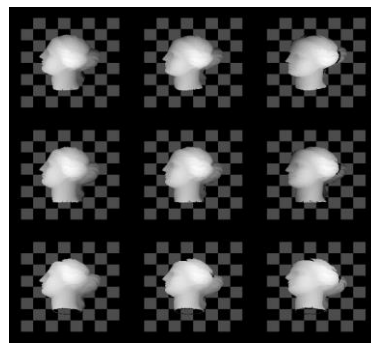


**Fig. 1. Generated orthographic images by low density point cloud**

In this paper, we proposed a computer-generated hologram system of a real-existing scene by depth camera using orthographic projection based images and depth map. Real scene captured by depth camera in 3d scanning mode, then the point cloud model and corresponding color information is processed to generating orthographic projection images and depth map. Hidden point remove was used in point cloud to orthographic projection image (and depth map) conversion. And the hole filling method will be used. Finally, the orthographic projection images and depth map will be used to compute hologram with low angular sampling.

## Acknowledgment

This work was supported by Institute for Information & communications Technology Promotion(IITP) grant funded by the Korea government (No.2017-0-00417, Openholo library technology development for digital holographic contents and simulation). This research was supported by the Korea government, under the ITRC (Information Technology Research Center) support program (IITP-2017-2015-0-00448) supervised by the IITP (Institute for Information & communications Technology Promotion).

## References

1. Y. Ohsawa, Computer-generated holograms using multiview images captured by a small number of sparsely arranged cameras, *Applied Optics*, pp. A167-A176, 2013.
2. J. H. Park, Fresnel and fourier hologram generation using orthographic projection image, *Optics express* Vol. 17, No. 8, pp. 6320-6334, 2009.
3. T. Mishina, Calculation of holograms from elemental images captured by integral photography, *Applied optics*. Vol. 45, No. 17, pp. 4026-4036, 2006.

# Analysis of 360-degree Non-mechanical Table Top Electronic Holographic Display System

Soobin Kim and Hwi Kim

Dept. of Electronics and Information Engineering, Korea University, Sejong 30019, Korea

Tel.: 82-44-860-1736, E-mail: hwikim@korea.ac.kr

**OCIS codes:** (090.1995) Digital holography; (090.2870) Holographic display; (120.4820) Optical systems

Three-dimensional (3D) holographic displays are considered as the ultimate display and the challenge for researchers. A table-top holographic display system is an issue and promising candidate for next generation 3D holographic display system. Recently, the 360-degree holographic table-top display was introduced in Giga Korea Project which was supported by the Korean Federation of Science and Technology Societies(KOFST). This system consists of digital micromirror device (DMD) for color image representation, 4- $f$  Fourier filtering systems, a parabolic mirror for 3D observation and a mechanical motor for 360-degree images on the viewing circumference [1]. However, the design of an electronic system which has the mechanical rotary motor has not yet accomplished, and this problem is remained as a challenge of the system.

In this paper, we carried out analysis and design of non-mechanical table-top type display system based on geometric and wave optics. Our suggested system consists of multi-sub panel, 4- $f$  system, parabolic mirror, field lens and two types of prisms. Multi-sub panel is a high-resolution panel and divided by sub-region. Because of these sub-regions, the system has more viewpoint. And the incident beams are refracted by each prism [2].

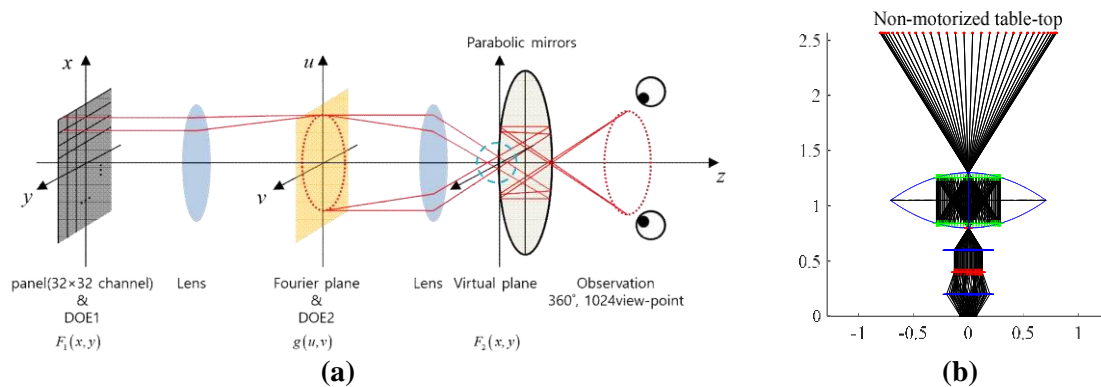


**Fig. 1. (a) Schematic diagram of proposed system, and (b) result of simulation based on geometric optics**

The schematic diagram shown in Fig. 1. (a) is designed for the proposed system. It consists of 32 by 32 region panel, resolution of each sub-panel is 256 by 256, and two types of prisms. The fig. 1 (b) shows the result of simulation based on geometric optics for proposed system. The final goal of this research is design of RGB full-color system increasing of viewpoints to 1,024.

## Acknowledgment

This work was supported by GigaKOREA Project (GK17D0100, Development of Telecommunications Terminal with Digital Holographic Tabletop Display).

## References

1. Y. Lim, K. Hong, H. Kim, H.-E. Kim, E.-Y. Chang, S. Lee, et al., "360-degree tabletop electronic holographic display," *Opt. Express* 24, 24999-25009 (2016).
2. Marios Papas, Thomas Houit, Derek Nowrouzezahrai, Markus Gross, Wojciech Jarosz. *The Magic Lens: Refractive Steganography*. ACM Transactions on Graphics (Proceedings of SIGGRAPH Asia), 31(6), November 2012.



# Geometrical optical modeling and diffraction efficiency analysis of diffractive augmented reality system

*JungBeom Choi, JongHa Park, SooBin Kim, and Hwi Kim*

Dept. of Electronics and Information Engineering, Korea University, Sejong 30019, Korea

Tel.:82-44-860-1736, E-mail: hwikim@korea.ac.kr

**OCIS codes:** (090.2820) Heads-up displays; (050.1950) Diffraction gratings; (120.4820) Optical systems;

Augmented Reality (AR) is the significant technology of head-mounted-display (HMD) which is one of the next-generation displays, and has received great attention in recent years. Accordingly, Microsoft HoloLens is at the forefront of augmented reality technologies that is commonly used with diffractive optical elements. However, further research for the Microsoft HoloLens is needed because it has achieved high performance through a thin combiner without using a lens. In this paper, we show the numerical model based on the electromagnetic analysis with the accurate structural design of the combiner of the diffractive optical element, which is implemented in the diffractive AR system.

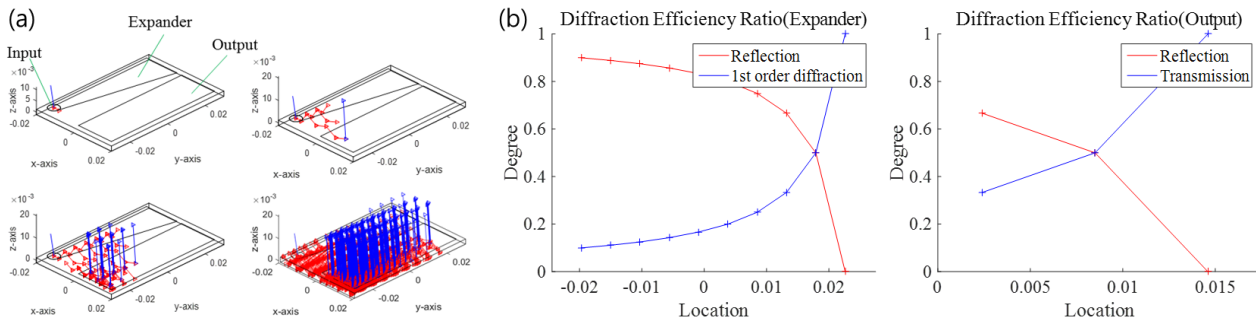


**Fig. 1. Geometrical optical modeling and diffraction efficiency ratio**

Fig. 1. (a) shows the simulation of geometrical optical modeling for a combining system of the diffractive AR. When light passes through the input grating structure, the diffraction is occurred in the direction of the expanded grating structure. In this diffracted light, the next diffraction is occurred in the direction of the output lattice structure by the expanded lattice structure, and it is replicated at the same time. This replicated light continues to diffract and replicate continuously by the expansion grating structure, and the incident light on the output grating structure is output in a parallel direction to the input light. These processes allow we could duplicated one light to multitude of lights, which is forming a field of view (FOV).

The diffraction efficiency distributions of the expander and output gratings obtained by simple calculation theory as shown in Fig. 1 (b). The gratings with these efficiencies could be designed using Fourier Modal Method (FMM) and could be applied to the expander and output gratings that has a final goal of uniform light efficiency. If the light efficiency is uniform, an image in the retina is clearly formed when the light beam from the output grating is entering to the eye. [1].

In this paper, we carried out the analysis of the optical structure for a diffractive AR by hybrid modeling of geometrical optics and electromagnetic field analysis as described above, and ultimately propose a new optical structure to improve yield of the grating process, FOV and light emitting efficiency.

## Acknowledgment

## References

1. H. Kim and B. Lee, "Rigorous Fourier modal analysis on slab structures with finite thickness and one-dimensional arbitrary permittivity and permeability profiles," The 11th Micro-optics Conference Tokyo, Japan, Oct.-Nov. 2005.

# Fast Calculation Method of High-Definition Computer-Generated Hologram

*Sungjae Park, Jonghyun Lee and Hwi Kim\**

Department of Electronics and Information Engineering, Korea University, Sejong 30019, Korea

Tel.: 82-44-860-1428, E-mail: [hwikim@korea.ac.kr](mailto:hwikim@korea.ac.kr)

**OCIS codes:** (090.2870) Holographic display; (090.1760) Computer holography; (090.1705) Color holography

High-definition (HD) computer-generated hologram (CGH) has been actively researched because it can solve the problems of holographic 3D display that narrow viewing angle and limited resolution [1-2]. Also it can display realistic and high quality holographic 3D images. HD CGH is a large scale that requires huge computational time and great memory, so the enhancement in efficiency of computation algorithm is important issue [3]. In this paper, we proposed a method to calculate the large scale of HD CGH by the localized light wave computation of polygon mesh and the viewing zone division technique.

As a first method, a conceptual diagram and mathematical formula of segmentation method for large-scale CGH calculation are shown in Fig. 1. (a). The second method is the local polygon calculation as shown in Fig. 1(b). Our proposed method that ultimate final solution is to calculate CGH by hybridization of these two techniques. The first step of this technique is to divide and calculate in the viewing zone. The second step is localized calculation of angular spectrum of the polygon mesh for the segmented area. This step calculates only some areas depending on the polygon size, unlike the traditional method of calculating the entire area for calculating one polygon. Finally, the locally computed small fields are stamped on their original large field, respectively. This procedure improves memory efficiency and enables fast HD CGH calculations.

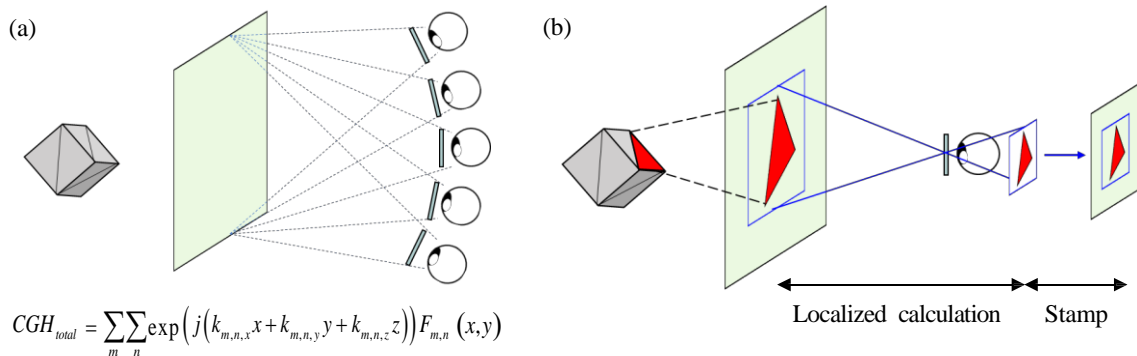


**Fig. 1. Conceptual diagram of (a) viewing zone segmentation method and (b) localized polygon calculation**

The proposed method can efficiently calculate HD CGH and is useful for many applications. Our future work is to calculate a 160K by 160K full color HD CGH and build a system for the practical CGH content generation process.

## Acknowledgment

This work was supported by the Industrial Strategic technology development program (10052641, Development of the commercialization platform technology for diffractive optical element based on 3D surface nanostructure for full-color implementation) funded by the Ministry of Trade, industry & Energy (MI, Korea).

## References

1. Y. Tsuchiyama, K. Matsushima, S. Nakahara, and Y. Sakamoto, "Full-Color High-Definition CGH Using Color Filter and Filter Design Based on Simulation," in Imaging and Applied Optics 2016, OSA Technical Digest (online) (Optical Society of America, 2016), paper DW51.4.
2. K. Matsushima and S. Nakahara, "Extremely high-definition fullparallax computer-generated hologram created by the poly-gon-based method," Applied optics 48, H54-H63 (2009).
3. J. Cho, J. Hahn, and H. Kim, "Fast reconfiguration algorithm of computer generated holograms for adaptive view direction change in holographic three-dimensional display," Optics Express 20, pp. 28282-28291, (2012).

# Analysis of Moiré Deflectometry in Display System using Talbot Effect

*Junghwan Park and Hwi Kim*

Dept. of Electronics and Information Engineering, Korea University, Sejong 30019, Korea

Tel.: 82-44-860-1736, E-mail: hwikim@korea.ac.kr

**OCIS codes:** (120.4120) Moire' techniques; (070.6760); Talbot and self-imaging effects; (090.1760) Computer holography

When the display system is manufactured, various optical functional panels are integrated inside of two glasses. In the combination of panels between two sheets of glasses, because of complicated optical interactions, accurate alignment is the crucial key point for the appropriate result. In this paper, the simulation was carried out for generating Moiré patterns using Talbot effect, and analyzing the generated Moiré pattern to confirm that the panels are properly bonded. Through this process, we can measure the displacement, rotation angle [1], and tilt angle between upper and lower plates.

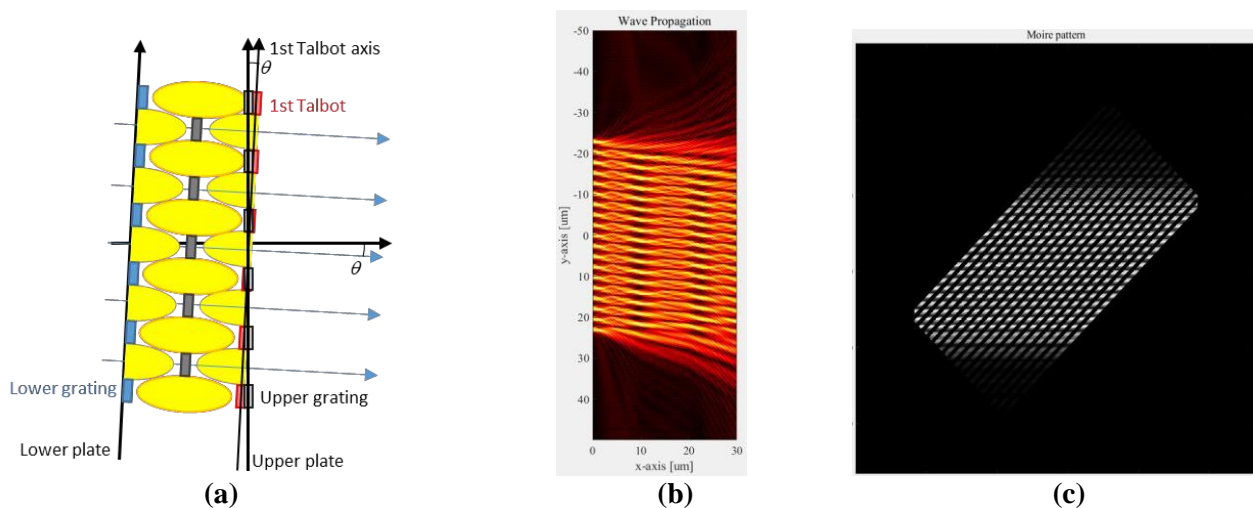


**Fig. 1. (a) Schematic of simulation, (b) Simulated Talbot pattern, (c) Results of Moiré pattern**

Fig. 1. (a) shows the basic schematic of simulation assuming that the upper plate is tilted as much as  $\theta$ . The 1<sup>st</sup> order Talbot pattern by the grating structure of the lower plate occurs on the grating of the upper plate, and the Moiré pattern is generated by this 1<sup>st</sup> Talbot pattern on the upper grating. In the simulation result in Fig 1. (b), we can see the Talbot pattern by the grating of lower plate. The Talbot distance is adjustable by regulating the grating period in this system [2]. The incident angle  $\theta$  is 10 degree and the medium is composed of free space and glass. Finally, the simulated Moiré pattern is shown in Fig 1.(c). It is occurred by interference of upper grating and Talbot pattern of lower grating. As a conclusion, we can determine the tilt angle  $\theta$  of upper and lower plates by analyzing the Moiré pattern in Fourier domain.

## Acknowledgment

This work was supported by LG display Co. LTD.

## References

1. B.J. Kim, K.C. Yuk, S.I. Lee, S. Chang, "Use of a phase type elongated circular grating in Talbot moiré deflectometry", In *Optik - International Journal for Light and Electron Optics*, Volume 115, Issue 3, Pages 121-128, (2004)
2. Yoshiaki Nakano and Kazumi Murata, "Measurements of phase objects using the Talbot effect and moiré techniques," *Appl. Opt.* 23, 2296-2299 (1984)

# Localization Method of Depth-map Computer Generated Hologram for Fast Calculation

*JongHa Park, JiSung Yoon, SungJae Park, JongHyun Lee and Hwi Kim*

Department of Electronics and Information Engineering, Korea University, Sejong 30019, Korea

Tel.:82-44-860-1428, E-mail: [hwikim@korea.ac.kr](mailto:hwikim@korea.ac.kr)

**OCIS codes:** (090.1760) Computer holography; (050.1970) Diffractive optics;

Real-time CGH calculations is essential for the implementation of HMD type holographic display. As the HMD industry grew, more research on the technology of generating real-time CGH became necessary. The crucial key point of depth-map CGH generation which is one of the real-time CGH technology is the cascaded FFT method. So, it is important to reduce the calculation time of process in cascaded FFT for the fast calculation. In this paper, we propose the localization method of depth-map CGH for the fast calculation. The first step is area segmentation as shown in Fig. 1. (a). Generally, the computation amount of depth-map CGH from SLM of  $N$  by  $N$  resolution is described as  $N^2 \log_2 N^2$ . However, the amount from  $m$  by  $m$  by using area segmentation method is described as  $N^2 (\log_2 N^2 - \log_2 m^2)$ . Therefore, the proposed method is much faster than conventional area segmentation method. The second step is local area calculation method as shown in Fig. 1. (b). When the object with multiple depth is divided to 2D images with different depth, the images are composed of very sparse images. Thus, the FFT computation of the entire area of image is a huge waste of computation. Therefore, the depth-map CGH should be calculated by only the meaningful region of the image for the effective calculation.

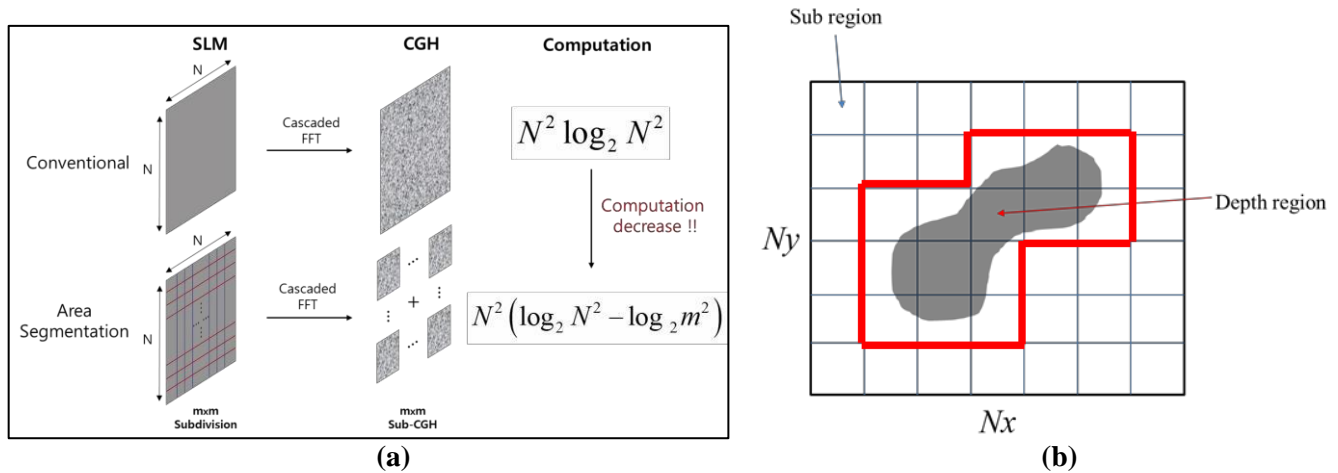


**Fig. 1. (a) Schematic of area segmentation method (b) Schematic of local area calculation method**

The proposed fast computation algorithm of the depth-map CGH assumes that the same object is created by CGH with multiple focus. Therefore, the FFT process of propagation from the pupil to the retina have been performed the same calculation process as different depth CGH which is located at the same distance from the eye. Consequently, it is not necessary to recalculate CGH when creating other CGH of different depth.

## Acknowledgment

This work was supported by Samsung Electronics Co., Ltd.

## References

1. T. Senoh, K. Yamamoto, R. Oi, T. Mishina, & M. Okui, Computer generated electronic holography of natural scene from 2D multi-view images and depth map, In Universal Communication, ISUC'08. Second International Symposium (2008).

# Comparison of LED and LD as a light source for near-eye holographic display

*Dukho Lee, Gang Li, Byounghyo Lee and Byoungho Lee\**

School of Electrical and Computer Engineering, Seoul National University, Gwanak-Gu Gwanakro 1, Seoul 151-744, Korea

\*byoungho@snu.ac.kr

**OCIS codes:** (090.2870) Holographic display; (090.1995) Digital holography

## 1. Introduction

Recently, as interest in augmented reality (AR) and virtual reality (VR) increases, the market for head mounted display is growing. Various research groups and companies are studying on near-eye displays, but it is not enough to be commercialized yet. The near-eye displays should offer wide viewing angle, fast frame rates, high resolution images, and small form factors, but the most important factor is to provide more natural 3D images so that users can watch the display for a long time without visual fatigue [1]. Various approaches using light field technique have been studied [2], but there is a fundamental limitation of wavefront approximation. Therefore, ultimately, the holographic display capable of fully reproducing wavefront should be applied to AR and VR systems. However, requirement of high coherence light source such as laser makes it difficult to develop a compact near-eye holographic display system.

In this paper, we compare light emitting diode (LED) and laser diode (LD) as a light source for near-eye holographic display to determine which light source is more suitable. To demonstrate better light source selection, several experiments which reconstruct holograms at different depth planes using the light sources are carried out.

## 2. Experiment analysis

There are two types of coherence: spatial coherence and temporal coherence. The former one determines the image contrast which increases as the size of the light source decreases. The latter one determines the depth range of holographic display while the high temporal coherence induces severe speckle noise. Thus, there is a trade-off between depth range and speckle noise in selecting coherence time. It is necessary to decide optimal coherence time for near-eye holographic display. Fig. 1 shows the coherence time versus spectral width graph of the light source. In the experiment, we used LED (Thorlabs, M530F2) and LD (Thorlabs, CPS532) light source shown in red circle and green circle in Fig. 1. The wavelengths of LED and LD are 530 nm and 532 nm, respectively, and the bandwidth (FWHM) of each light source is 30 nm and 0.8 nm, respectively. A holographic display system using a reflection type spatial light modulator (Jasper Display Corp., JD4704) is implemented as shown in Fig. 2.

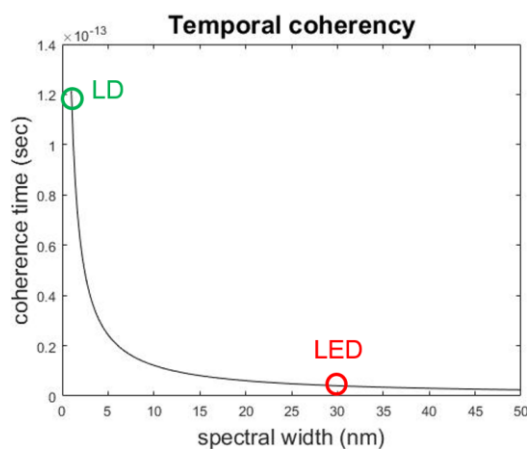


**Fig. 1. Coherence time of LED and LD**

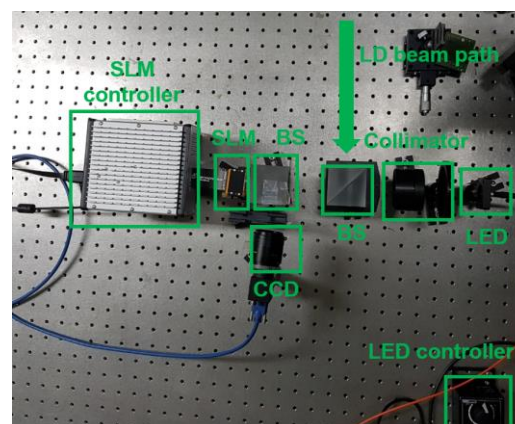


**Fig. 2. Experimental setup**



Fig. 3 shows the reconstruction images corresponding to different depths. Fig. 3(a) shows the case of using LED, and (b) shows the results of using LD. It is confirmed that the image can be reconstructed up to 170 mm depth using LED, and the severe speckle noise appear in the region farther than 280 mm using LD. If we combine an eye piece lens of focal length less than 170 mm and LED, images can be reconstructed from the eye piece lens plane to infinity depth without speckle noise [3].

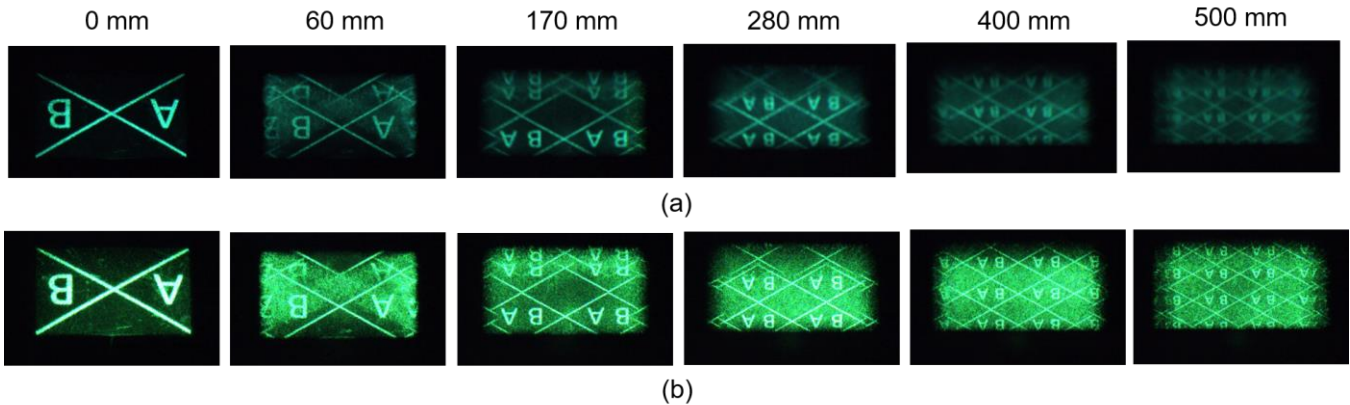


**Fig. 3. Reconstruction images using (a) the LED and (b) the LD light source**

### 3. Conclusion

In this paper, the LED and the LD are used as a light source of holographic display. When an LED light source with coherence length of 50 nm and a wavelength of 530 nm was used, images can be reconstructed up to 170 mm. In conventional near-eye holographic display system, the focal length of eye piece lens is shorter than 170 mm, so LED light source could be used for near-eye holographic display.

### Acknowledgment

This research was supported by Projects for Research and Development of Police Science and Technology under Center for Research and Development of Police science and Technology and Korean National Police Agency. (Grant No. PA-H000001)

### References

1. B. Lee, "Three-dimensional displays, past and present," *Phys. Today* **66**(4), 36-41 (2013).
2. S. Lee, C. Jang, S. Moon, J. Cho, and B. Lee, "Additive light field displays: realization of augmented reality with holographic optical elements," *ACM Transactions on Graphics* **35**(4), 60 (2016).
3. A. Maimone, A. Georgiou, J. S. Kollin, "Holographic near-eye displays for virtual and augmented reality," *ACM Transactions on Graphics* **36**(4), 85 (2017).



# Augmented-Reality Display for Supporting Ametropia using Maxwellian view and Edge Enhancement

Byounghyo Lee<sup>1</sup>, Seungjae Lee<sup>1</sup>, Dukho Lee<sup>1</sup>, Hee-Jin Choi<sup>2</sup> and Byoungho Lee<sup>1,\*</sup>

<sup>1</sup>School of Electrical and Computer Engineering, Seoul National University, Seoul 151-744, Korea

<sup>2</sup>Department of Physics, Sejong University, Seoul 143-747, Korea

\*byoungho@snu.ac.kr

**OCIS codes:** (170.0170) Medical optics and biotechnology; (110.6880) Three-dimensional image acquisition; (100.6890) Three-dimensional image processing.

## 1. Introduction

There are numbers of people who have the ametropia that an error of refraction occurs since the eye lens fails to form the focused image of objects. With recent rapid improvements in augmented reality (AR) head mounted display (HMD), some approaches to support the patients by enhancing or correcting the perceived view have been researched [1, 2]. These prior works, however, do not actively provide focused augmented views as changing the users focal states since the conventional optical elements in them form virtual image at a fixed depth. In this paper, we present ametropia supporting AR HMD with an edge enhanced Maxwellian view which forms a focused image on retinal surface despite the change of focal states of eye lens.

## 2. Principles and demonstration of the proposed method

The entire system is schematized in Fig. 1(a). Our system adopts a Maxwellian view system which consists of a laser projector, a collimating lens, a waveguide, and a holographic lens as shown in Fig. 1(b). The holographic lens functions as a see-through combiner [3]. After being collimated and guided, the virtual image forms the Maxwellian view through the holographic lens. The Maxwellian view directly projects the virtual image to the retina so that it can make a focused view regardless of focal states of the users. In addition, we process the virtual image to have higher contrast as enhancing the edge. Fig. 2 shows the experimental results of the proposed system. Figs. 2(a) and 2(b) indicate the perceived views without and with vision enhancement by the augmented images, respectively. We simulate the ametropia as changing the focal length of CCD lens to induce the blur. While the real-world views are expected to be seen blurred to the ametropia patients, the AR images can support the perception of environmental objects by providing a focused vision-aid images to all type of the patients as shown in Fig. 2(b).

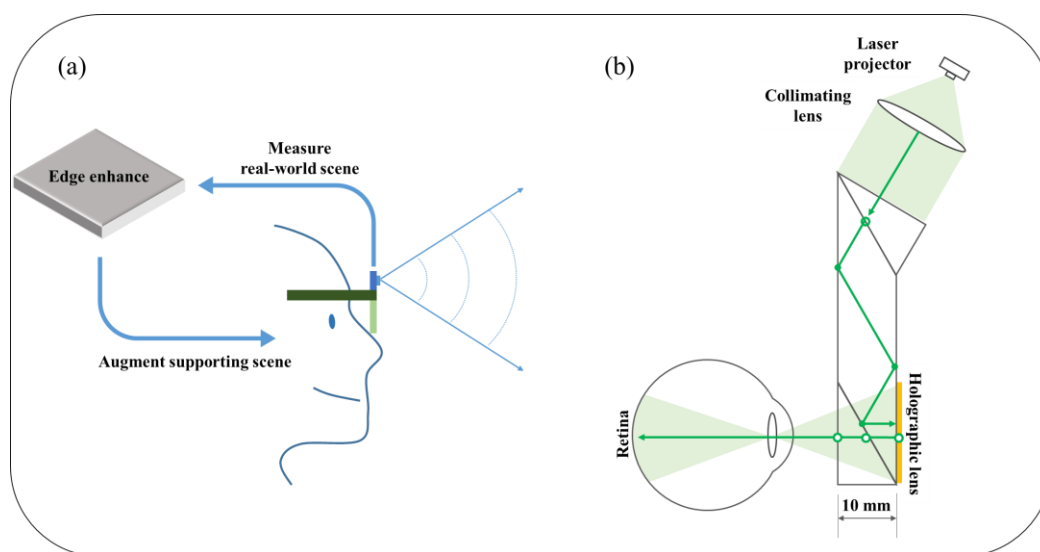


**Fig. 1. (a) The entire system of the proposed method. (b) The optical schematic of the proposed AR HMD.**

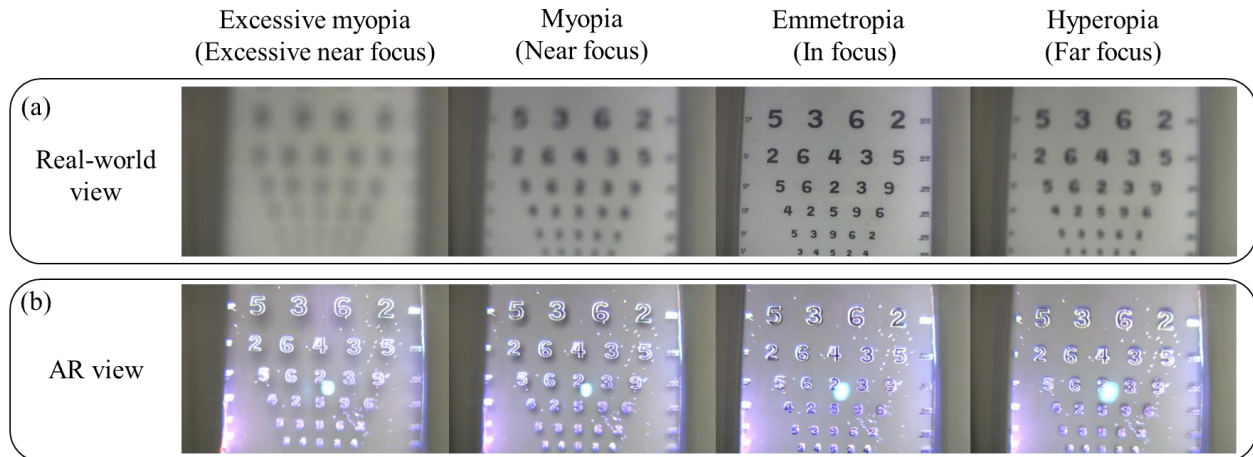


**Fig. 2. Experimental results. The perceived views of ametropic patient as changing the focal states (a) without and (b) with the proposed AR device.**

### 3. Conclusion

In this paper, we present an AR device that provides Maxwellian view using holographic lens. Since the holographic AR device can provide a Maxwellian view to make all in-focus virtual image for low vision aid, our prototype can support all types of the ametropia patients suffering from the error of refraction. Moreover, it improves the contrast of AR image by enhancing the edge components of real-world view.

### Acknowledgment

This work was supported by Institute for Information & Communications Technology Promotion (IITP) grant funded by the Korean government (MSIT) (No. 2017-0-00787, Development of vision assistant HMD and contents for the legally blind and low visions).

### References

1. A. D. Hwang and E. Peli. "Augmented edge enhancement for vision impairment using Google glass," *SID Symposium Digest of Technical Papers* **45**, 305-307, (2014).
2. F.-C. Huang *et al.*, "Eyeglasses-free display: towards correcting visual aberrations with computational light field displays," *ACM Transactions on Graphics (TOG)* **33**(4), 59 (2014).
3. S. Lee, B. Lee, J. Cho, C. Jang, J. Kim, B. Lee, "Analysis and implementation of hologram lenses for see-through head-mounted display," *IEEE Photonics Technology Letters* **29**(1), 82-85 (2017).

## Apparatus for measuring large field of view embossed hologram

*Sunggyun Ahn, Geunseop Choi, Mugeon Kim and Joonku Hahn*

School of Electronics Engineering, Kyungpook National University, 80 Daehak-ro, Buk-gu, Daegu, 41566, South Korea

Tel.: 82-53-950-5514, E-mail: [jhahn@knu.ac.kr](mailto:jhahn@knu.ac.kr)

**OCIS codes:** (090.1760) Computer holography; (090.6186) Spectral holography

In recent years, various holograms have been proposed. Among them, nano-structured imprinting hologram is one of promising hologram in commercial aspect. Since it needs simple manufacturing process, it can be supplied at low price and be a popular for the public. Then, when we try to measure the hologram, there are some limitations due to high resolution holograms with the size of 25mm x 25mm and 1 $\mu$ m pixel pitch. A lens with high numerical aperture and a camera with high resolution are necessary for measurement. To solve this problem, the method to rotate the camera with telecentric lens was proposed. It operates as a bandpass filter and accept only narrow bandwidth. Without the high NA lens and the high resolution camera, it is possible to measure the reconstruction images. But, the rotating of observation part may also makes some problems. For example, if a large scale sample is concerned, the size of lens and observation part will matter and it is difficult to rotate the heavy observation part.

So we propose a new system to rotate the specimen including the light source. The movement of specimen makes it possible to obtain the angular spectrum of hologram without high NA lens. Furthermore, we can replace the light source, collimation lens and pinhole. It allows to change the coherence, the divergence and the wavelength of the light source. The spherical bearing is also customized for large rotation angle of the specimen.

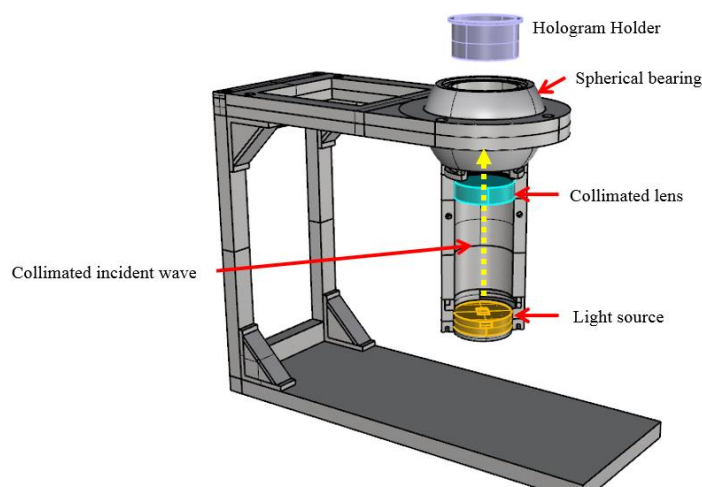


**Fig. 1. A schematic of apparatus for measuring large field of view embossed hologram**

### Acknowledgment

This work was supported by the Industrial Strategic technology development program (10052641) funded by the Ministry of Trade, Industry & Energy (MI, Korea).

### References

1. J. Hong, Y. Kim, H.-J. Choi, J. Hahn, J.-H. Park, H. Kim, S.-W. Min, N. Chen, and B. Lee, "Three-dimensional display technologies of recent interest: principles, status, and issues," *Appl. Opt.* **50**, H87-H115 (2011).
2. L. Dong, J. Tian, "An accurate calibration method for a camera with telecentric lenses," *Optics and Lasers in Engineering* **51**(5), 538-541(2013).
3. W. Moon, J. Kwon, H. Kim and J. Hahn, "Electronic holographic device based on macro-pixel with local coherence," *Proc. SPIE* **9626**, 51-56 (2015).

# Time division multiplexed holographic display using electronic beam steering method

Hyun-Eui Kim<sup>1</sup>, Min-Sik Park<sup>1</sup> and Jinwoong Kim<sup>1</sup>

<sup>1</sup>Electronics and Telecommunications Research Institute, Korea

E-mail: turnn@etri.re.kr

**OCIS codes:** (909.1995) Digital holography; (090.2970) Holographic display

We propose a time division multiplexed(TDM) holographic display structure with electronic beam steering method using SLM. The holographic display structure of the TDM scheme is continuously studied by many groups<sup>1,2</sup> as a method of expanding SBP through optical scanner. In this way, the optical scanner is a major component that greatly affects performance, such as reconstructed image size or viewing angle of the display. In the conventional TDM method, the mechanical scanning methods of changing the direction of the beam combined with the actuator and the mirror were used to achieve the desired result of viewing angle or reconstructed image size expansion. However, mechanical scanning methods have problems such as mechanical complexity, low reliability, high power consumption, narrow beam steering area, and phase aberration in the wavefront of a steered beam. We have solved the disadvantages of the above-mentioned mechanical beam steering system by using electronic beam steering using SLM.

The beam steering was performed using a phase SLM with a single-dimensional array, and applied to the holographic display structure to extend the horizontal viewing zone. The wrapped phase profile to steer the beam in an arbitrary direction  $\alpha$  is derived from  $\varphi_n(\alpha) = 2\pi/\lambda \cdot x_n \sin \alpha + \varphi_0$ . Where  $\varphi_n(\alpha)$  is a wrapped phase profile with arbitrary steering angle  $\alpha$ ,  $x_n$  is the spatial coordinate in the SLM, and  $\varphi_0$  is the arbitrary constant phase offset.  $\lambda$  is the wavelength of the light source. The obtained phase profile is quantized according to the modulation level of SLM. Figure 1 is a schematic of a holographic display applying the principle of the proposed method.

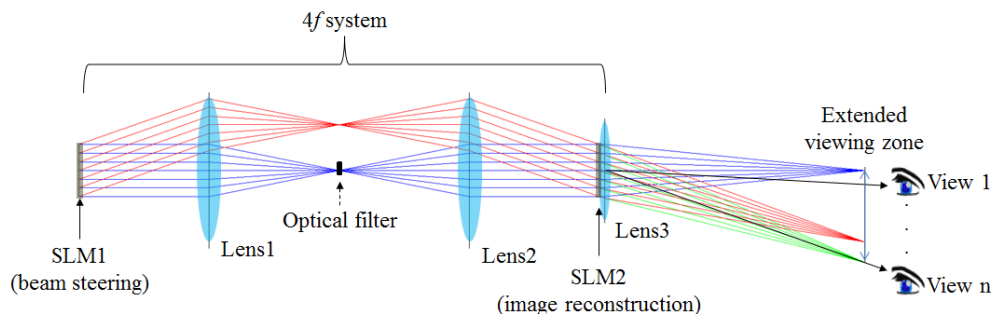


**Fig. 1. Schematics of proposed holographic display**

## Acknowledgment

This work was supported by 'The Cross-Ministry Giga KOREA Project' grant funded by the Korea government(MSIT) (GK17D0100, Development of Telecommunications Terminal with Digital Holographic Table-top Display)

## References

1. H. Kang, et al. *Digital Holography and Three-Dimensional Imaging*. Optical Society of America, p. DM3E. 5 (2016)
2. Y. Takaki, et al. *Optics express* 24.16 (2016)

# Improving the image quality of a digital holographic display system by estimating a virtual spatial light modulator plane

*Yongjun Lim, Keehoon Hong, Minsik Park and Jinwoong Kim*

5G Giga Communication Research Laboratory, Electronics and Telecommunications Research Institute, 218 Gajeong-ro Yuseong-gu Daejeon 34129, South Korea

Tel.:82-42-860-5984, E-mail: yongjun@etri.re.kr

**OCIS codes:** (090.0090) Holography; (090.1995) Digital holography

In a general digital holographic display system, it is necessary to filter out unwanted signals given by high-order diffraction components and a direct current(DC) component emanating from spatial light modulators(SLMs) when illuminated by coherent light sources. To achieve this,  $4-f$  optics configuration is conventionally applied, and the imaged plane after passing through the  $4-f$  optics is required to be estimated. In specific, the digital holographic system fundamentally based on a viewing window depends on the imaged SLM plane, or the virtual SLM plane [1,2]. Here, we are to estimate the virtual SLM plane by adopting two methods. One is a non-interferometric method, and the other is an intrerferometric method. After capturing the virtual SLM plane by adopting those two methods, we try to find degrading factors and to improve the reconstructed hologram image by compensating for them.

In Fig. 1(a), the experimental setup is shown, where both the interferometric method and the non-interferometric method are established to estimate the virtual SLM plane. In our experiment, a digital micro-mirror device(DMD), which has the minimum pixel pitch of  $13.68\ \mu\text{m}$  and the resolution of  $1024 \times 768$ , is used as an SLM. Two lenses with the focal length of  $180\ \text{mm}$  and one spatial filter inserted between them constitute  $4-f$  optics configuration, so the unwanted signals can be filtered out. The captured image of the virtual DMD plane is shown in Fig. 1(b). After analyzing the captured image of the virtual DMD plane, we tried to improve the image quality of the reconstructed hologram. Fig. 1(c) shows the reconstructed hologram image before improvement, and Fig. 1(d) is the one after improvement.

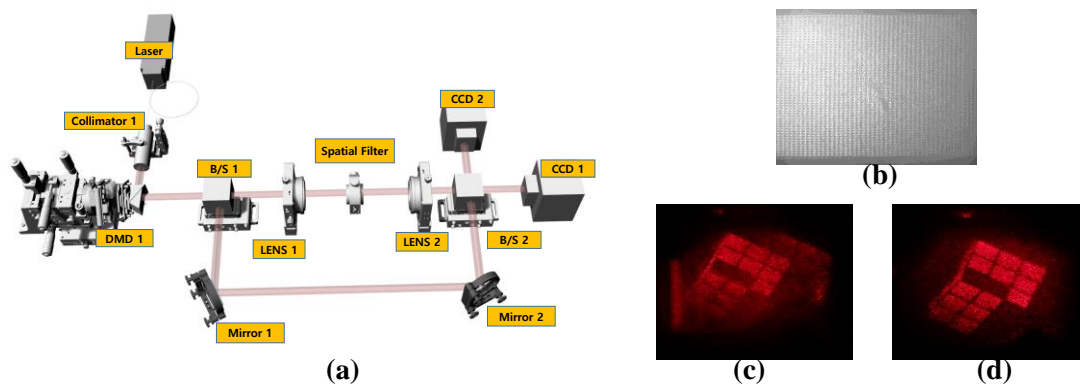


**Fig. 1. (a) Experimental setup (b) Captured image of a virtual DMD plane (c) Reconstructed hologram (before compensation) (d) Reconstructed hologram (after compensation)**

## Acknowledgment

This work was supported by ‘The Cross-Ministry Giga KOREA Project’ grant from the Ministry of Science, ICT and Future Planning, Korea.

## References

1. R. Häussler, S. Reichelt, N. Leister, E. Zschau, R. Missbach, A. Schwerdtner, Proc. SPIE 7237, Stereoscopic Displays and Applications XX, 72370S (2009)
2. Y. Lim, K. Hong, H. Kim, H. Kim, E. Chang, S. Lee, T. Kim, J. Nam, H. Choo, J. Kim, and J. Hahn, *Opt. Express*, 24(22), 24999-25009 (2016).

## 3D Smart Table Display

*Sang-Hyeok Mun, Muhan Choi\**

**School of Electronics Engineering, Kyungpook National University, Daegu 41566, South Korea**

*\*Tel.:82-53-950-5520, E-mail: mhchoi@ee.knu.ac.kr*

**OCIS codes:** (110.6880) Three-dimensional image acquisition

We devised and produced a 3D Smart Table that could transform the appearance according to needs and requests of the users. The size of the outer frame made of wood is  $700 \times 700 \times 410$  in millimeters, and the size of each block inside is  $40 \times 40 \times 80$  in millimeters. The array structure of the block has a square shape as a whole. In a row, 15 blocks are arranged and 15 blocks are arranged in a column. The driving part of the servo motor moves 180 degrees from the bottom to the top. The wire connecting the servo motor to each block turns the circular motion of the servo motor into a linear movement of the block, allowing each block to move up and down to 4 centimeters.

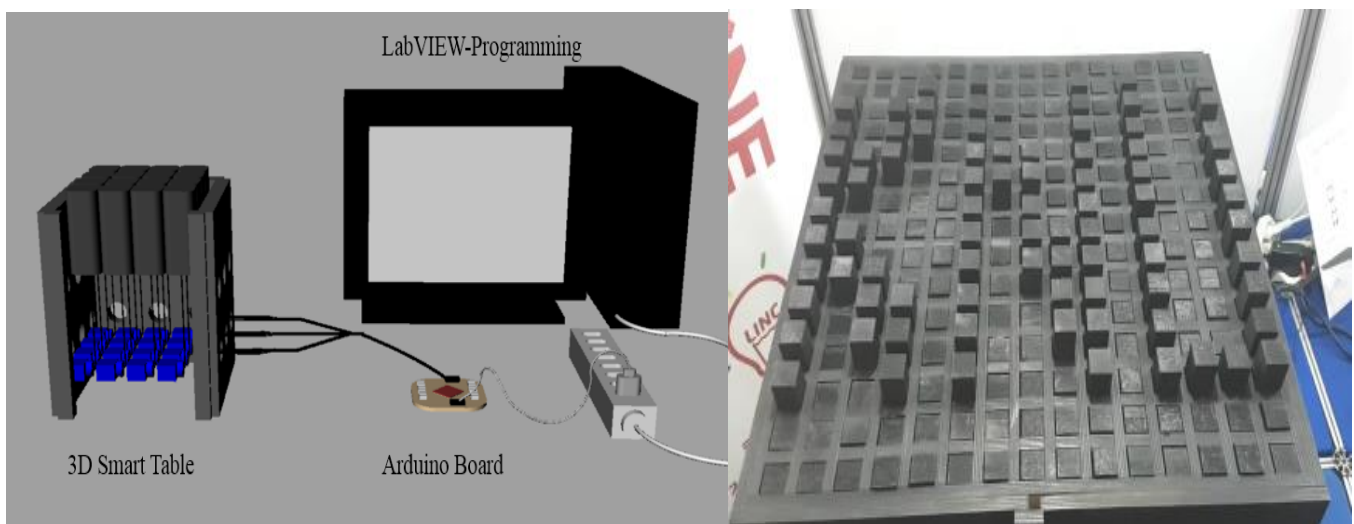


**Fig. 1. 3D Smart Table with Block Structure**  
( Control system of structure and 3D Smart Table showing the letters 'KNU' )

Control of the 3D Smart Table is realized by interlocking the structure with the Arduino board and LabVIEW programming. The 225 servo motors are divided into 9 parts and connected to 9 servo motor controllers (Arduino boards). These 9 servo motor controllers are driven by LabVIEW programming, and each servo motor-block part is individually controlled.

We designed a 3D Smart Table that can be changed in appearance to suit individual characteristics and can be used semi-permanently. When IoT (Internet of things) technology is associated with furniture, it would be interesting to apply 3D Smart Table to it. We think it is meaningful that we have implemented a 3D display of analog ideas.

### References

1. G. W. Johnson, LABVIEW GRAPHICAL PROGRAMMING, *McGraw-Hill*, Now York, (1997).
2. S. B. Hong, RHINO 3D 4.0, *TaeHakWon*, (2008)
3. Monk, Simon, Programming Arduino, *McGraw-Hill*, (2016)



## Tunable Graphene Metasurface Applicataion

*Yong-Hoon Lee, Sang-Hyeok Mun, Inbo Kim and Muhan Choi\**

School of Electronics Engineering, Kyungpook National University, Daegu 41566, South Korea

\*Tel.:82-53-950-5520, E-mail: mhchoi@ee.knu.ac.kr

**OCIS codes:** (090.1760) Computer holography

The focal length of a lens is determined by its geometric structure. Recently to overcome this limitation, meta-lens technology for controlling path of light wave through the spatial properties and the surface properties at the interface of medium has been actively studied. However, it is impossible to actively control the transmission characteristics including the focal length because the unit atoms constituting the conventional meta-lens consist of nanoscale structures made of metal or dielectric

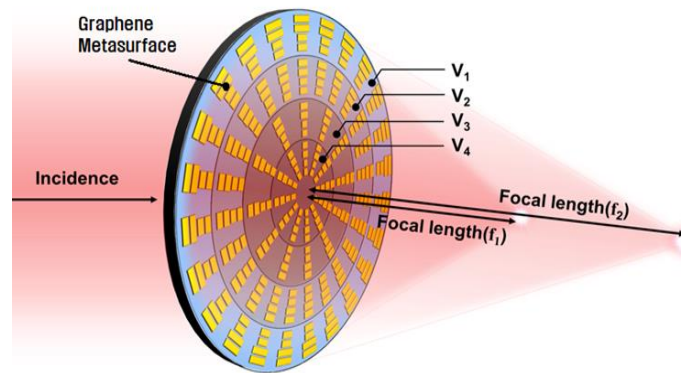


**Fig. 1. Terahertz Graphene Meta-lens**

In this study, we try to actively control the electrical properties of the meta-surface in block units by replacing the metal and dielectric unit atoms with metal and graphene. To do this, it is necessary to establish high-precision transferring technology of graphene. And it is also required to adjust the phase shift to  $2\pi$  through optimal meta-atom design which enables effective gate control and maximizes changes in optical characteristics. Through the ion-gel patterning we control the gate voltage of the each graphene meta-atom block individually. The large scale transferring of graphene is performed by polydimethylsiloxane (PDMS) stamp technique and it is used to enable precise transfer on the substrate of the meta-lens. Based on polarization-independent meta-atom design, we also implement a meta-lens that operates regardless of the polarization of the incident wave. The variable focus meta-lens we are aiming for is very thin and can be driven at super high speed. So it is expected that this active meta-lens with graphene patterning will be applied to various devices in terahertz and mid-infrared range.

### References

1. Muhan Choi, Seung Hoon Lee, et al., *Nature*, 470, 369 (2011)
2. Seung Hoon Lee, Muhan Choi, et al., *Nature Materials*, 11, 936 (2012)
3. Keun Soo Kim, Yue Zhao, et al., *Nature*, 457, 706 (2009)
4. Lei Zhang, Ghengtao Mei, Cheng-Wei Qiu, *Adv. Optical Mater.*, 4, 818 (2016)

# Compressive holographic optical sectioning

*Junkyu Yim, Seungwhi Yoo, and Sung-Wook Min*

Dept. of Information Display, Kyung Hee University, 26 Kyunghee-daero, Dongdaemun-gu, Seoul 130-701, Korea

*E-mail: mins@khu.ac.kr*

**OCIS codes:** (110.6880) Three-dimensional image acquisition; (100.6890) Three-dimensional image processing; (090.1760) Computer holography

Compressive holography enables us to reconstruct the voxels of three-dimensional volume with the high probability provided those are sparse at the certain domains and the system matrix satisfies the restricted isometry property(RIP) condition [1]. With the restricted number of measurements equal to the sensor pixel numbers, it is possible for getting better 3D reconstruction compared to Fresnel back propagation, where the sectional 2D planes are reconstructed by the multiplication with the interference pattern signal and the conjugation of quadratic phase terms. Specifically, the bounds for the reconstruction of Fresnel holography are investigated as follows [2]:

$$S \leq 0.5(1 + 1/\mu) \quad (1)$$

where the  $S$  is the number of the non-zero elements of 3D object signal(voxels) and  $\mu$  is the coherence term. The coherence term is the significant index which means the maximum correlation between the point spread functions of 2D sectional planes if the reconstruction process is conducted at the spatial domain. As shown in the equation (1), the lower coherence, the better reconstruction in the compressive holography. In terms of the optical sectioning, we can get the higher axial resolution with the lower coherence. If only two section planes are considered, the sensing mechanism of Fresnel holography can be expressed as the vector-matrix multiplication form:

$$g = \Phi f = [\Phi_1 \Phi_2] \begin{bmatrix} f_1 \\ f_2 \end{bmatrix} \quad (2)$$

where the  $g$  is the interference pattern,  $\Phi$  the sensing matrix, and  $f$  the section plane. In this case, the coherence is the maximum correlation between two sensing matrices  $\Phi_1$  and  $\Phi_2$ .

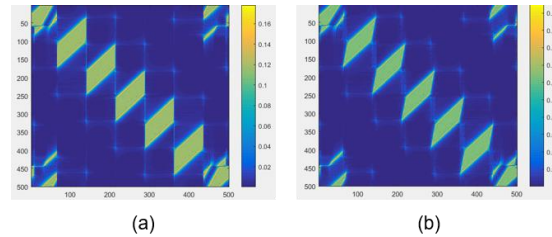


**Fig. 1. System matrices for two section planes**

Figure 1 shows the system matrices of Fresnel holography for two different section planes. Each matrix is the multiplication of the toeplitz matrices such as some propagation matrices and lens phase matrix. In this case, coherence is the similiarity between two matrices. We can adjust the numerical aperture of the optics system or increase the distance between two section planes to get the low coherence. Therefore, the axial resolution of the system can be further with the same measurements(sensor pixel numbers).

## Acknowledgment

This work was supported by 'The Cross-Ministry Giga KOREA Project' grant funded by the Korea government(MSIT) GK17C0200, Development of Full-3D Mobile Display Terminal and its Contents)

## References

1. David J. Brady, Kerkil Choi, Daniel L.Marks, Ryoichi Horisaki and Sehoon Lim, "Compressive Holography", Opt.Express, 17, pp.13040-13049 (2009).
2. Tianlong Man, Yuhong Wan, Fan Wu, and Dayong Wang, "Self-interference compressive digital holography with improved axial resolution and signal-to-noise ratio", Appl.Opt. 56, pp.F91-F96, (2017).

# Digital Holographic Tabletop display with vertical parallax by pupil tracking

*Jaehan Kim, Hyongon Choo, Minsik Park and Jinwoong Kim*  
 Digital Holography Research Section, ETRI, 218 Gajeong-ro, Daejeon, Korea  
 Tel.:82-42-860-1061, E-mail: [kimjhan@etri.re.kr](mailto:kimjhan@etri.re.kr)

**OCIS codes:** (090.2870) Holographic display; (090.5694) Real-time holography

We have implemented a holographic display capable of viewing 360 degrees in a horizontal direction by horizontally concatenating many holograms with a narrow viewing angle using a spatio-temporal multiplexing method[1][2]. In addition, vertical parallax was provided by using the pupil tracking method to find the 3D position of the eye and streaming technique of the hologram data at the corresponding position.

In this paper, we describe the structure and method of providing vertical parallax in holographic display as shown in Fig.1. According to the proposed method, a holographic display with vertical parallax using pupil tracking information is implemented as shown in Fig.2. In order to verify the proper operation, we reconstructed different holograms according to the six-step elevation angle of the pupil position, and finally confirmed the required functions for the vertical parallax.

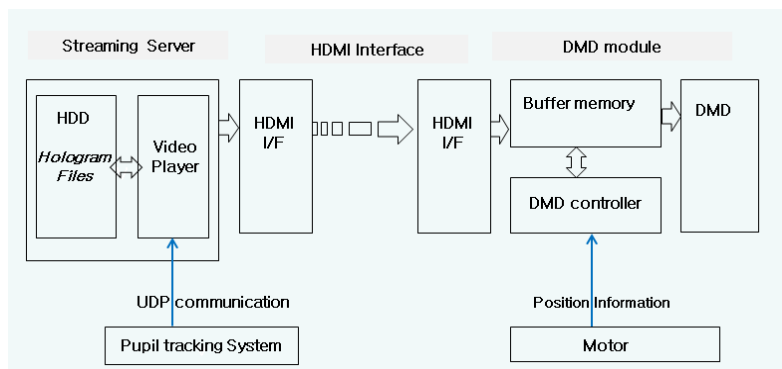


**Fig. 1. Functional block diagram for providing vertical parallax on the holographic display**

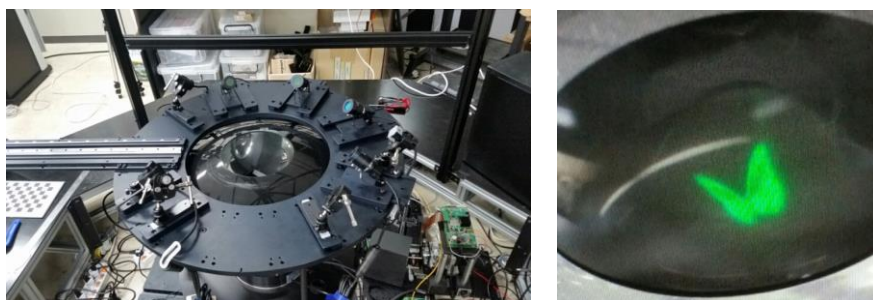


**Fig. 2. Digital holographic table-top display system with vertical parallax**

## Acknowledgment

This work was supported by ‘Giga KOREA Project’ granted from the Ministry of Science and ICT, KOREA. (GK-17D0100 : Development of Telecommunications Terminal with Digital Holographic Tabletop Display)

## References

1. J. Kim, K. Hong, Y. Lim, J-H Kim, and H-G Choo, *IDW'16*, 3D1-1 (2016).
2. J-H. Kim, K. Seol, E. Chang, K. Hong, H. Kim, M-S. Park, and J. Kim, *IMID2017*, P2-228 (2017).

## Optical design of table-top light field display

*Kwangsoo Kim, Daerak Heo, and Joonku Hahn*

School of Electronics Engineering, Kyungpook National University, 80 Daehak-ro, Buk-gu, Daegu 41566,  
South Korea

*Tel.:82-53-950-5514, E-mail: jhahn@knu.ac.kr*

**OCIS codes:** (100.6890) Three-dimensional image processing; (220.0220) Optical design and fabrication.

Table-top three-dimensional (3D) displays have a potential to change a flat table-top into 3D space. These displays require large field of view in comparison of 3D display on the wall since the observer watches the display at the end of the table. Various technologies have been applied to table-top style displays. S. Yoshida implemented his display with plural small projectors to form multiple views[1] and Y. Lim et. al suggested a table-top holographic display with a high speed spatial light modulator[2]. Light field method with microlens array has a benefit to make the system thin due to its scalability[3] and it may be possible to replace the top plate of the table with 3D display.



**Fig. 1. Concept of table-top light field display.**

Figure 1 shows a concept of Table-top light field display. This system is currently under construction and it consists of plural small projectors in order to realize high resolution image on the screen and then light field is formed by micro-lens array. In this system, we designed the optical components including additional projection lens attached to a conventional projector and micro-lens array for defining directions of views.

### Acknowledgment

This work was supported by Civil-Military Technology Cooperation under Project Number 16-CM-DP-06.

### References

1. S. Yoshida, "fVisiOn: interactive glasses-free tabletop 3D images floated by conical screen and modular projector arrays," SIGGRAPH Asia 2015 Emerging Technologies (SA '15), p. 12.
2. Y. Lim, K. Hong, H. Kim, H. Kim, E. Chang, S. Lee, T. Kim, J. Nam, H. Choo, J. Kim, and J. Hahn, "360-degree tabletop electronic holographic display," *Opt. Express* **24**, 24999-25009 (2016).
3. Thomas L. Burnett, "Light-field Display Architecture and the Challenge of Synthetic Light-field Radiance Image Rendering," *SID Symposium Digest of Technical Papers* **48**, 899-902 (2017).

# Augmented Reality Near-eye Light-field 3D Display Using Retroreflector

*Hyeongkyu Do, Young Min Kim, Hyunsik Sung, Ki-Hong Choi, Sungwon Choi and Sung-Wook Min*

**Dept. of Information Display, KyungHee University, Seoul, Korea**

*E-mail: mins@khu.ac.kr*

**OCIS codes:** (120.2040) Displays; (120.2820) Heads-up displays; (120.4570) Optical design of instruments; (330.7338) Visually coupled optical systems; (110.6880) Three-dimensional image acquisition.

We propose an augmented reality near-eye light-field three-dimensional display system which leads the accommodation cue. This system has simple optical components such as pinhole array, aperture, lens, and etc., which are compared with the complex optical components like the freeform lens or the holographic optical elements.

By the retroreflector and the beam splitter, the conjugated images of the display, and aperture are formed inside of the human eye. Because the eye pupil restricts the light-field, the 2 mm aperture which is smaller than the minimum human eye pupil diameter can ignore the eye pupil size change. The pinhole array that has 1.104 mm pitch and 0.184 mm size of the hole is used for imaging component in specific depth plane by integral imaging. The image source is 5.46" full-color liquid crystal display (LCD) panel with 3840\*2160 pixels. The lens used for the improvement of the image sharpness has 75.4 mm focal length which is the distance from the display to the aperture. The distance from display to pinhole array is 42 mm.

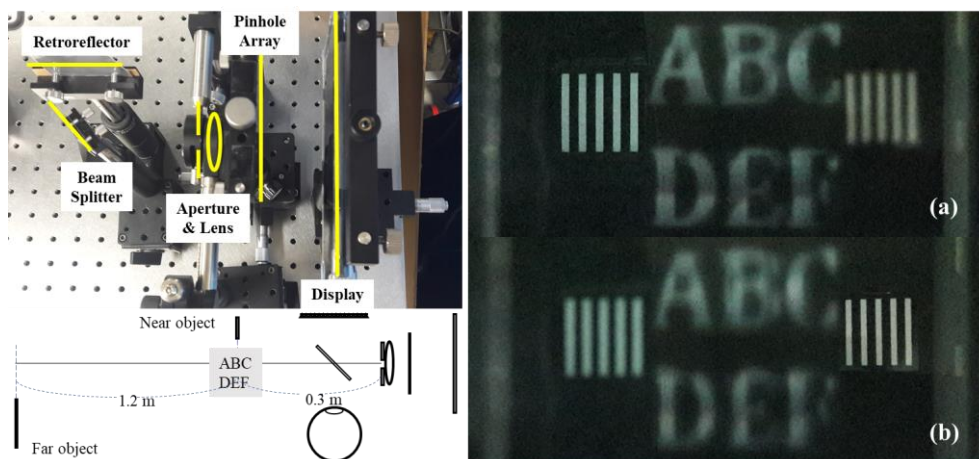


**Fig. 1. Experimental setup (left) and result (right)**

The experimental setup and results are shown in fig. 1. The stripe object in fig. 1 is left to right reversal image caused by the beam splitter, so left stripe is 0.3 m near object and right stripe is 1.5 m far object. The alphabet in middle of the result is the integrated image that has accommodation in 0.3 m. When the camera focuses on near stripe object, in fig. 1-(a), the alphabet image is focused. But the camera focus is on 1.5 m far object, the alphabet image is defocused with near object, shown in fig. 1-(b).

## Acknowledgment

This work was supported by the National Research Foundation of Korea(NRF) grant funded by the Korea government(MSIT) (No.2011-0030079)

## References

1. H. Hua and B. Javidi, *Opt. Express* 22, 13484-13491 (2014).
2. A. Maimone, D. Lanman, K. Rathinavel, K. Keller, D. Luebke, and H. Fuchs, in *ACM SIGGRAPH Emerging Technologies*, 20 (2014)
3. A. Maimone, A. Georgiou, and J. S. Kollin, *ACM Trans. Graph*, 36, 4, Article 85 (2017)



# Improvement in Phase Pattern Design for Holographic Shack-Hartmann Wavefront Sensor with High Sensitivity

*Yusuke Saita and Takanori Nomura*

Faculty of Systems Engineering, Wakayama University, 930 Sakaedani, Wakayama, 640-8510, Japan  
Tel.: +81-73-457-8184, E-mail: [saita@sys.wakayama-u.ac.jp](mailto:saita@sys.wakayama-u.ac.jp)

**OCIS codes:** (090.2890) Holographic optical elements; (120.3940) Metrology; (120.5050) Phase measurement

A Shack-Hartmann wavefront sensor (SHWFS) which is composed of a microlens array and an image sensor is a well-known way to measure wavefront aberrations in an adaptive optics system widely used in astronomical and bio-medical fields<sup>1,2</sup>. An SHWFS has two important parameters to evaluate its capability. One is the dynamic range which indicates the maximum measurable wavefront gradient and depends on the focal length of a microlens array, the other is the sensitivity. The latter indicates the minimum detectable wavefront gradient and also depends on the focal length of a microlens array. Although the longer focal length leads to higher sensitivity, the dynamic range becomes smaller conversely. It is not easy that these parameters are compatible due to this trade-off relationship. We have proposed the dynamic range expansion method without dependence on the focal length, which is called the holographic Shack-Hartmann wavefront sensor (H-SHWFS)<sup>3</sup>. In this study, we try to improve the sensitivity without decreasing the dynamic range by using the H-SHWFS.

The H-SHWFS has an arrangement of individually-designed computer-generated phase holograms (microhologram array) instead of a conventional microlens array. The discriminable patterns are obtained as reconstructed images from a microhologram array in an image sensor plane, and the expansion of the dynamic range is achieved owing to the patterns. It is possible to improve the sensitivity without decreasing the dynamic range by the H-SHWFS with longer focal length. However, the size of patterns becomes larger, and adjacent patterns are subject to be overlap in the condition. To solve the problem, the design method of a microhologram array is modified from the Fourier transform type to the lightwave propagation one based on the angular spectrum. Figure 1 shows the reconstructed patterns from a microhologram array designed by the modified design method. Although the size of dots constructing a pattern is larger as the focal length is longer, the whole size of patterns is almost invariant.

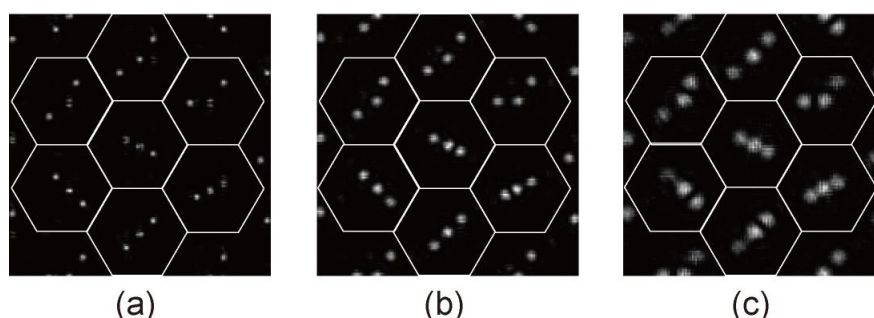


**Fig. 1. Reconstructed patterns from modified microhologram arrays with the focal length of (a) 7mm, (b) 14mm, and (c) 21mm.**

The numerical simulation was demonstrated to confirm the high sensitivity by the H-SHWFS with longer focal length. As a result, the focal length of 14mm was better than one of 7mm. However, the low quality of the pattern with 21mm degraded the sensitivity through the reduction of the measurement accuracy. In the longer focal length, shapes of the patterns must be robust for the low image quality.

## References

1. H. Takami, *et al.*, Publ. Astron. Soc. Japan **56**, 225 (2004).
2. D. X. Hammer, *et al.*, Opt. Express **14**, 3354 (2006).
3. Y. Saita, *et al.*, Optica **2**, 411 (2015).



# GPU acceleration of hologram calculation using an orthographic ray-sampling plane

*Shunsuke Igarashi<sup>1</sup>, Tomoya Nakamura<sup>1,2</sup>, Kyoji Matsushima<sup>3</sup>, and Masahiro Yamaguchi<sup>1</sup>*

<sup>1</sup>School of Engineering, Tokyo Institute of Technology, Yokohama, Kanagawa, 226-8503, Japan

Tel.: +81-45-924-5296, E-mail: [igarashi.s.ab@m.titech.ac.jp](mailto:igarashi.s.ab@m.titech.ac.jp)

<sup>2</sup>PRESTO, Japan Science and Technology Agency, Chiyoda, Tokyo 102-0075, Japan

<sup>3</sup>Faculty of Engineering Science, Kansai University, Suita, Osaka, 564-8680, Japan

**OCIS codes:** (090.1760) Computer holography; (090.2870) Holographic display; (090.1995) Digital holography

## Abstract

Calculation of large-scale (over 10 gigapixels) holographic displays in high-resolution and realistic appearance is a difficult problem in terms of computational cost. We previously proposed an algorithm using an orthographic ray-sampling plane to calculate such holograms. In this paper, the calculation is accelerated by efficiently utilizing a GPU. The proposed method enables us efficient calculation on GPUs by the division of the input light-ray data of 3D objects. In the experiment, a 128K × 128K hologram was computed and the acceleration effect of the proposed method was verified comparing computational time with the calculation only using a CPU. The generated fringe pattern was fabricated as an amplitude mask. We confirmed a realistic and detailed 3D image is reconstructed through the generated hologram.

## 1. Introduction

Holographic 3D display satisfies all depth cues by reconstructing the wavefront from objects. In principle, it is possible to display 3D objects in their actual size and distance even if the objects are large and at far away from the hologram. However, synthesis of such computer generated holograms (CGHs) is not realized because of the computational load. Especially in case of large-scale, realistic and detailed objects, a new method must be invented.

The difficulty of calculating the large-scale and realistic holographic display comes from the required sampling number of the wavefront and the computational complexity of the simulation of its propagation. If we adequately sample a 100mm × 100mm wavefront in  $\pm 30$  degrees, it should be sampled in  $0.5\mu\text{m}$  pitch when the color is green. This means the wavefront data is sampled as  $40 \times 10^9$  points. Simulation of wave propagation in this scale takes infeasible time. We previously proposed a calculation method to generate such holograms using an orthographic ray-sampling (ORS) plane [1], however, it still takes 13 hours to compute 128K × 128K holograms.

In this paper, we utilized a GPU to accelerate the calculation of the ORS plane method. We confirmed the proposed method takes 1 hour to compute the 128K × 128K hologram, which is 13 times faster than our previous method. The generated fringe pattern was fabricated as a binary amplitude mask. We also confirmed that a realistic and detailed 3D image is reconstructed through the hologram.

## 2. ORS plane method and its acceleration using GPUs

Schematic of the proposed method is shown in Fig. 1. In the CGH calculation using ORS plane, a plane is defined near the objects, and parallel light-rays emitted from the target object are sampled. The sampled light-rays correspond to orthographic images. In other words, an orthographic image is a set of spatially distributed parallel light-rays. In this method, orthographic images are captured from various angles in order to obtain the light-field passing through the ORS plane. Each captured orthographic image physically corresponds to discontinuously sampled wavefront propagating toward a certain angle, thus the Fourier transform of an orthographic image is a small region of Fourier transformed whole wavefront at the ORS plane, which also means the angular spectrum of objects. After the ray sampling, fast Fourier transform (FFT), the spectrum is multiplied with the transfer function for wave propagation. The transfer function derived from Fresnel propagation, shifted angular spectrum method, or any other wave-propagation model can be adapted. Finally, the wavefront at the hologram is obtained by inverse FFT after the multiplication of the transfer function. In this paper, the hologram plane is divided into small number

of pixel to efficiently utilize a GPU.

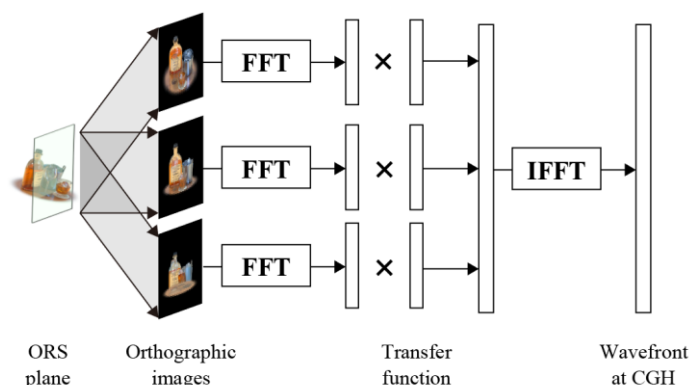


**Fig. 1. Schematic of CGH calculation using an orthographic ray-sampling plane.**

### 3. Experimental results

In the experiment, we calculated a  $128K \times 128K$  hologram. In the calculation using only a CPU, the hologram is divided into  $8 \times 8$  blocks. The calculation time of fringe pattern except the rendering time was around 13 hours. Note that we used an Intel Core i7 4790K CPU (4.0 GHz) and a 32GB RAM and around 6 hours for rendering time in both methods. In the calculation using a GPU additionally, the hologram was divided into  $64 \times 64$  blocks that have  $2048 \times 2048$  pixels. Each hologram tile was computed by a GPU (GeForce GTX 980), and the calculation time was around 1 hour, which was 13 times faster than the CPU case.

The generated CGH was fabricated as an amplitude mask by the laser-lithography technique of Kan-Dai Digital Holo Studio [2]. The pixel pitch of the mask is  $0.8\mu\text{m}$ , which achieves  $\pm 23.3$  degrees of viewing angle for a red light. A 3D image reconstructed from the hologram illuminated by the laser light was shown in Fig. 2. A realistic and detailed  $100\text{mm} \times 60\text{mm} \times 50\text{mm}$  3D image is reconstructed through the generated hologram. The 3D object is 80mm away from the hologram plane and the resolution of the 3D object is still high even in the distance.



**Fig. 2. Optical reconstruction of a 3D image from the hologram generated by the proposed method.**

### 4. Conclusion

We proposed an efficient method of calculating large-scale CGHs that reconstruct realistic and detailed 3D objects using GPUs. The efficiency of the proposed method is confirmed by comparing the computational time with the previous method. The feasibility of reconstructing high-quality 3D images is also demonstrated by the experiment.

A part of this work was supported by the MEXT strategic research foundation at private universities (2013–2017) and Kan-Dai Digital Holo-Studio in Kansai University.

### References

1. S. Igarashi, T. Nakamura, and M. Yamaguchi, “Fast method of calculating a realistic hologram based on orthographic ray-wavefront conversion,” *Opt. Lett.* **41**, 1396–1399 (2016).
2. Kansai University, “Kan-Dai Digital Holo Studio,” <http://holography.ordist.kansai-u.ac.jp/digitalholostudio>

# Angular spectrum convolution based occlusion processing in computer generated hologram

*Mehdi Askari and Jae-Hyeung Park\**

Dept. of Information and communication Engineering, Inha University, 100 Inha-ro, Nam-gu, Incheon, 22212, South Korea

Email: [\\*jh.park@inha.ac.kr](mailto:*jh.park@inha.ac.kr)

OSIC codes: (090.1760) Computer holography

In this paper, we propose an occlusion processing technique based on the fully-analytic triangular mesh based computer generated holography (CGH) to tackle the problem called non-occluding effect as shown in Fig. 1. The proposed method performs the occlusion processing not in the spatial domain like conventional methods but in the angular spectrum domain.

The proposed algorithm for occlusion handling using convolution technique [1] is explained by,

$$AS_{1:2}(\mathbf{f}_{x,y}) = AS_1(\mathbf{f}_{x,y}) - AS_{1,2}(\mathbf{f}_{x,y}) + AS_2(\mathbf{f}_{x,y}),$$

The global angular spectrum of the rear mesh  $AS_1(\mathbf{f}_{x,y})$  is convoluted with the global angular spectrum of the current mesh  $AS_2(\mathbf{f}_{x,y})$  to determine the angular spectrum part  $AS_{1,2}(\mathbf{f}_{x,y})$  that should be occluded by the current mesh as shown in Fig. 1. The convolution operation is performed in the hologram plane, not in the individual local mesh plane. Therefore, the numerical propagations between the silhouette mask planes are not required, which reduces the computational cost of the proposed method. The global angular spectrum convolution achieves the blocking of the rear wave field in the tilted local mesh plane, not in the plane parallel to the hologram as in Fig. 1(e). Therefore, the proposed method is exact, being free from oblique angle artifacts of the previous silhouette methods [2].

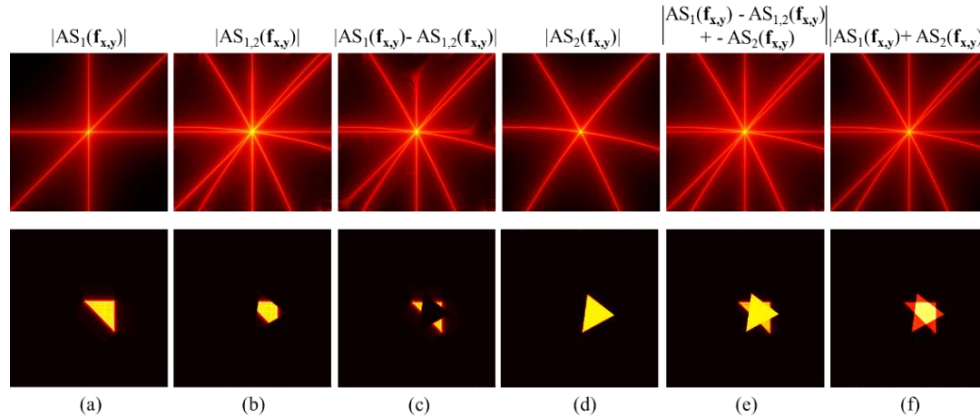


**Fig. 1. (a)-(e) shows angular spectrum and reconstruction in current mesh plane, (f) shows reconstruction without occlusion processing.**

## References

1. H.-J. Yeom and J.-H. Park, "Calculation of reflectance distribution using angular spectrum convolution in mesh-based computer-generated hologram," *Opt. Express* **24**(17), 19801-19813 (2016).
2. K. Matsushima, M. Nakamura, and S. Nakahara, "Silhouette method for hidden surface removal in computer holography and its acceleration using the switch-back technique," *Opt. Express* **22**(20), 24450-24465 (2014).

# Speckle reduction using angular spectrum interleaving for triangular mesh based computer generated hologram

Seok-Beom Ko and Jae-Hyeung Park\*

Dept. of Information and communication Engineering, Inha University, 100 Inha-ro, Nam-gu, Incheon, 22212, Korea

E-mail: \*[jh.park@inha.ac.kr](mailto:jh.park@inha.ac.kr)

OCIS codes: (090.1760) Computer holography

In this paper, we propose a method that eliminates speckle artifacts in the reconstruction of triangular mesh based computer generated hologram. The proposed method generates a number of holograms with different sets of the interleaved plane carrier waves. The generated holograms are displayed sequentially with time-multiplexing, achieving speckle-free reconstruction without sacrificing the viewing angle or depth of focus. We show the results of the proposed method in comparison with the conventional temporal averaging method [1] as shown Fig. 1

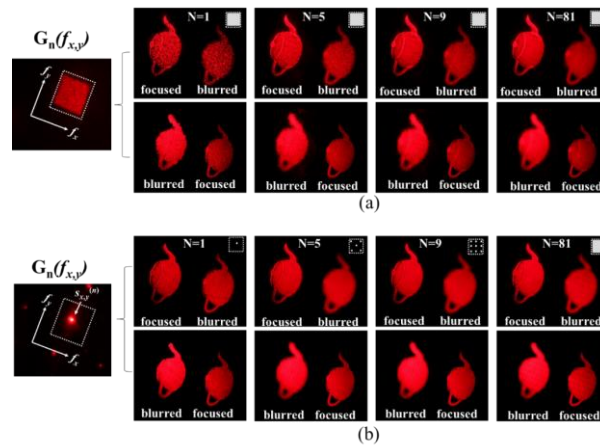


**Figure 1. Experimental result**  
(a) conventional temporal averaging method (b) proposed method

For the quantitative speckle measurement, we used a planar scene with uniform amplitude as the target object. Figure 2 shows the measured speckle contrast. As can be seen in Fig. 2, the proposed method shows lower speckle contrast in all time-multiplexing cases and it reaches the minimum speckle contrast level at  $N=5$ , which means the number of time-multiplexing required in the proposed method can be as small as 5.

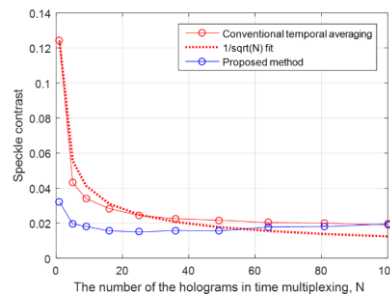


**Figure 2. Measured speckle contrast**

## References

1. W.F. Hsu and C.F. Yet, "Speckle suppression in holographic projection displays using temporal integration of speckle images from diffractive optical elements," Appl. Opt. 50(34), H50-H55 (2011).

## See-through Maxwellian display using waveguide and multiplexing holographic optical element

*Seong-Bok Kim, Jae-Hyeung Park\**

**Department of Information and Communication Engineering, Inha University, Korea**

*Tel.: +82-32-860-7432, E-mail: \*jh.park@inha.ac.kr*

**OCIS codes:** (110.6880) Three-dimensional image acquisition; (100.6890) Three-dimensional image processing; (090.1760) Computer holography

Commercially available augmented reality (AR) / virtual reality (VR) devices in the form of head-mounted displays (HMDs) present two-dimensional (2D) images using flat panel displays and lenses, and offer sense of depth by giving binocular parallax. However, these devices generate vergence accommodation conflict (VAC) and users can feel eye fatigue. To solve this problem, there are solutions generating 3D images like light field and holographic displays or removing the focal cue (accommodation) like Maxwellian displays. At this time, Maxwellian displays are more suitable for HMD than 3D displays because the displays have low computational load and less degradation in resolution. In Maxwellian displays, the collimated beam modulated by a display panel is focused at the center of the eye pupil by using a lens to write images onto the retina directly. Therefore users can always see clear images regardless of changing focal length of the user's eye. Currently available commercial Maxwellian displays consist of a scanning mirror and a concave mirror. So users can not see see-through views where the mirror is located. The device is complicated and bulky because mechanical equipment such as a scanning mirror are used. Also, the principle of Maxwellian display accompanies disadvantages that the eyebox size is limited to the pupil size. To solve these disadvantages, we propose a transmissive Maxwellian display using a multiplexed HOE and waveguide with a beveled surface

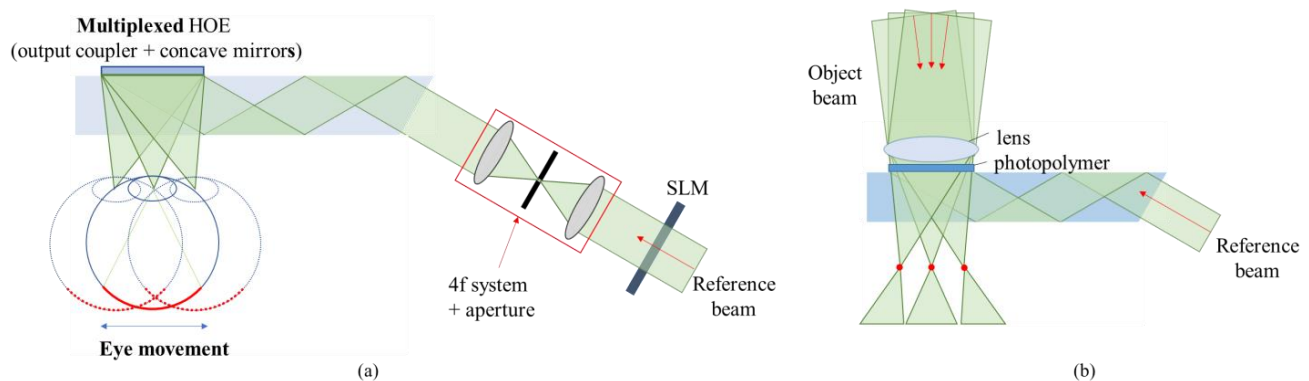


**Fig. 1. (a) proposed system configuration, (b) HOE recording setup**

Figure 1(a) shows the structure of the proposed system. The system is composed of a waveguide with a oblique side and a HOE that acts as multiple concave mirrors, 4-f system, aperture, transparent sparital light modulator (SLM). The parallel beam passes through the SLM and its high order diffraction terms are removed using the 4-f system and aperture. The collimated beam is incident perpendicular to the oblique surface of the waveguide and delivered to the HOE by total internal reflections. The HOE focuses the incident beam onto three spots as shown in Fig. 1(b), giving extended eyebox to the user. The proposed system is optically-see-through and compact. Moreover, the proposed system increases the eyebox which has been one of the practical problems of the Maxwellian displays.

### References

1. H.-J. Yeom, H.-J. Kim, S.-B. Kim, H. Zhang, B. Li, Y.-M. Ji, S.-H. Kim, and J.-H. Park, "3D holographic head mounted display using holographic optical elements with astigmatism aberration compensation," *Opt. Express* 23(25), 32025-32034 (2015).



# Acceleration of fully analytic mesh based computer generated hologram using foveated rendering technique

Yeon-Gyeong Ju and Jae-Hyeung Park\*

Dept. of Information and communication Engineering, Inha University, 100 Inha-ro, Nam-gu, Incheon, 22212, South Korea

Email: [\\*jh.park@inha.ac.kr](mailto:jh.park@inha.ac.kr)

**OCIS codes:** (090.1760) Computer holography; (090.2870) Holographic display; (100.6890) Three-dimensional image processing

In this paper, we propose the method to accelerate the calculation of mesh based computer generated hologram (CGH) using foveated rendering technique. Mesh based CGH is one of the CGH techniques which use polygon mesh based computer graphical information. Foveated rendering is a technique used in head-mounted displays (HMDs) to reduce the computational load by reducing the image resolution in peripheral area. Human eyes can detect high details not within entire field of view, but within only tiny area around the center of our field of view. Using this characteristic of human eyes, we can reduce the image quality outside of the eye fixation area, while maintaining the perceived image quality. We applied this foveated rendering to mesh based CGH to reduce the computation time without perceived quality degradation.

Figure 1 shows the simulation result of the proposed method. Figure 1(a) and 1(d) are the hologram and its reconstruction of the full resolution case, i.e. when the proposed method is not applied. Figure 1(b), 1(c), 1(e), and 1(f) are the foveated rendered case, when we supposed the yellow circular area is the eye fixation area. Table 1 shows the computation time reduction when we implement the proposed method. The result is the case of Fig. 1(b), and 1(e). The computation time of the mesh based CGH is proportional to the number of meshes, and it can be found that the computation time is reduced by about 46%.

We have presented the method to accelerate the calculation of mesh based CGH, in the case of HMD. We expect the proposed technique would find its applications in the contents generation for holographic 3D HMDs.

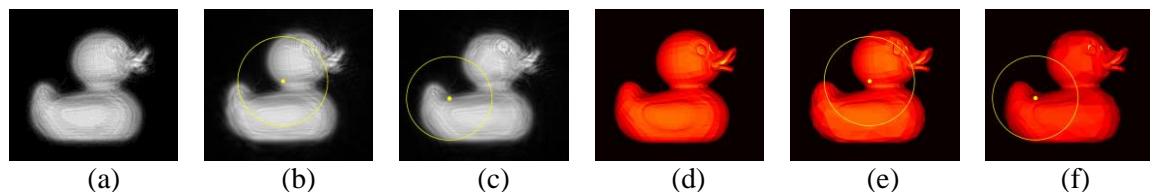


**Fig. 1. Comparison the hologram and their reconstruction between the full resolution and the foveated rendered case. (a): Hologram of the full resolution case. (b),(c): Hologram of the foveated rendered case. (d)-(f): Reconstruction of (a)-(c).**

	Full Resolution Case	Foveated Rendered Case
# of meshes outside the focusing area	2722	544
# of meshes in the whole area	4212	2034
Computation time	66.25s	30.72s

**Tab. 1. Comparison the computation time and the number of the meshes between full resolution and foveated rendered case**

## References

1. M. Askari, S. B. Kim, K. S. Shin, S. B. Ko, S. H. Kim, D. Y. Park, Y. G. Ju, and J. H. Park, *Occlusion handling using angular spectrum convolution in fully analytical mesh based computer generated hologram*, Opt. Express, vol. 25, no. 21, pp. 25867-25878 (2017).
2. J. S. Hong, Y. M. Kim, S. H. Hong, C. S. Shin, and H. J. Kang, *Gaze contingent hologram synthesis for holographic head-mounted-display*, SPIE, vol 9771, pp. 97710K 6 (2016).





## Full-parallax light-field and holographic displays

Masahiro Yamaguchi

School of Engineering, Tokyo Institute of Technology, Yokohama, Japan

Tel.:81-45-924-5137, E-mail: yamaguchi.m.aa@m.titech.ac.jp

**OCIS codes:** (090.2870) Holographic display; (100.6890) Three-dimensional image processing; (090.1760) Computer holography

A light-field display (LFD) reproduces the light-rays from a display screen so that virtual or real images are generated, and an observer can perceive natural 3D image in the air without using 3D glasses or goggle. However, there are some limitations in LFD, such as the sampling of light-rays and the diffraction at the screen plane, and the resolution of image far from the screen plane becomes low. On the other hand, holography, which is wavefront reconstruction technology, can also reconstruct light-field, while it is free from above limitations and high-resolution image is obtained even in deep 3D scene. Thus, ray-based LFD is suitable for lower-resolution large displays, esp the 3D image near the screen, whereas wavefront-based LFD is advantageous in higher-resolution deep 3D scene<sup>[1]</sup>. We apply the concept of integrating ray-based and wavefront-based techniques to computational holography<sup>[2-4]</sup> and interactive 3D touch display<sup>[5]</sup>.

In the calculation of computer generated hologram (CGH), rendering is done by using off-the-shelf 3D CG software, while the light propagation is calculated based on wavefront [Fig. 1]. Then, realistic images are generated using 3D CG software, and high-resolution 3D images are reconstructed in a deep 3D scene [Fig. 2].

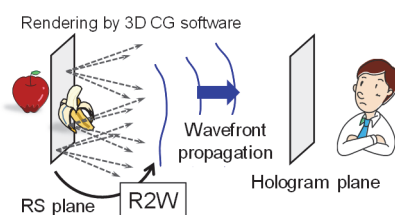


**Fig. 1 Hologram computation using R2W conversion**

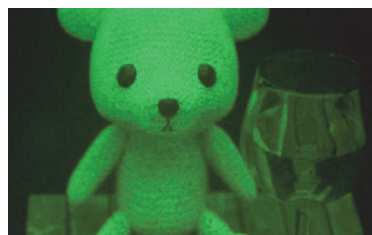


**Fig. 2 Reconstructed image from the CGH.**

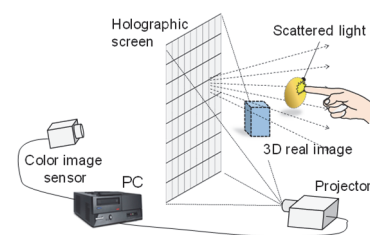


**Fig. 3 The 3D touch sensing display using holographic LFD.**

For the interactive 3D user interface, a hologram is used as an optical element for generating light-field, and image data are projected by a high-resolution projector [Fig. 3]. Then, we can generate interactive light-field display with floating 3D image, which is a real image. If a user touches the image, the top of fingertip is irradiated by the reconstructed real image. The color of scattered light is detected by a color camera, and it is used for user interface.

The integration of light-field and holography will provide great advantage. The examples are demonstrated in the computation of high-quality hologram and the interactive 3D touch interface, assisted by light-field technology.

### Acknowledgment

This work is performed in collaboration with Prof. Kyoji Matsushima, Kansai Univ. and our Lab members, Ryo Higashida, Shunsuke Igarashi, and Dr. Tomoya Nakamura.

### References

1. M. Yamaguchi, "Full-Parallax Holographic Light-Field 3-D Displays and Interactive 3-D Touch," *Proc. of the IEEE*, 105, 5, 947-959 (2017).
2. K. Wakunami and M. Yamaguchi, "Calculation for computer generated hologram using ray-sampling plane," *Opt. Express* 19, 10, 9086-9101 (2011)
3. S. Igarashi, T. Nakamura, and M. Yamaguchi, "Fast method of calculating a photorealistic hologram based on orthographic ray-wavefront conversion," *Opt. Lett.* 41, 7, 1396-1399 (2016).
4. S. Igarashi, T. Nakamura, M. Yamaguchi, K. Matsushima, "Efficient calculation method for realistic deep 3D scene hologram using orthographic projection," *Proc. SPIE*, 9771, 977100, (2016).
5. M. Yamaguchi, R. Higashida, "3D touchable holographic light-field display," *Appl. Opt.* 55, 3, A178-A183, (2016).

## Table-top Holographic Display with Full Parallax

*Minsik Park, Yongjun Lim, Keehoon Hong, Eun-Young Chang, Hayan Kim, Jaehan Kim and Jinwoong Kim*  
 Electronics and Telecommunications Research Institute (ETRI), 218 Gajeong-ro, Daejeon, 34129, South Korea  
 Tel.:82-42-860-1231, E-mail: pms@etri.re.kr

**OCIS codes:** (090.2870) Holographic display; (090.1760) Computer holography

Digital holographic display has been actively researched for the development of an ultimate three-dimensional display because it can obviously solve the vergence-accommodation conflict problem of an existing three-dimensional display [1]. Digital holographic display, however, can't have a sufficient spatial bandwidth due to the limited performance of a commercialized spatial light modulator (SLM), which results in limitations on both a size and a viewing angle of the image reconstructed from hologram. In order to remove such restrictions, we have not only studied a flat-panel holographic display using spatial multiplexing [2] but also developed a table-top holographic display using temporal multiplexing [3] to expand a spatial bandwidth. A high-speed DMD is applied as a SLM to realize the temporal-multiplexing in table-top holographic display. Figure 1 shows the system structure of the implemented table-top holographic display. It consists of combination optics including three DMDs corresponding to each RGB light source for reconstructing a colour hologram, 4F optics not only for removing spatial noise (DC and twin image) but also for optically magnifying the reconstructed hologram image, and rotation optics including the hollow motor synchronized with the RGB DMDs to display colour hologram images in a 360-degree direction.

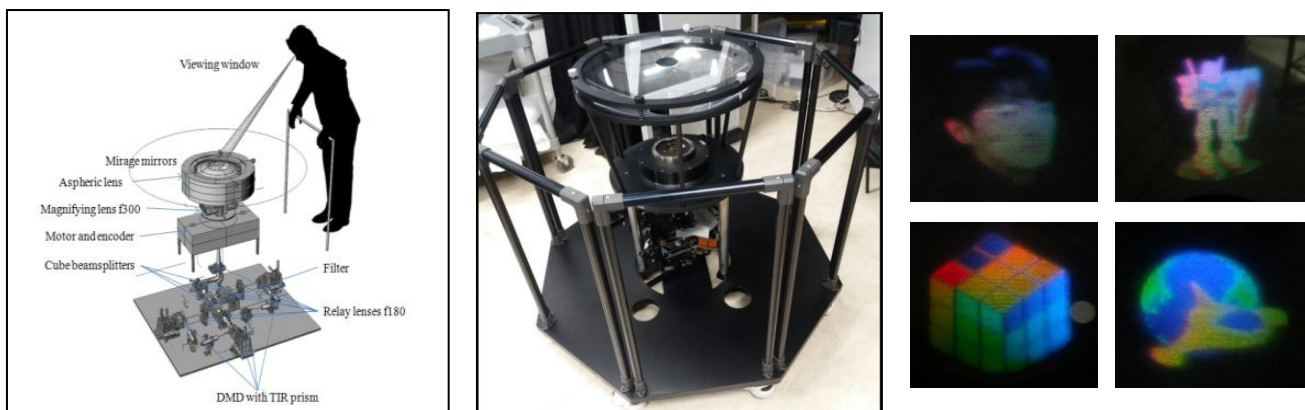


**Fig.1. Table-top Holographic Display**

In addition, we have tried to develop a vertical parallax in 20-degree for the verification purpose of the feasibility to support a full parallax in table-top holographic display by integrating both an eye-tracking function of camera system and a projection function of DMD. We will elaborately discuss the optical design to realize the floating hologram image, the principle to apply the temporal-multiplexing and the method to implement the full parallax in the table-top holographic display.

### Acknowledgment

This research was supported by GigaKOREA project, (GK17D0100, Development of Telecommunications Terminal with Digital Holographic Table-top Display).

### References

1. J. Hong et al., "Three-dimensional display technologies of recent interest: principles, status, and issues," *Appl. Opt.* vol. 50, pp. H87-H115, 2011.
2. M.S. Park et al., "Digital holographic display system with large screen based on viewing window movement for 3D video service," *ETRI Journal*, vol. 36, no. 2, pp. 232-241, 2014.
3. Y. Lim et al., "360-degree tabletop electronic holographic display", *Opt. Express*, 24(22), 24999-25009, 2016.

## Enlargement of viewing zone of holographic 3D display using a parabolic mirror

Yusuke Sando<sup>3</sup>, Kazuo Satoh<sup>3</sup>, Takahiro Kitagawa<sup>3</sup>, Makoto Kawamura<sup>3</sup>, Daisuke Barada<sup>1,2</sup> and Toyohiko Yatagai<sup>1</sup>

<sup>1</sup>Center for Optical Research & Education, Utsunomiya University, 7-1-2 Yoto, Utsunomiya, Tochigi 321-8585, Japan

<sup>2</sup>Graduate School of Engineering, Utsunomiya University, 7-1-2 Yoto, Utsunomiya, Tochigi 321-8585, Japan

<sup>3</sup>Osaka Research Institute of Industrial Science and Technology, 2-7-1 Ayumino, Izumi, Osaka 594-1157, Japan

Tel.: 81-725-51-2713, E-mail: sando@tri-osaka.jp

**OCIS codes:** (090.1760) Computer holography

Recently, holographic 3D display has been actively researched. To put the holographic 3D display into practical use, the problem of the narrow viewing zone must be solved. However, the view zone of the hologram is limited in principle due to the shape. For example, in the planar hologram, no one can never observe reconstructed images from the opposite or lateral sides of the hologram. To overcome this shape-based limitation, we propose one approach of the introduction of a convex parabolic mirror between the hologram and viewers to realize the extremely wide viewing zone. Differently from other techniques, it should be noted that the vertical viewing zone can be also enlarged in addition to the horizontal viewing zone. The enlargement effect is the same as that of a hemispherical-shaped hologram.

The schematic of a holographic 3D display using a convex parabolic mirror is illustrated in Fig. 1. The wavefront modulated by a hologram is Fourier-transformed by a lens. The non-diffracting wave and the conjugate wave are removed by a single sideband filter placed at the back focal plane of the lens. Then, the wavefront enters the convex parabolic mirror, and reflects radially. If the Fourier-transform type hologram is properly designed considering the parabolic mirror reflection, a 3D image can be reconstructed as a virtual images near the focal point of the parabolic mirror. Because the diverging angle of this reflected wavefront is quite large, extremely wide viewing zone is realized. The extended viewing zone of the horizontal (azimuthal) and vertical (zenithal) directions are  $180^\circ$  and  $90^\circ$ , respectively. Some optically reconstructed images observed from various directions are shown in Fig. 2. The 3D object used for this experiment is a dice.  $\theta$  and  $\varphi$  indicates vertical and horizontal angles. As can be seen from Fig. 2, the proper perspective images are reconstructed in accordance with observation directions, and extremely large viewing zone has been demonstrated.

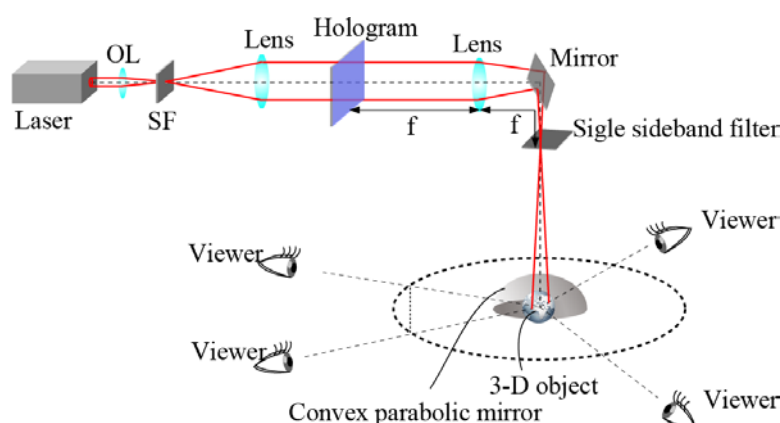


**Fig. 1. Schematic of holographic 3D display using a convex parabolic mirror.** OL: objective lens, SF: spatial filter, f: focal length of the lens.

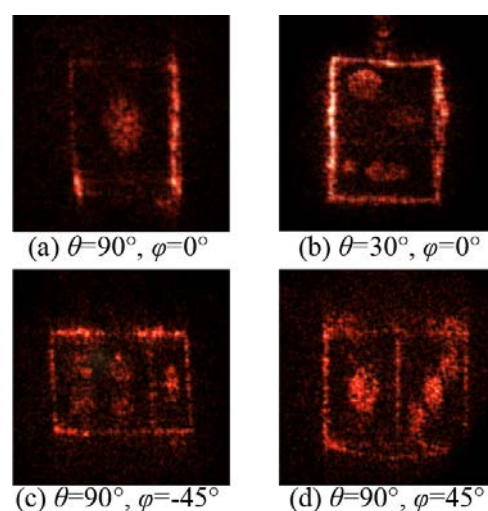


**Fig. 2. Optically reconstructed images.**

### Acknowledgment

This research was partially supported by JSPS KAKENHI Grant Number JP15K21699.

# Formation of dynamic viewing zone in autostereoscopic 3D display

Sung-Kyu Kim\*, Ky-Hyuk Yoon, and Min-Koo Kang

Imaging Media Research Center, KIST, Seoul, Korea

\*e-mail: kkk@kist.re.

**Abstract:** Conventional autostereoscopic multiview 3D displays suffer from the crosstalk and freedom of viewing condition. Two type of dynamic viewing zone methods are developed to reduce the crosstalk and observation freedom; they are based on the viewing z

one fusion (VZF) and dynamic maximal viewing zone (DMVZ). These methods are verified in the developed parallax type multiview and HDMV 3D displays.

## 1. Introduction

Glasses-based 3D displays should wear uncomfortable special glasses. For this reason, popularization of 3D displays is delayed. For that reason, the development of an autostereoscopic 3D display is important. However, in the case of the non-eyeglass system, 3D resolution is degraded and the degree of freedom of observation is known to be a problem. VZF proposed a solution to the problem of crosstalk and limitation of observation freedom. (1~3) And DMVZ presents its findings in a way that can improve the 3D resolution in the case of HDMV or SMV and at the same time relax the limit of observer position. (4)

## 2. Concepts of VZF and DMVZ

The concept of VZF is at Fig.1 and the basic idea of DMVZ is at Fig. 2.

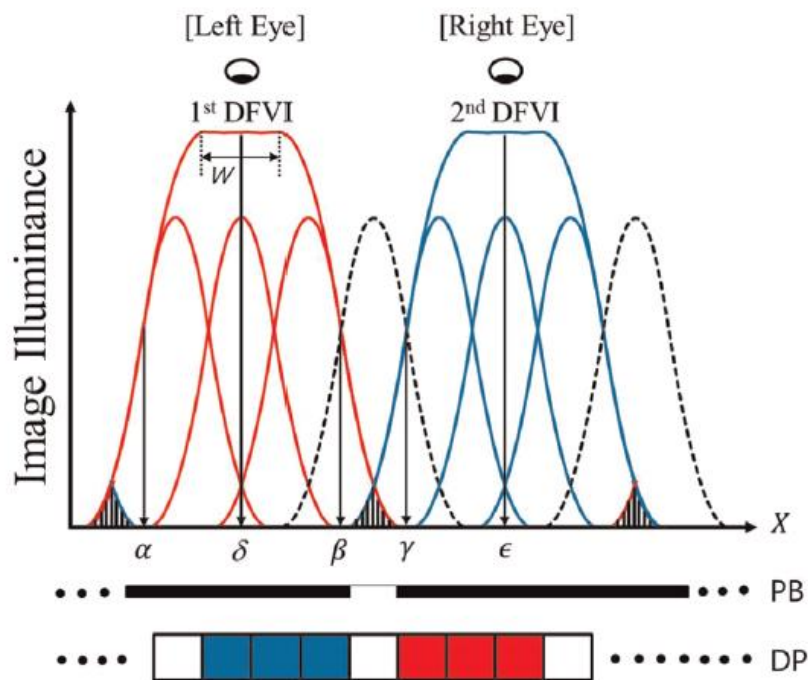


Fig. 1 Concept of VZF



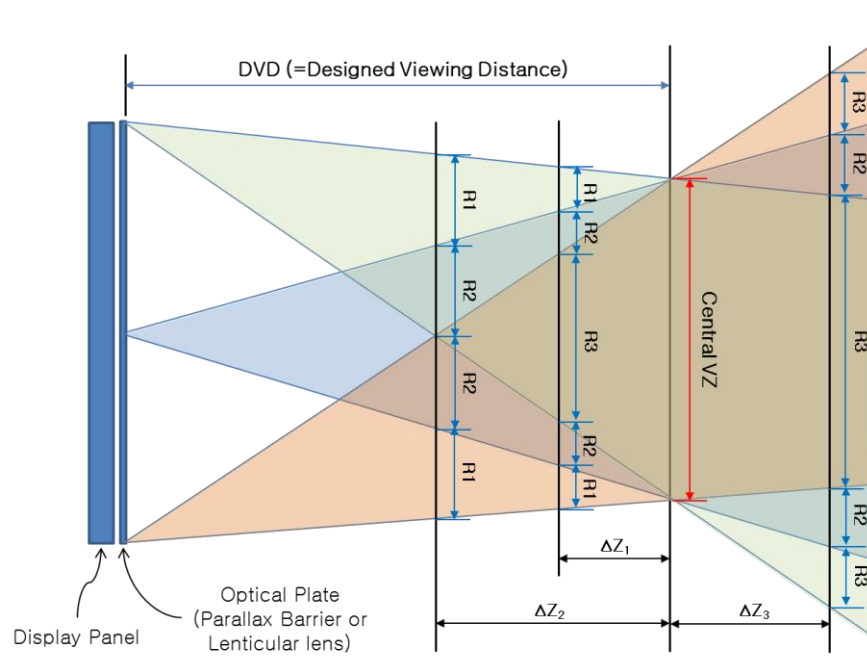


Fig. 2 Concept of DMVZ

### 3. Conclusions

In this presentation, we discuss on the low crosstalk technique using eye-tracking system and wide 3DOF viewing position based on face tracking system. Additionally both methods support full parallax when real time rendering activates.

### 4. References

1. Sung-Kyu Kim, Ki-Hyuk Yoon, Seon Kyu Yoon, and Heongkyu Ju, "Defragmented image based autostereoscopic 3D displays with dynamic eye tracking," *Optics Communications*, 357, pp.185-192, (2015)
2. Korea Patent, "10-1073512, 3-dimensional displaying apparatus and driving method thereof,"(2011).
3. Korea Patent, "10-2012-0072384, Apparatus for 3-dimensional displaying using dynamic viewing zone enlargement for multiple observers and method thereof" (2012).
- 4 Korea Patent, "2017-0103605, Autostereoscopic 3D display using DMVZ," (2017).



## Aerial Multi-Modal Information Display

*Hirotsugu Yamamoto<sup>1,2</sup>, Tomoyuki Okamoto<sup>1</sup>, Shusei Ito<sup>1</sup>, and Ryosuke Kujime<sup>1,2</sup>*

<sup>1</sup>Dept. of Optical Engineering, Utsunomiya Univ., Utsunomiya City, Tochigi 321-0904, Japan

Tel.: 81-28-689-7074, E-mail: [hirotsugu@yamamotolab.science](mailto:hirotsugu@yamamotolab.science)

<sup>2</sup>ACCEL, JST, Utsunomiya City, Tochigi, Japan

**OCIS codes:** (120.2040) Displays; (110.6820) Thermal imaging; (110.7170) Ultrasound

Aerial display enables us to handle visual information directly in the mid-air. Because there is no hardware at the aerial screen position, it is important to give appropriate feedback for a viewer. This paper proposes some techniques to give multi-modal sensation for the viewer of an aerial display. We have developed an aerial display technique, called aerial imaging by retro-reflection (AIRR)<sup>1</sup>, which features a wide viewing angle, scalability, and mass-productivity. In order to converge sound and ultrasonic wave, we have fabricated a crossed-mirror array (CMA), which is made of transparent acrylic plates with hollow apertures. Furthermore, we have formed an aerial heater by converging far-infrared radiations with double-layered arrays of rectangular mirror (WARM)<sup>2</sup>.

This paper reports our developments on aerial multi-modal display in combination of AIRR, CMA, and WARM. We have developed a visual, thermal and acoustic floating aerial display<sup>3</sup>. The composition of our system is shown in Fig. 1 (a). Aerial images are formed in the air, as shown in Fig. 1 (b). We have placed a electric heater to warm up an aerial image of fire. By placing a thermo-chromic screen, as shown in Fig. 1 (c), we have confirmed that only a part of the aerial images is heated. Because a parametric speaker and a CMA are installed in the left side of the aerial screen, sound pressure is locally increased in the mid-air. Thus, our visual, thermal, and acoustic aerial display gives multi-modal sensations for users.

Another application of multi-modality is to guide a viewer to the viewing position of a secure aerial display<sup>4</sup>. We have introduced an ultrasonic transducer array to give haptic sensation for a viewer<sup>5</sup>. As shown in Fig. 1 (e), by adjusting the phases of the transducers, Haptic sensation is given at an arbitrary position. This haptics is used to present the limited viewing position of the aerial secure display.

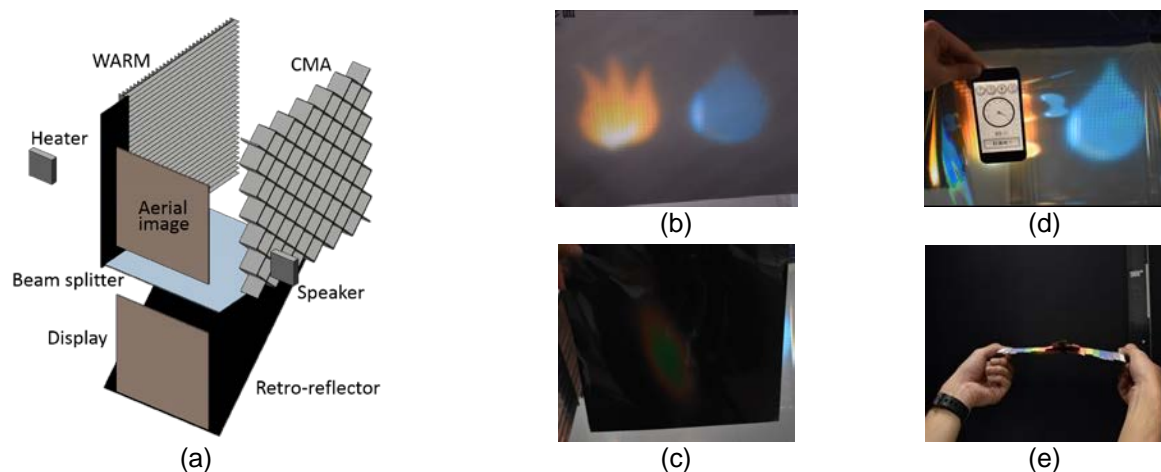


**Fig. 1.** (a) Composition of our developed aerial multi-modal information display. (b) Observation of formed aerial images on a screen. (c) Observation of the formed aerial thermal image on a thermo-chromic screen. (d) Conversing sound in the mid-air. (e) Haptic sensation by use of an ultrasonic transducer array.

### References

1. H. Yamamoto, *et al.*, *Opt. Exp.*, 22(22), 26919 (2014).
2. T. Okamoto, *et al.*, *Proc. IDW/AD'16*, 3D6/3DSA7-4 (2016).
3. H. Yamamoto, *et al.*, *SIGGRAPH Posters 2017*, 16 (2017).
4. K. Uchida, *et al.*, *Opt. Rev.*, 24 (1), 72 (2017).
5. S. Ito, *et al.*, *Proc. IDW'17*, HAPp1-4 (2017).

## Metasurfaces for holograms

*Byoungho Lee\* and Gun-Yeal Lee*

School of Electrical and Computer Engineering and Inter-University Semiconductor Research Center,  
Seoul National University, Gwanak-Gu Gwanak-ro 1, Seoul 08826, Korea

\*Tel.:82-2-880-7245, E-mail: byoungho@snu.ac.kr

**OCIS codes:** (110.6880) Three-dimensional image acquisition; (100.6890) Three-dimensional image processing; (090.1760) Computer holography

Holography, which is an optical technology that reconstructs the wavefront of electromagnetic waves to provide vivid three-dimensional images, has been of great interest due to its potential for the next generation imaging technology. In general, conventional digital holography has been based on various optoelectronic devices such as a spatial light modulator and a digital micromirror device. However, these kinds of devices have been suffering from several issues due to their large pixel size compared to operating wavelengths, leading to low resolution, narrow viewing angle, and severe noises generated from undesirable diffraction orders and twin images. More importantly, conventional holographic technologies are usually based on either amplitude- or phase-only modulation scheme with incomplete approximations of object images. It is notable that a subwavelength scale of the pixel is required for realizing enough viewing angles and high spatial resolutions of holographic images.

Metasurfaces, which are planar optical elements with composition of artificially fabricated subwavelength-structures, have been extensively studied recently. It was found that wide ranges of light-matter interactions can be obtained by designing the morphologies of subwavelength nanoantennas in metasurfaces [1]. Recently, metasurfaces are expected to pave the path for high quality spatial light modulators that can overcome the limitations of conventional optical components. Various metasurfaces have been investigated as holographic devices with control of phase and polarization of light, and show great performances including wide viewing angles, high resolutions, and no diffraction orders in holographic images.

In this presentation, several metasurface platforms for holographic generation and manipulation of electromagnetic waves will be presented. First, we will briefly explain the physical mechanisms and concepts of the holographic metasurfaces. Various types of meta-atoms providing phase modulations will be introduced in this presentation, and their applications will also be discussed [2, 3]. Moreover, we would like to introduce the next step of those kinds of metasurfaces, which provides not only phase-modulations but also amplitude-modulations, leading to complex-amplitude modulations. In particular, C-shaped nanostructures for generating ultra-compact Airy beams will be first introduced where the C-shaped metasurface provides both full phase-modulations and binary amplitude-modulations [4]. Then, X-shaped silicon metasurfaces, which provide complete control of both amplitude and phase of visible light, will be introduced, and their physical mechanisms will be explained [5]. Based on the X-shaped metasurfaces, full complex-amplitude modulated holograms with subwavelength spatial resolutions will be suggested as a promising application of this metasurface platform. Finally, conclusions with the future direction of the metasurface holography study will be briefly discussed.

### Acknowledgment

This research was supported by Basic Science Research Program through the National Research Foundation of Korea (NRF) funded by the Ministry of Science, ICT & Future Planning (2017R1A2B2006676).

### References

1. N. Meinzer *et al.*, *Nat. Photon.* 8, 889–898 (2014).
2. G. Zheng *et al.*, *Nat. Nanotech.* 10, 308–312 (2015).
3. A. Arbabi *et al.*, *Nat. Nanotech.*, 10, 937–943 (2015).
4. E.-Y. Song *et al.*, *Adv. Opt. Mater.* 5(10), 161028 (2017).
5. G.-Y. Lee *et al.*, arXiv:1706.09632 (2017).

## Common-path incoherent digital holography

Osamu Matoba<sup>1</sup>, Xiangyu Quan<sup>1</sup> and Yasuhiro Awatsuji<sup>2</sup>

<sup>1</sup>Graduate School of System Informatics, Kobe University, Rokkodai 1-1, Nada, Kobe 657-8501, Japan

Tel.:81-78-803-6235, E-mail: matoba@kobe-u.ac.jp

<sup>2</sup>Graduate School of Science and Technology, Kyoto Institute of Technology, Matsugasaki, Sakyo-ku, Kyoto 606-8585, Japan

**OCIS codes:** Digital holography; (110.6880) Three-dimensional image acquisition; (180.2520) Fluorescence microscopy; (090.1970) Diffractive optics

Incoherent digital holography is one of the hot topics in digital holography because it can be applied to biological tissue in fluorescence imaging. There are two configurations. One is Michelson-type interferometer. It can realize an off-axis holography, but two separated arms are required and then it is difficult to make the system compact. The other configuration is a common-path geometry using diffractive optical elements. FINCH is one of the pioneer works of the incoherent digital holography. In this system, two focusing lenses implemented by a phase-mode spatial light modulator can generate two diffracted waves from the fluorescence light, and then two waves are interfered in the image sensor. Phase shifting method is applied to improve the reconstructed quality. However, it prevents from the single shot measurement. Recently, we have proposed an off-axis incoherent digital holography in a common-path configuration [1]. This configuration is suitable for the multi-modal imaging where the phase and the fluorescence 3D distributions can be measured simultaneously [2, 3].

Figure 1 shows our concept of the common-path off-axis incoherent digital holography. In this setup, the two focusing lenses with diffraction gratings are used to implement an off-axis configuration. In this setup, the modulated signals travels in different directions from the optical axis and then the unmodulated waves including the surface reflection of the optical elements and spatial light modulator can be eliminated. This setup is very stable and makes the system compact. These properties are suitable for optical microscope. Figure 2 shows the preliminary experiment by using a quasi-point light source using a LED. From Fig. 2(a), the off-axis hologram can be seen and the original point light source is reconstructed well by changing the reconstruction distance. In the presentation, we will discuss the possibility of the fluorescence measurement and the biological samples.

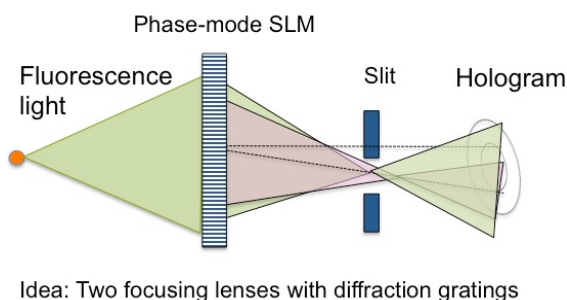


**Fig. 1. Concept of common-path off-axis incoherent digital holography.**

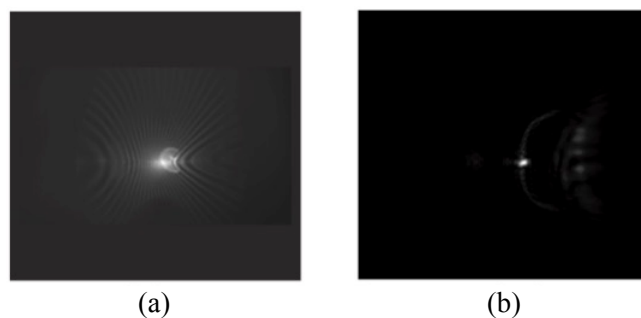


**Fig. 2. Experimental results using a point-like source by LED. (a) hologram and (b) reconstructed image.**

### Acknowledgment

A part of this work was supported by JSPS KAKENHI Grant Number 15H03580 and JSPS KAKENHI Grant Number 16J05689.

### References

1. X. Quan, O. Matoba, and Y. Awatsuji, *Opt. Lett.*, 42(3), 383 (2017).
2. X. Quan, K. Nitta, O. Matoba, P. Xia, and Y. Awatsuji, *Opt. Rev.*, 22, 349 (2015).
3. O. Matoba, X. Quan, P. Xia, Y. Awatsuji, and T. Nomura, *Proc. of the IEEE*, 105(5), 906 (2017).

## Photonic meta-devices based on optical path control

Muhan Choi\*, Inbo Kim, Jinhang Cho, Sang-Hyeok Mun

School of Electronics Engineering, Kyungpook National University, Daegu 41566, South Korea

\*Tel.:82-53-950-5520, E-mail: mhchoi@ee.knu.ac.kr

**OCIS codes:** (160.3918) Metamaterials, (140.3945) Microcavities,

### 1. Gradient index micro-cavity designed by transformation optics

The optical mode properties of dielectric cavities, such as quality factor and emission directionality, can be tailored at will by using transformation optics [1-3]. The dielectric microcavity with the spatially varying refractive index profile can be implemented by drilling subwavelength-scale air holes in a dielectric slab. The proposed design scheme of microcavities based on the transformation optics can be applied to new kinds of laser beyond the conventional microcavity laser diodes.

### 2. Active graphene meta-lens operating in terahertz regime

The variable focus meta-lens has been designed by using actively controllable metasurface blocks. The meta-surface blocks are composed of metallic unitcells and a graphene layer in which optical conductivity can be controlled individually by the gate voltage through the ion-gel gate. The metalens is very thin and can be operated with very high modulation speed. It is expected that the active meta-lens will be applied to various devices in terahertz and mid-infrared range.[4-7]

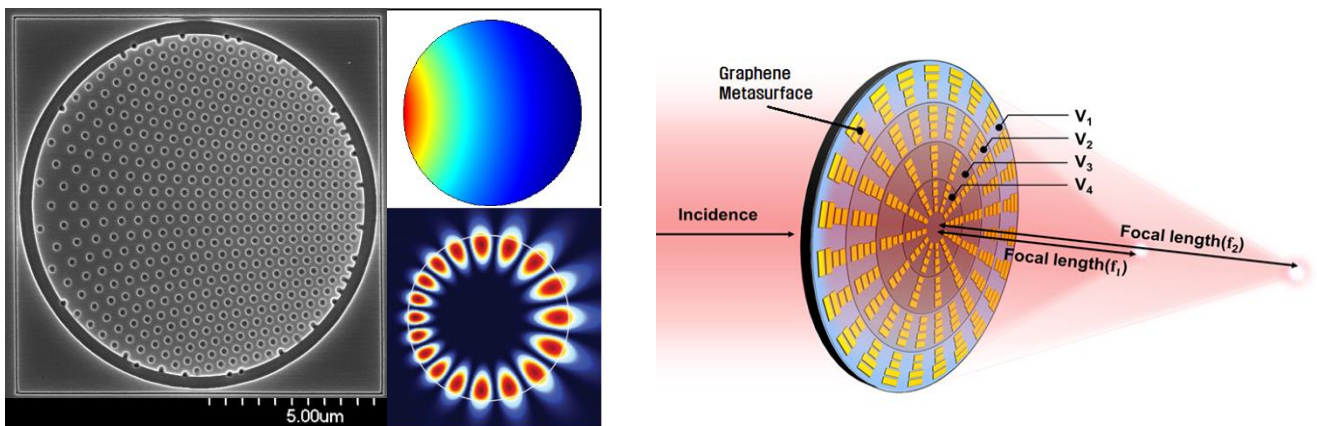


**Fig. 1.** Gradient index microcavity designed by transformation optic and Terahertz Graphene Meta-lens

### References

1. J. B. Pendry, D. Schuring, and D. R. Smith, *Science*, **312**, 1780, (2006)
2. Leonhardt, U., *Science*, **312**, 1777 (2006)
3. Yushin Lee, et al., *Nature Photonics*, **10**, 647 (2016)
4. Hoon Lee, et al., *Nature*, **470**, 369 (2011)
5. Seung Hoon Lee, Muhan Choi, et al., *Nature Materials*, **11**, 936 (2012)
6. Keun Soo Kim, Yue Zhao, et al., *Nature*, **457**, 706 (2009)
7. Lei Zhang, Ghengtao Mei, Cheng-Wei Qiu, *Adv. Optical Mater.*, **4**, 818 (2016)

# Multidimensional imaging with phase-shifting interferometry

Tatsuki Tahara<sup>1,2</sup>, Reo Otani<sup>3</sup>, Yasuhiko Arai<sup>1</sup> and Yasuhiro Takaki<sup>4</sup>

<sup>1</sup>Faculty of Engineering Science, Kansai University, 3-3-35 Yamate-cho, Suita, Osaka, 564-8680, Japan

Tel.: 81-6-6368-1757, E-mail: tahara@kansai-u.ac.jp

<sup>2</sup>PRESTO, Japan Science and Technology Agency, 4-1-8 Honcho, Kawaguchi, Saitama, 332-0012, Japan

<sup>3</sup>SIGMAKOKI CO. LTD., 17-2, Shimotakahagi-shinden, Hidaka-shi, Saitama 350-1297, Japan

<sup>4</sup>Institute of Engineering, Tokyo University of Agriculture and Technology, 2-24-16 Naka-cho, Koganei, Tokyo 184-8588, Japan

**OCIS codes:** (090.0090) Holography; (090.1995) Digital holography; (090.1705) Color holography.

Digital holography is a technique to obtain 3-D information without a mechanical scan by recording a digital hologram and reconstructing a 3-D image using a computer [1]. The technique has the ability for sensing multidimensional information such as 3-D space, phase, and multiple wavelengths simultaneously. Phase-shifting interferometry is a powerful technique that can utilize a full space-bandwidth product of an image sensor with a high signal-to-noise ratio [2]. As a method to record multidimensional information with phase-shifting, we have presented phase-shifting interferometry selectively extracting wavelength information since 2013 [3-6].

Figure 1 illustrates the principle of the presented multiwavelength digital holographic technique [3-6]. A monochrome image sensor records wavelength-multiplexed phase-shifted holograms sequentially. As a result, wavelength information is superimposed on space and spatial frequency domains and is separated in the polar coordinate plane. Based on phase-shifting interferometry, an object wave at the desired wavelength is selectively extracted and complex amplitude images at multiple wavelengths are reconstructed. It is worth noting that  $2N + 1$  wavelength-multiplexed holograms are sufficient in the initially proposed scheme [3,4,6] where  $N$  is the number of wavelengths measured and the number can be decreased to  $2N$  [5]. In the talk we describe numerical and experimental results and also introduce single-shot incoherent digital holography with phase-shifting [7].

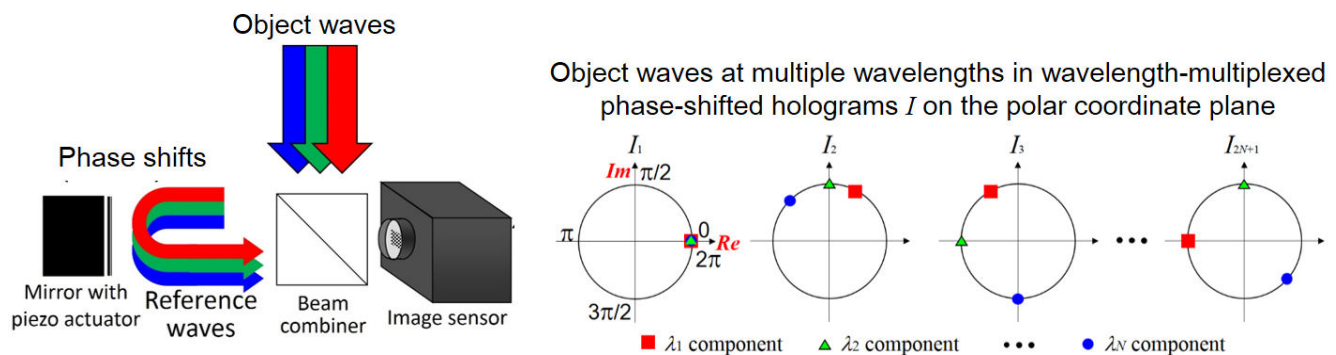


**Fig. 1. Principle of phase-shifting interferometry selectively extracting wavelength information.**

## Acknowledgments

This study was partially supported by Japan Science and Technology Agency (JST), PRESTO, Grant number: JPMJPR16P8, Konica Minolta Science and Technology Foundation, the Japan Society for the Promotion of Science (JSPS), MEXT-Supported Program for the Strategic Research Foundation at Private Universities, and Research Foundation for Opt-Science and Technology.

## References

1. Y. Takaki, H. Kawai, and H. Ohzu, *Appl. Opt.* **38**, 4990 (1999).
2. J. H. Bruning, *et al.*, *Appl. Opt.* **13**, 2693 (1974).
3. T. Tahara, S. Kikunaga, Y. Arai, and Y. Takaki, in *Proceedings of Optics and Photonics Japan 2013 (OPJ)*, 13aE9, Nara, Japan, Nov. 13, 2013. (in Japanese)
4. T. Tahara, R. Mori, S. Kikunaga, Y. Arai, and Y. Takaki, *Opt. Lett.* **40**, 2810 (2015).
5. T. Tahara, R. Mori, Y. Arai, and Y. Takaki, *J. Opt. (IOP Publishing)* **17**(12), 125707 (2015).
6. T. Tahara, R. Otani, K. Omae, T. Gotohda, Y. Arai, Y. Takaki, *Opt. Express* **25**, 11157 (2017).
7. T. Tahara, T. Kanno, Y. Arai, and T. Ozawa, *J. Opt. (IOP Publishing)* **19**, 065705 (2017).



## Quantitative verification for whether LF display system can serve accommodative function to the observer

Kwang-Hoon Lee<sup>1,\*</sup> and Seon Kyu Yoon<sup>1</sup>

<sup>1</sup>Spatial Optical Information Research Center, Korea Photonics Technology Institute, Gwangju, Korea

Tel.: 82-62-605-9324, \*E-mail: [geniuspb@kopti.re.kr](mailto:geniuspb@kopti.re.kr)

**OCIS codes:** (110.6880) Three-dimensional image acquisition; (100.6890) Three-dimensional image processing

The purpose of this approach is that verifying whether the LF display provides accommodative function, and quantifying the focusable range at the reconstruction image space in which permitted by the focusable power served by the display. Our point of view is quite different compared to the existing reports. They had only dealt with the subjective accommodation inducing by observer, in this work, but we had focused to the objective accommodation providing by the LF display in contrast.

The proposed objective accommodation assessment system is consisted by several core parts such as the optical system mimicked the model of pseudo human eye, the spatial filter dividing direction of rays which are passed the two-holes of Hartmann mask located in front of the cornea lens, the optical circumstance given deep depth of field over  $f/4$ , and the designed special pattern optimized to the display in which verifying either the formed image on the detection plane was focused or not. The LF display used in the investigation is designed that it serves 72 multi-views with 7mm of the inter distance between adjacent center positions of each viewing zone. The entrance pupil size (as the cornea lens) of the optical system in the equipment was designed that it can be acceptable three adjacent viewing zone widths. The positions of three virtual objects (Near, Middle – on the display and Far) are represented the couple of the rays having each direction toward to the optical system, and the objects were patterned to the superposed multi-view image within the special window area. Also the window area satisfied the focusable range providing by the display.

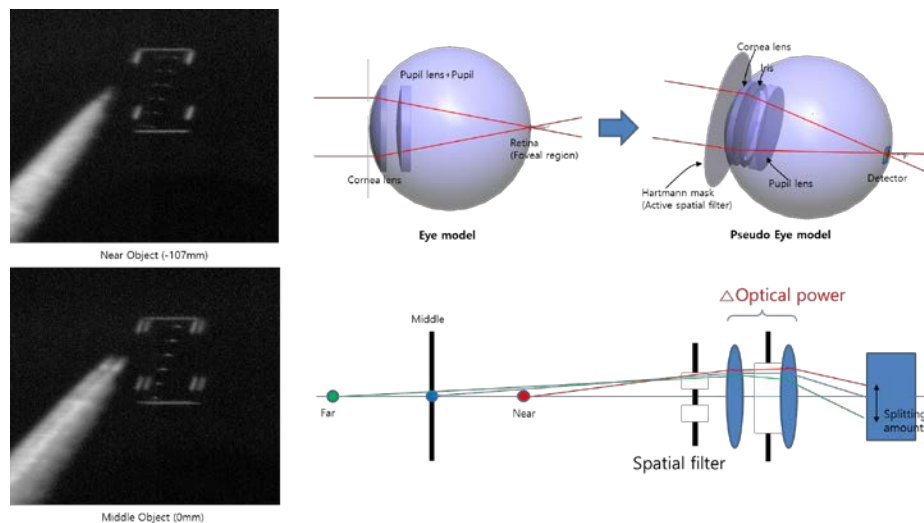


**Fig. 1. Experimental results by the designed optical system verifying objective accommodation served by LF display**

Consequently, we verified that LF display (based on horizontal parallax only model) can serve the objective accommodation function to the observer at the special condition. In the experimental result, non-focused object image was split on the detector as double image form which is not affected blur effect induced by optical system, and its form was contrasted to the focused case. Additionally, the result showed that the amount of split in the double image represents proportionally to the relative object distances in the object space.

### Acknowledgment

This work was supported by 'The Cross-Ministry Giga KOREA Project' grant funded by the Korea government (MSIT) (No.GK17C0200, Development of full-3D mobile display terminal and its contents )

### References

1. David A. Atchison, G. Smith, *Optics of the Human Eye*, Butterworth-Heinemann press, (2000)



## How to control polarization color

*Kenji Harada, Toshiki Matsuzaki and Huangyi Qin*

Department of Computer Science, Kitami Institute of Technology,

165 Koen-cho, Kitami, Hokkaido 090-8507, Japan

Tel.:81-157-26-9323, E-mail: harakan@cs.kitami-it.ac.jp

**OCIS codes:** (100.0100) Image Processing; (100.4998) Pattern recognition, optical security and encryption; (330.5000) Vision - patterns and recognition

A birefringent cellophane tape or a polymer sheet exhibits polarization color (interference color) by polarizer. We propose a novel technique for viewing images using polarization. The polarization color is controlled by changing the total retardation of the birefringent materials. Various colors can be displayed without color filters, which can be applied to color imaging device. There are various ways to control the polarization color. In this presentation, we show how to control the polarization color.

Figure 1(a) shows the conventional optical arrangement. The angle between the transmission axis of a polarizer and the retarder axis of a retarder film is  $45^\circ$  or  $135^\circ$  because the maximum transmittance is obtained at these angles. Figure 1(b) shows the proposed optical arrangement. The angle between the transmission axis of a polarizer and the retarder axis of a retarder film can be varied, and up to four retarder films are stacked. Using this proposed setup, we can display a high chroma image.

Figure 1(c) shows the composition the of polarization color display with stacking order dependence. Four retarder films (films 1, 2, 3, and 4) are inserted between two crossed polarizers such that the retarder axes of the retarder films are  $45^\circ$ ,  $0^\circ$ ,  $135^\circ$ , and  $0^\circ$ , respectively. The retardation of films 1 and 3 are 140 nm. In this composition, the displayed polarization color only depends on the retardation of film 2. By changing the position of images 1 and 2, the displayed polarization color changes. Figure 1(d) shows the optical arrangement of a stereoscopic imaging setup using polarization color. In general, stereoscopic imaging involves polarization, and polarized glasses with orthogonal polarization ( $\pm 45^\circ$  linear polarization or circular polarization) are used. A complementary color is observed with each eye when we apply this arrangement for viewing stereoscopic images using polarization color. In our stereoscopic arrangement, the polarization axes of both eyes are fixed to  $\theta = \pm 22.5^\circ$  (or  $\theta = \mp 67.5^\circ$ ) to separate the left-eye and right-eye images.

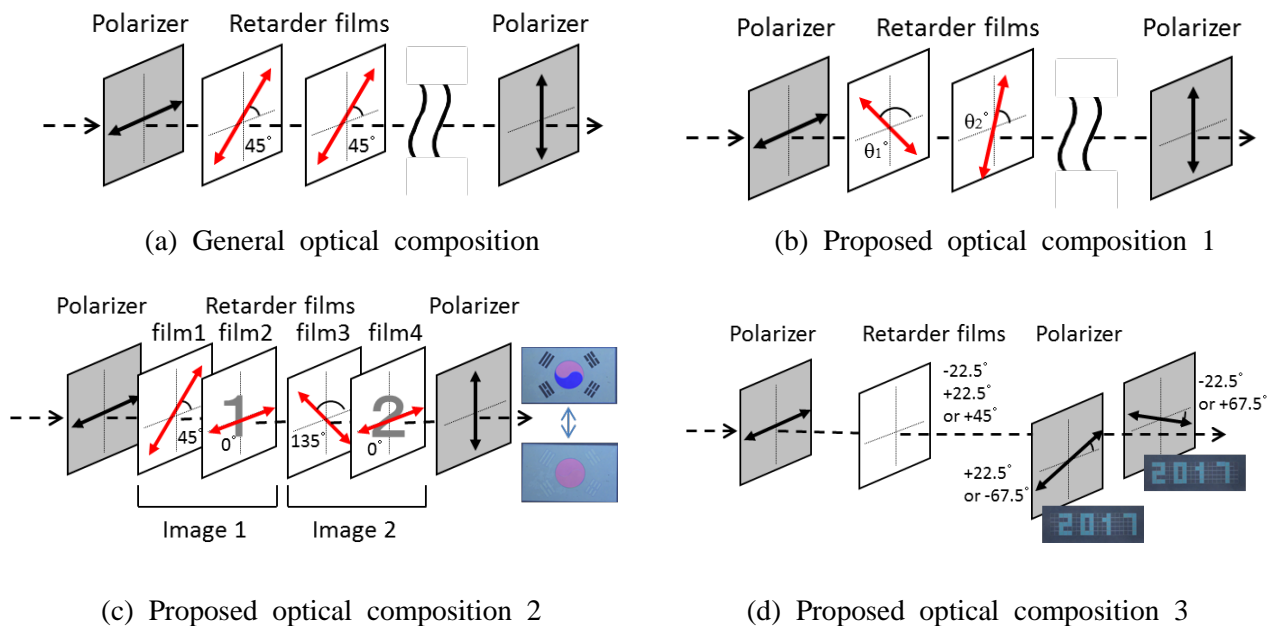


**Fig. 1. Optical composition for viewing polarization color image**

## Researches on effects of physiological depth cues on the visual discomfort of augmented reality displays

Hee-Jin Choi\*, Hanul Lee, Minyoung Park, and Jaehee Seo

<sup>1</sup>Dept. of Physics, Sejong University, Seoul 05006, Korea

Tel.:82-2-3408-3208, \*E-mail: hjchoi@sejong.ac.kr

**OCIS codes:** (110.3000) Image quality assessment; (100.6890) Three-dimensional image processing.

Recently, there are fast progresses in the field of augmented reality(AR) to overlap a virtual image including additional information to the object of interest by realizing a see-through optical system. Since the AR device can emerge the digital information with the objects in the real world, it attracts increasing attention for various applications. However, there are still some bottlenecks to be overcome for the AR devices to become popular. Among them, the human factor issue is one of the most important research subjects to be analyzed carefully. In this paper, we introduce our researches on the effects of physiological depth cues which can be the potential causes of the visual discomfort of current AR displays[1].

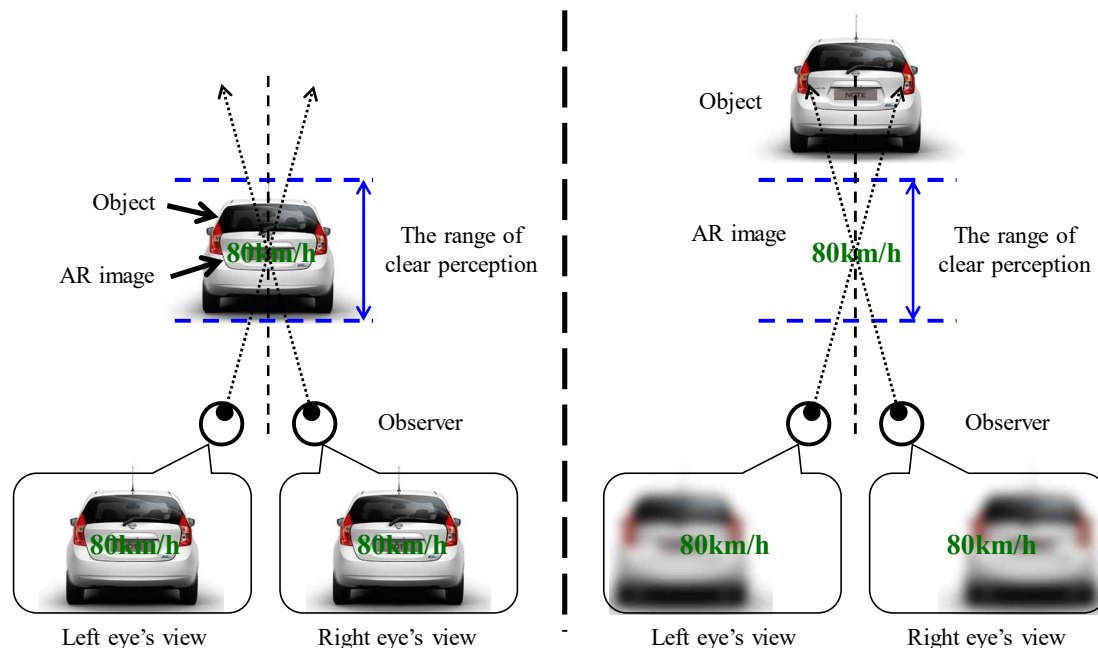


**Fig. 1. Effect of physiological depth cues in current AR devices**

We made the observer watch two images to be composed of odd/even half rows of a single digit number at different image planes (an AR image plane and an object image plane) and guess what the number is. Then, we measured the proportion of correct and the recognition time which the observer had consumed before making an answer. In order to evaluate the effect of the convergence and accommodation separately, we analyzed the response of the binocular viewing condition and monocular viewing condition respectively.

With the binocular viewing condition, the distance between the two image planes had a positive correlation with the recognition time whereas the proportion of correct decreases had a negative correlation. In contrast, there was no significant correlation between them in the monocular viewing condition. Therefore, it can be concluded that the cue of convergence has a larger affection to the visual discomfort than the accommodation and it is recommended to develop an improved AR devices to display the adapted AR images where the real object locates.

### References

1. H. Lee, M. Park, J. Seo, and H.-J. Choi, "Analysis on the range of clear perception of an augmented reality devices by measuring the recognition time of the observer," The 17th International Meeting on Information Display(IMID 2017), Busan, Korea, paper P1-119, August, 2017

# Volumetric Bubble Display

*Yoshio Hayasaki & Kota Kumagai*

Center for Optical Research and Education (CORE), Utsunomiya University

7-1-2 Yoto, Utsunomiya 321-8585, Japan

Tel.: +81-28-689-7114, E-mail: hayasaki@cc.utsunomiya-u.ac.jp

OCIS codes: (110.0110) Imaging systems; (300.0300) Spectroscopy; (110.1758) Computational imaging

Much attention has been paid to the development of three-dimensional volumetric displays in fields of optics and computer graphics, and it is a dream of we display researchers. They can render 3D graphics in real 3D space, and therefore, a volume image can be observed from any surrounding viewpoints without the user having to wear any special devices or experience physiological discomfort [1]. These optically-accessed volumetric displays have a wide viewing angle because they require no physical connection between the light source and the display volume. Therefore, reconfigurable and parallel connections are easily achieved, resulting in good accessibility and high drawing speed to the voxels. We developed three kind of volumetric displays with laser-excited fluorescence voxels[2], laser-produced plasma voxels[3], and laser-produced microbubble voxels[4]. In this presentation, we focus a volumetric display using light-scattering voxels formed of microbubbles induced by focused femtosecond laser pulses in high-viscosity liquid. This display is called as a volumetric bubble display.

Volumetric bubble display consisted of an amplified femtosecond laser source (Micra and Legend Elite Duo, Coherent), a 3D beam scanner composed of a 2D galvanometer mirror (GM-1010, Canon) and varifocal lens (EL-10-30- Ci, Optotune), a liquid-crystal on silicon SLM (LCOS-SLM; X10468-02, Hamamatsu Photonics) for holographic laser drawing, and glycerin in a glass cell. The femtosecond laser had a center wavelength of 800 nm, a repetition frequency of 1 kHz, and a pulse duration of <100 fs. The galvanometer scanner changed the focus position in the horizontal direction. A varifocal lens controlled the focus position in the axial direction. The 3D focal position was changed by these devices to render the 3D graphics. The LCOS-SLM displayed Fourier CGHs at a frame rate of 10 Hz. The Fourier CGHs were optimized by the optimal rotating angle method to generate parallel beams. The screen was glycerin sealed in a glass cell with dimensions 10 mm × 10 mm × 100 mm.

Figure 1(a) shows 3D bubble graphics viewed from different observation directions. These graphics were rendered by scanning 100 2D outlines of cross-sectional images from ear to foot, and were illuminated by the halogen lamp. The irradiation energy was 4.3 μJ. The volumetric graphics was successfully rendered by using femtosecond laser-induced microbubbles. Figure 1(b) shows the bubble graphics illuminated by light of different colors. The illumination light was emitted by a high-power full-color LED capable of outputting light of different colors. The center wavelengths were 624 nm (red), 525 nm (green), and 470 nm (blue). The irradiation pulse energy was 5.4 μJ. Although these results are monochrome graphics with different colors, it will be easy to form full-color bubble graphics by changing the color of the illumination light.

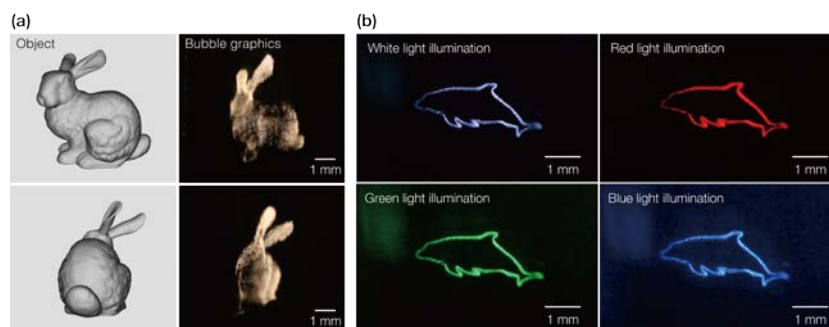


Fig. 1 (a) Volumetric graphics of “Stanford bunny” rendered by femtosecond laser-induced microbubbles. (b) 2D bubble graphics of “Dolphin” with illumination light having different colors.

## References

- [1] B. G. Blundell and A. J. Schwarz, IEEE Trans. Vis. Comput. Graph. **8**, 66–75 (2002).
- [2] K. Kumagai, D. Suzuki, S. Hasegawa and Y. Hayasaki, Opt. Lett., **40**, 3356–3359 (2015).
- [3] Y. Ochiai, K. Kumagai, T. Hoshi, J. Rekimoto, S. Hasegawa, Y. Hayasaki, ACM Trans. Graph. **35**, 1–14 (2016).
- [4] K. Kumagai, S. Hasegawa and Y. Hayasaki, Optica **40**, 298–302 (2017).

# Accommodative optical-see-through near-to-eye displays using waveguide and holographic optical elements

Jae-Hyeung Park\*, Seong-Bok Kim, Seok-Beom Ko, Kwang-Soo Shin, Yeon-Gyeong Ju, Dae-Yeol Park, and Askari Mehdi

Dept. of Information and Communication Engineering, Inha University, Incheon, 22212, Korea

Tel.: 82-32-860-7432, E-mail: jh.park@inha.ac.kr

**OCIS codes:** (110.6880) Three-dimensional image acquisition; (100.6890) Three-dimensional image processing; (090.1760) Computer holography

Optical see-through near-to-eye displays (NEDs) are highly demanding in augmented reality (AR) applications. Currently available NEDs usually present stereoscopic views of a 3D scene. Despite of depth perception by the binocular disparity, the individual image presented to each eye is 2D image at the conjugate plane of the display panel where the eye accommodates, and thus there is vergence-accommodation mismatch problem. We have developed several systems, solving this vergence-accommodation mismatch. One developed system is a waveguide-type holographic NED. This system delivers a holographic 3D image generated by a spatial light modulator (SLM) to the individual eye through the glass waveguide equipped with two holographic optical elements (HOEs) couplers. The aberration caused by the asymmetric diffraction of the HOEs is pre-compensated in the computer generated hologram (CGH) loaded in the SLM, presenting clear 3D images with true focal cues to each eye on top of the optical-see-through view of the real environment.[1]

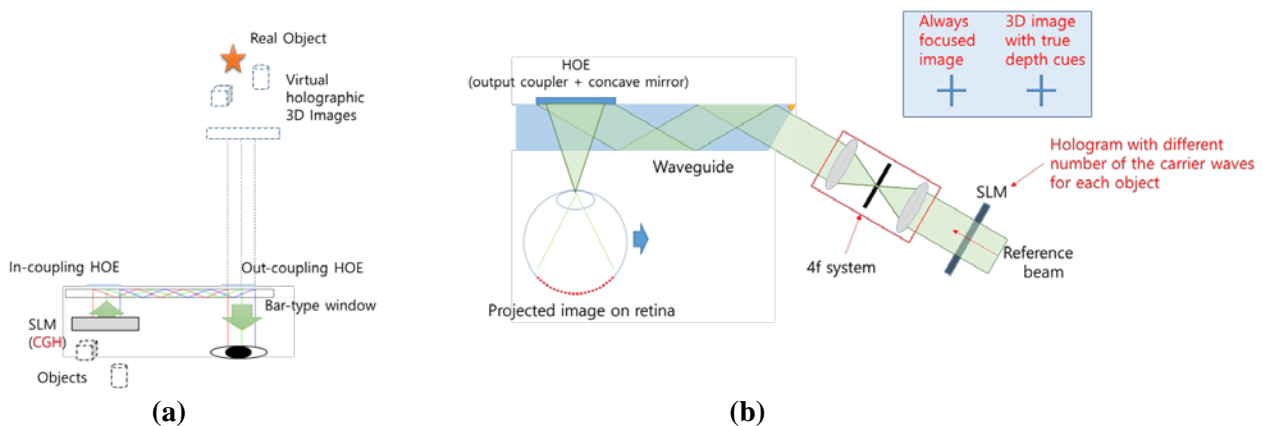


**Fig. 1. Waveguide type accommodative NEDs (a) holographic NED (b) Maxwellian NED**

A waveguide type Maxwellian display system has also been developed. In this system, the HOE works as the transparent multiplexed concave mirrors to give always-focused images to each eye. The multiple spots in the eye pupil plane generated by the single HOE contributes to the enlargement of the eyebox, solving small eyebox problem of conventional Maxwellian displays. We have also developed a technique to present the always-focused images and the true 3D images at the same time by using CGH as the display contents of the SLM in the Maxwellian displays.[2] We expect this technique can be applied to wide range of applications of AR.

## Acknowledgment

This work was supported by the Basic Science Research Program, National Research Foundation of Korea (NRF) [NRF-2017R1A2B2011084].

## References

1. H.-J. Yeom, H.-J. Kim, S.-B. Kim, H. Zhang, B. Li, Y.-M. Ji, S.-H. Kim, and J.-H. Park, *Optics Express* **23**(25), 32025 (2015).
2. J.-H. Park, OSA Frontiers in Optics 2017 (FiO 2017), Washington, DC, USA, paper FW5C.3, (2017).

## Incoherent holography without depth of field

*Takanori Nomura<sup>1</sup> and Takuya Matsuda<sup>2</sup>*

<sup>1</sup>Faculty of Systems Engineering, Wakayama University, Wakayama, Wakayama, Japan

Tel.:81-73-457-8174, E-mail: nom@sys.wakayama-u.ac.jp

<sup>2</sup>Graduate School of Systems Engineering, Wakayama University, Wakayama, Wakayama, Japan

**OCIS codes:** (090.1995) Digital holography; (110.1758) Computational imaging; (100.3195) Interferometric imaging

It is common to observe objects which exist at different depths by a microscope. However, it is impossible to observe all in-focus objects. To obtain all in-focus images, a number of methods have been proposed. In this paper, alternative method to obtain all in-focus image is introduced.

For pattern matching of incoherent objects, the use of the cosine transformation of an object have been proposed<sup>1)</sup>. The cosine transformation of an object is obtained by a rotational shearing interferometer. If the power distribution of a spatially incoherent object with a wavenumber  $k$  is given by  $P(x,y)$ , the obtained intensity distribution, incoherent hologram  $I(\mu,\nu)$  obtained at a detector plane whose distance from an object is  $z$ , is given by

$$I(\mu, \nu) = \frac{1}{2} \iint_{-\infty}^{\infty} P(x, y) dx dy + \frac{1}{2} \iint_{-\infty}^{\infty} P(x, y) \cos \left\{ k \frac{2 \sin \theta}{z} (-x\nu + y\mu) \right\} dx dy, \quad (1)$$

where,  $\theta$  denotes the rotational shearing angle given by the interferometer. The distance  $z$  affects only the magnification of the Fourier transformation. Therefore, all focused images can be obtained by the inverse Fourier transformation of an incoherent hologram given by Eq. (1). The images shown in Fig. 1 are the preliminary experimental results of this method. In the experiments, the object was a Chinese character consisting four squares displayed on a liquid crystal display whose backlight was green LEDs. The object was placed at different distances (210 mm and 240 mm from the image sensor). The sizes of reconstructed images are different. However, they are focused. This fact suggests the imaging without depth of focus based on a hologram obtained by a rotational shearing interferometer.

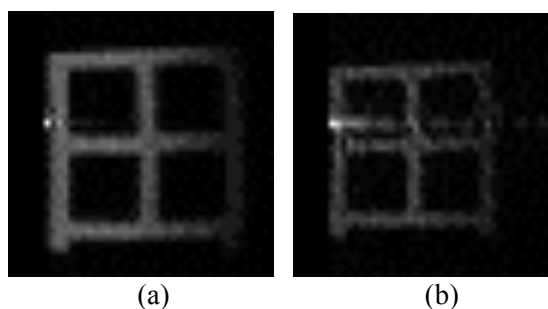


**Fig. 1. Reconstructed images of incoherent holograms obtained by a rotational sharing interferometer. The objects were placed at a distance of (a) 210 mm and (b) 240 mm.**

More detailed discussson of the reconstructed images including magnification and image quality will be given.

### References

1. T. Nomura, K. Itoh, and Y. Ichinoka, *Appl. Opt.*, 28(23), 4987 (1989).
2. K. Watanabe and T. Nomura, *Appl. Opt.*, 54(1), A18 (2015).
3. T. Matsuda and T. Nomura, ISOM'17 Tu-J-10 (2017).



## Recent researches for two type 3D screens: Reflection-type and Transmission-type

*Sung-Wook Min\* and Hyunsik Sung*

Dept. of Inform. Display, Kyung Hee University, Dongdaemun-gu, Seoul 02447, Korea

\*E-mail: mins@khu.ac.kr

**OCIS codes:** (110.6880) Three-dimensional image acquisition; (100.6890) Three-dimensional image processing; (090.1760) Computer holography

The projection-type display system has been used in the display industry because the displaying region is enlarged easily. However, in the projection-type display system, the projection image has low diverging angle due to the limitation of exit pupil. Therefore, when we use the projection system, we need the diffuser as the screen for observing image presented by the projector. The projection-type display system is often used in three-dimensional (3D) display system due to its advantages. However, the projection-type 3D display system also has same problem for the limited field of view. So we cannot observe 3D image without any screen. To resolve this problem, we use the diffuser in the projection-type 3D display system. But, this solution is not effective because the diffuser can help improve the visibility of image located on the screen, and other images is blurred. Therefore, we need the new screen for the projection-type 3D display system, which is called 3D screen.

In previous research, the optical depth converter (ODC), consisted of two lens arrays, was proposed as the screen in the projection-type integral imaging system [1]. The ODC can be used to resolve the pseudoscopic problem in integral imaging system because the ODC arranges the 3D integrated images in the reverse order. Besides, the ODC can retain the depth information in the space. Thanks to its characteristic, the ODC can be used as the 3D screen of the projection-type 3D display system.

The 3D screen is divided into two types: reflection-type and transmission-type. The reflection-type 3D screen generally uses a lens array and a reflecting device as the equivalent system for the ODC. The reflection-type 3D screen using the simple mirror has the problem that the image flipping occurs the reflected image by the mirror after passing through the adjacent elemental lens. To resolve the problem, we use the retroreflector film, which reflects the reflected light in the direction of the incident, in the reflection-type 3D screen. To optimize the reflection-type 3D screen using the retroreflector film, we analyze the distance between the retroreflector film and the lens array [2]. The transmission-type 3D screen can be instrumented using ODC or adding other optical devices in the ODC. The ODC has same problem of the image flipping. To resolve this problem, we adapt the micro hole-mirror array (MHA) in the transmission-type 3D screen. However, because it is difficult to fabricate the MHA, and so we propose the new structure fabricated easily and name it the roof mirror array [3].

In this paper, to optimize the transmission-type 3D screen, we confirm the image simulation of the MHA using Light Tools 8.3 and compare the imaging simulation results shown in Fig. 1 according to the incident angle. In addition, we fabricate the proto-type the MHA to compare with the simulation results.

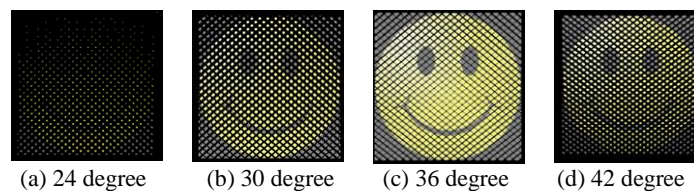


**Fig. 1. Image simulation results**

### Acknowledgment

This work was supported by the National Research Foundation of Korea(NRF) grant funded by the Korea government(MSIT) (No.2011-0030079)

### References

1. S-W. Min et al, "Analysis of an optical depth converter used in a three dimensional integral imaging system," Appl. Opt. 43(23), 4539-4549 (2004).
2. Y. M. Kim et al, "Projection-type integral imaging system using a three-dimensional screen composed of a lens array and a retroreflector film," Appl. Opt. 56(13), F105-F111 (2017)
3. S-W. Min et al, "Recent research about 3D screen," in the Sixth Japan-Korea workshop on Digital Holography and Information Photonics. (Optical Society of Japan & Optical Society of Korea, Sapporo, 2016)